

MECHANICAL AND THERMAL PROPERTIES OF
RENEWABLE OIL PALM SHELL LIGHTWEIGHT
CONCRETE REINFORCED WITH SYNTHETIC
POLYPROPYLENE FIBRES

LOH LEONG TATT

MASTER OF ENGINEERING SCIENCE

LEE KONG CHIAN
FACULTY OF ENGINEERING AND SCIENCE
UNIVERSITI TUNKU ABDUL RAHMAN
MAY 2021

**MECHANICAL AND THERMAL PROPERTIES OF RENEWABLE OIL
PALM SHELL LIGHTWEIGHT CONCRETE REINFORCED WITH
SYNTHETIC POLYPROPYLENE FIBRES**

By

Loh Leong Tatt

A dissertation submitted to the Department of Civil Engineering,
Lee Kong Chian Faculty of Engineering and Science,
Universiti Tunku Abdul Rahman,
in partial fulfillment of the requirements for the degree of
Master of Engineering Science
May 2021

ABSTRACT

MECHANICAL AND THERMAL PROPERTIES OF RENEWABLE OIL PALM SHELL LIGHTWEIGHT CONCRETE REINFORCED WITH SYNTHETIC POLYPROPYLENE FIBRES

Loh Leong Tatt

Being the second largest exporter of palm oil globally, Malaysia generated approximately 6.3 million tonnes of oil palm shell (OPS) in 2018. OPS are solid waste products from the palm oil mill. Researches of using OPS as aggregates in concrete have been initiated as the specific gravity of the shells is 1.1 – 1.4 g/cm³, which falls within the range of lightweight aggregates. Previous studies show that the mechanical performance of oil palm shell lightweight concrete is lower than other types of lightweight aggregate concrete. Therefore, synthetic polypropylene fibres are added to enhance the mechanical properties, especially in splitting tensile strength and modulus of rupture. The effects of two different types of synthetic polypropylene fibres on the mechanical and thermal properties of OPS concrete are investigated in this research. The fibres are singly and hybrid reinforced in different volume fractions (0.1%, 0.3% and 0.4%). The oven-dried density of the OPS concrete produced is between 1936.7 kg/m³ to 1976.5 kg/m³ with compressive strength of more than 25 MPa at 28-days. A new mixing method has been proposed, which shows significant improvement in workability and compressive strength. The research outcome has proven that the inclusion of fibres is more prominent in improving the residual strength properties of OPS concrete. The

research finding has proven that the bridging effect of fibres modifies the failure modes of OPS concrete. In addition, synthetic polymer fibres of small diameter increase the thermal conductivity; while synthetic polymer fibres of large diameter decrease the thermal conductivity. Hence, the findings of this study prove that synthetic polypropylene fibres can be used to enhance the mechanical and thermal properties of OPS lightweight concrete.

ACKNOWLEDGEMENTS

First and foremost, I would like to express my deepest and sincere gratitude to my supervisor, Dr. Yew Ming Kun and my co-supervisor, Ts. Dr. Yew Ming Chian for their invaluable guidance, constructive advices and considerate assistance throughout this research. They are always available for consultation and always willing to share their ideas and knowledge selflessly. With patience, they elaborate with clear and detailed explanation to ensure my understanding during discussion.

Furthermore, I would like to appreciate the laboratory staffs for their assistance in providing technical support to my experimental work. At the same time, I would also like to thank my fellow coursemates, who offered their help and encouragement whenever I encountered any difficulties.


Also, I would like to deliver my acknowledgement to the UTAR Research Fund under the vote number of 6200/Y52 for the financial support in the execution of the research work.

Last but not least, the emotional support from my family and friends is very much appreciated. Without their support, I would not be able to complete my research.

APPROVAL SHEET

This dissertation/thesis entitled “MECHANICAL AND THERMAL PROPERTIES OF RENEWABLE OIL PALM SHELL LIGHTWEIGHT CONCRETE REINFORCED WITH SYNTHETIC POLYPROPYLENE FIBRES” was prepared by LOH LEONG TATT and submitted as partial fulfillment of the requirements for the degree of Master of Engineering Science at Universiti Tunku Abdul Rahman.

Approved by:



(Ts. Dr. Yew Ming Kun)

Date: ...6/5/2021/...

Assistant Professor/Supervisor

Department of Civil Engineering

Lee Kong Chian Faculty of Engineering and Science

Universiti Tunku Abdul Rahman



(Ts. Dr. Yew Ming Chian)

Date: ...6/5/2021/...

Assistant Professor/Co-supervisor

Department of Mechanical and Material Engineering

Lee Kong Chian Faculty of Engineering and Science

Universiti Tunku Abdul Rahman

**LEE KONG CHIAN FACULTY OF ENGINEERING SCIENCE
UNIVERSITI TUNKU ABDUL RAHMAN**

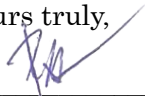
Date: 5-5-2021

SUBMISSION OF DISSERTATION

It is hereby certified that LOH LEONG TATT (ID No: 17UEM05509) has completed this dissertation entitled "MECHANICAL AND THERMAL PROPERTIES OF RENEWABLE OIL PALM SHELL LIGHTWEIGHT CONCRETE REINFORCED WITH SYNTHETIC POLYPROPYLENE FIBRES" under the supervision of Dr. Yew Ming Kun (Supervisor) from the Department of Civil Engineering, Faculty of Engineering Science, and Ts. Dr. Yew Ming Chian (Co-Supervisor) from the Department of Mechanical and Material Engineering, Faculty of Engineering Science.

I understand that University will upload softcopy of my dissertation in pdf format into UTAR Institutional Repository, which may be made accessible to UTAR community and public.

Yours truly,



(LOH LEONG TATT)

DECLARATION

I hereby declare that the dissertation is based on my original work except for quotations and citations which have been duly acknowledged. I also declare that it has not been previously or concurrently submitted for any other degree at UTAR or other institutions.

Name Loh Leong Tatt

Date 5/5/2021

TABLE OF CONTENTS

	Page
ABSTRACT	II
ACKNOWLEDGEMENTS	IV
APPROVAL SHEET	V
SUBMISSION OF DISSERTATION	VI
DECLARATION	VII
TABLE OF CONTENTS	VIII
LIST OF TABLES	XI
LIST OF FIGURES	XIII
LIST OF ABBREVIATIONS	XVI
LIST OF SYMBOLS	XVIII
CHAPTER	
1 INTRODUCTION	20
1.1 Research Background	20
1.2 Problem Statement	23
1.3 Research Objectives	24
1.4 Scope of Research	24
1.5 Significance of Research	25
1.6 Outline of Thesis	26
2 LITERATURE REVIEW	27
2.1 Introduction	27
2.2 Lightweight Aggregate Concrete	27
2.3 Oil Palm Shell (OPS)	28
2.3.1 Specification of OPS	31
2.3.2 Application of OPSLWC in Malaysia	32
2.4 Fibres	33
2.4.1 Characteristics of Fibres	36
2.4.1.1 Geometrical Properties	36
2.4.1.2 Aspect Ratio	40
2.4.1.3 Volume Fraction	40
2.4.2 Polypropylene Fibres	41
2.4.3 Fibres Hybridisation	42
2.4.4 Role of Fibres	45
2.5 Effects of Fibres on OPSLWC	46
2.5.1 Compressive Strength	46
2.5.2 Splitting Tensile Strength	47
2.5.3 Flexural Strength	48
2.5.4 Residual Strength	50

2.5.5	Thermal Conductivity	50
2.5.6	Temperature Gradient	51
2.6	Mixing Method	52
2.7	Summary	53
3	METHODOLOGY OF RESEARCH	54
3.1	Introduction	54
3.2	Materials	55
3.2.1	Cement	55
3.2.2	Fine Aggregates	57
3.2.3	OPS Coarse Aggregates	57
3.2.4	Polypropylene (PP) Fibres	58
3.2.5	Water	59
3.2.6	Superplasticiser	59
3.3	Mix Design	60
3.3.1	Absolute Volume Method	60
3.3.1.1	Sample Calculation of the Mix	61
3.3.1.2	Sample Calculation of the Fibre Volume	61
3.4	Mixing Method	62
3.4.1	Conventional Mixing Method (CMM)	62
3.4.2	New Mixing Method (NMM)	63
3.5	Water Curing	64
3.6	Fresh Concrete Tests	65
3.6.1	Fresh Density of Concrete	66
3.6.2	Slump Test	67
3.6.3	Vebe Test	68
3.7	Hardened Concrete Tests	70
3.7.1	UPV Test (Non-Destructive Test)	71
3.7.2	Compression Test (Destructive Test)	73
3.7.3	Splitting Tension Test (Destructive Test)	75
3.7.4	Flexure Test (Destructive Test)	77
3.8	Thermal Properties Tests	79
3.8.1	Thermal Conductivity Test	80
3.8.2	Temperature Gradient Test	82
3.9	Summary	84
4	RESULTS AND DISCUSSIONS	85
4.1	Introduction	85
4.2	Trial Mix	85
4.2.1	Mix Design	86
4.2.2	Workability	87
4.2.3	Compressive Strength	88
4.2.4	Comparison of Workability between CMM and NMM	89
4.2.5	Comparison of 28-days Compressive Strength between CMM and NMM	91
4.3	Actual Mix	92
4.3.1	Mix Design	92
4.3.2	Fresh Properties	93

4.3.2.1	Fresh Density	93
4.3.2.2	Workability	94
4.3.3	Hardened Properties	96
4.3.3.1	Density	96
4.3.3.2	UPV Test (Uniformity)	97
4.3.3.3	Compressive Strength	99
4.3.3.4	Residual Compressive Strength	103
4.3.3.5	Splitting Tensile Strength	107
4.3.3.6	Residual Splitting Tensile Strength	109
4.3.3.7	Flexural Strength	113
4.3.4	Performance Index	116
4.3.4.1	Performance Index of Compressive Strength	116
4.3.4.2	Performance Index of Splitting Tensile Strength	117
4.3.4.3	Performance Index of Flexural Strength	118
4.3.4	Thermal Properties	119
4.3.4.1	Thermal Conductivity	120
4.3.4.2	Temperature Gradient	122
4.4	Summary	119
5	CONCLUSIONS AND RECOMMENDATIONS	127
5.1	Conclusions	127
5.2	Recommendations for Future Research Work	130
	REFERENCES	131
	APPENDICES	139
	LIST OF PUBLICATIONS	158

LIST OF TABLES

Table		Page
2.1	Species of Oil Palm Fruits	30
2.2	Basic Properties of Various Fibres Type	35
2.3	Classifications of Fibres Made from Polymeric Materials	38
2.4	Volume Fractions of Fibres in Concrete Composites	41
2.5	Properties of Polypropylene Fibres	42
2.6	Mechanical Properties of OPSFRC of Previous Researches	49
2.7	Mixing Stages of Different Mixing Methods	52
3.1	Specifications of OPC	56
3.2	Main Compounds of OPC	56
3.3	Specifications of OPS	57
3.4	Specifications of PP Fibres	59
3.5	Sample Calculation of Absolute Volume Method	61
3.6	Sample Calculation of the Mass of PP Fibres	62
3.7	Types of Specimens and Age of Testing of Different Tests	84
4.1	Mix Proportions of Trial Mixes	86
4.2	Mix Codes for All Mixes	93
4.3	Fresh Density of All Mixes	94
4.4	Workability of All Mixes	94
4.5	Densities of All Mixes	97
4.6	Category of Concrete Quality Based on UPV	98
4.7	Compressive Strength of All Mixes at Different Ages	100
4.8	Residual Compressive Strength of All Mixes at 28-days	104

4.9	Residual Splitting Tensile Strength of All Mixes at 28-days	111
4.10	Temperature Changes of All Specimens	123

LIST OF FIGURES

Figures		Page
2.1	World Palm Oil Production by Country in 2018	29
2.2	Crushed OPS of Different Shapes	31
2.3	Footbridge Constructed with OPS Concrete	33
2.4	Model Low-cost House Built with OPS Concrete	33
2.5	Typical Profiles of Steel Fibres Commonly Used in Concrete	36
2.6	Illustration of the Role of Fibres during Cracking	39
2.7	Mechanism of the Cracking Control by Large and Micro Fibres and the Effects on Stress-Strain Relation	39
2.8	Mechanisms of Interactions between Fibres and Cement Matrix: (1) debonding (2) bridging (3) pull-out (4) failure	45
2.9	Crack Pattern in the Elements of RC and FRC Subjected to Tension Loading	46
2.10	Schematic Diagram of the Thermal Insulation Performance Test Equipment	51
3.1	Flowchart of the Experimental Program	55
3.2	Crushed OPS Coarse Aggregates	58
3.3	Flowchart of the Conventional Mixing Method (CMM)	63
3.4	Flowchart of the New Mixing Method (NMM)	64
3.5	Specimens in the Water Tank for Curing	65
3.6	Measurement of Fresh Density	67
3.7	Measurement of Slump Value	68
3.8	Vebe Test Apparatus	70
3.9	UPV Test Apparatus	72
3.10	Compression Test	74
3.11	Splitting Tension Test	76
3.12	Flexure Test	78
3.13	Test Equipment for Thermal Conductivity	80
3.14	Schematic Diagram of the Test Apparatus	83
3.15	Setup of the Test Apparatus	83

4.1	Workability of Trial Mixes	87
4.2	Compressive Strength of Trial Mixes at 28-days	89
4.3	Workability of Trial Mixes by Different Mixing Methods	90
4.4	Compressive Strength of Trial Mixes by Different Mixing Methods at 28-days	91
4.5	Relationship between Slump Value (mm) and Vebe Time (s)	96
4.6	UPV of Different Percentage of Fibres Content	99
4.7	Development of Compressive Strength at Different Ages	102
4.8	Correlation between Cube Compressive Strength and UPV	103
4.9	Comparison of RCS of All Mixes	105
4.10	Failure Pattern of OPSLWC (a) without Fibres (b) with Fibres after Third Loading	106
4.11	Linking Bridge between Fibres and Cement Matrices	106
4.12	Development of Splitting Tensile Strength of All Mixes	107
4.13	Stretching of Reinforced Fibres upon Splitting	109
4.14	Failure Mode of OPSLWC-CTR-0% after First Loading	110
4.15	Comparison of 28-days RSTS of All Mixes	111
4.16	Failure Mode of OPSLWC-HYB-0.4% after Third Loading	112
4.17	Flexural Strength of All Mixes at 7 and 28-days	113
4.18	Rupture Mode of Prisms (a)without Fibres and (b) with Fibres	115
4.19	Performance Index of Compressive Strength of OPSLWC Reinforced with PP Fibres of Various Volume Fractions at Different Ages	116
4.20	Performance Index of Splitting Tensile Strength of OPSLWC Reinforced with PP Fibres of Various Volume Fractions at Different Ages	118
4.21	Performance Index of Flexural Strength of OPSLWC Reinforced with PP Fibres of Various Volume Fractions at Different Ages	119

4.22	Thermal Conductivity of OPSLWC Incorporated with Various Percentage of Fibres at 7-days and 28-days	120
4.23	Temperature Gradient of OPSLWC with Various Percentage of Fibres	122
4.24	Cross-Section of OPSLWC-HYB-0.4% with Randomly Distributed Fibres	125

LIST OF ABBREVIATIONS

AR	Alkali Resistant
ACI	American Concrete Institute
ASTM	American Society for Testing and Materials
AD	Anno Domini
BPS	Barchip Polypropylene Straight
BC	Before Christ
CTR	Control
CMM	Conventional Mixing Method
DD	Demoulded Density
DT	Destructive Test
FRC	Fibre-reinforced Concrete
FROPSLWC	Fibre-reinforced Oil Palm Shell Lightweight Concrete
FLCS	First Loading Compressive Strength
FLSTS	First Loading Splitting Tensile Strength
FFB	Fresh Fruit Bunch
GFRC	Glass Fibres Reinforced Concrete
HPFRCC	High Performance Fibre Reinforced Cement Composites
HYB	Hybrid
RILEM	International Union of Laboratories and Experts in Construction Materials, System and Structures
LWA	Lightweight Aggregate
LWAC	Lightweight Aggregate Concrete
MOR	Modulus of Rupture
MPS	Monofilament Polypropylene Straight
NMM	New Mixing Method
NDT	Non-Destructive Test
Ny	Nylon
OPS	Oil Palm Shell
OPSLWC	Oil Palm Shell Lightweight Concrete
OPC	Ordinary Portland Cement
ODD	Oven Dried Density

PP	Polypropylene
PPFRC	Polypropylene Fibres Reinforced Concrete
PPTB	Polypropylene Twisted Bundle
PVA	Polyvinyl Alcohol
RCS	Residual Compressive Strength
RSTS	Residual Splitting Tensile Strength
SSD	Saturated Surface Dry
SEM	Scanning Electron Microscopy
SLCS	Second Loading Compressive Strength
SLSTS	Second Loading Splitting Tensile Strength
SCC	Self-Compacting Concrete
SG	Specific Gravity
ST	Steel
SFRC	Steel Fibres Reinforced Concrete
SLWC	Structural Lightweight Concrete
SP	Superplasticiser
TLCS	Third Loading Compressive Strength
TLSTS	Third Loading Splitting Tensile Strength
UPV	Ultrasonic Pulse Velocity

LIST OF SYMBOLS

a	Aspect Ratio
b	breadth
f_{cu}	Compressive Strength
ρ	Density
d	depth
D	diameter
L	distance
d_f	Equivalent Diameter
f_{ct}	Flexural Strength
l	Length
m	Mass
P	Peak Load
\emptyset	Power
S	Slump Value
f_{ct}	Splitting Tensile Strength
A	Surface Area
T	Temperature
k	Thermal Conductivity
t	Time
U_t	Transverse Ultrasonic Pulse Velocity
V_e	Vebe Time
v	Velocity
V	Volume
V_f	Volume Fraction
Al_2O_3	Aluminium Oxide
CaO	Calcium Oxide
C_2S	Dicalcium Silicate
Fe_2O_3	Iron (III) Oxide
MgO	Magnesium Oxide
C_3H_6	Propene

SiO_2	Silicon Dioxide
SO_3	Sulfur Trioxide
C_4AF	Tetracalcium Aluminoferrite
C_3A	Tricalcium Aluminate
C_3S	Tricalcium Silicate

CHAPTER 1

INTRODUCTION

1.1 Research Background

Along with the projection of the world's population, the scarcity of natural resources has become a major issue. Construction industry is one of the industries that will grow with the increasing population as to accommodate the demand for shelter and infrastructure. Concrete is the major construction material needed. In fact, the production of concrete consumes significant amount of natural resources, particularly natural aggregates which constitute 55% to 80% of concrete volume. The global market for aggregates in construction industry has an annual growth rate of 5.2% and is projected to reach 51.7 billion tonnes in 2019 (The Freedonia Group, 2016). Hence, the search for alternative aggregates has been initiated.

At the same time, energy crisis is now a worldwide recognised issue by government and industry leaders. Buildings are one of the major consumers of energy, which has accounted for about 40% of global energy demand. Building envelope plays an important role in energy efficiency buildings. High thermal and solar resistance is a key attribute of an energy efficiency building. Therefore, proper selection and design of suitable building materials can lead to a better indoor ambience to reduce the energy needed for heating and air-conditioning of a building. Thermal insulation of building envelope is a major

contributor practically and logically as a first step towards energy savings and can be defined by thermal conductivity of the material. Therefore, porous lightweight aggregates which are poor thermal conductor and are potential material for the construction of energy efficiency building.

In recent years, lightweight aggregate concrete (LWAC) is emerging as a solution to the depletion of natural aggregates. LWAC is defined by the replacement of conventional aggregates with aggregates of lower density to produce concrete with the density of 1600 kg/m^3 to 2000 kg/m^3 . Lightweight aggregates can be categorised into two different types, which are natural lightweight aggregates and artificial lightweight aggregates. Aggregates that are collected without undergoing any processes for the enhancement of properties are known as natural lightweight aggregates. Artificial lightweight aggregates are also known as industrial lightweight aggregates, which are obtained from the by-products of industrial processes. Processed natural aggregates are also categorised as industrial lightweight aggregates. From the aspect of strength, LWAC is lower than normal weight concrete. However, LWAC has advantages that favour its application over normal weight concrete in certain extent. One of the advantages is the lower construction cost due to its lower self-weight which reduces the dead load of the building as lesser formwork and reinforcement needed. In addition, lightweight aggregates are generally more porous than normal aggregates. Therefore, they are better in fire resistance and thermal insulation. These attributes favour their application in the construction of wall panels in energy efficiency buildings.

In fact, the search for alternative aggregate substituents has been extended to waste materials from the agricultural sector. The utilisation of waste materials gives many advantages, which include renewable, sustainable, domestic availability and innovation of value-added product. The tropical climate of Malaysia is a suitable ground for the plantation of palm oil trees. Due to its geological and metrological condition, Malaysia is the second largest exporter of palm oil, which contributes 27.7% to the total production of world palm oil trade, which is about 19.52 million tonnes (Malaysian Palm Oil Board, 2018b) (Ling, 2019). However, the biomass wastes generated from this sector has accounted for 85.5% of the total generation of biomass wastes in Malaysia (Phang & Lau, 2017). Waste disposal is a major problem for palm oil industry. OPS is one of the wastes generated from the manufacturing of palm oil. In a fresh fruit bunch (FFB) of palm oil, 6.4% is oil palm shell (OPS), which is one of the wastes generated from the manufacturing of palm oil (Hambali & Rivai, 2017). According to Malaysian Palm Oil Board (2018), the total production of FFB in 2018 was 98.42 million tonnes. Hence, approximately 6.30 million tonnes of OPS were produced in 2018. The potential of OPS as aggregate substituents in concrete has been investigated since three decades ago. Researches of replacing conventional coarse aggregates with lightweight crushed OPS had been initiated in 1984 by a Malaysian researcher (Abang, et al., 1984). The utilisation of OPS as lightweight aggregates is not only a solution for the disposal problem of palm oil industry, but it is also a way to relieve the depletion problem of natural resources.

In general, the mechanical performance of LWAC is lower than that of normal weight concrete. The addition of short randomly distributed fibres can be effective in improving the concrete strength and acts as cracking inhibitors. With the reinforcement of short fibres, the matrix is strengthened by the fibre-matrix bond. A bridging effect is induced within the bond by the frictional pull-out of fibres. Fibres have been first introduced in construction materials 3500 years ago in the form of horse hair and straw. Different types of fibres have been used according to their applications. In the early of 20th century, asbestos fibres were introduced. The application of asbestos fibres was then replaced after the discovery of their carcinogenic properties. Steel fibres, glass fibres and polypropylene (PP) fibres were then been used commercially in the last quarter of 20th century. Today, fibre-reinforced concrete (FRC) is widely applied structurally in construction with integrated code of practice.

1.2 Problem Statement

Although OPS approaches to be a potential alternate substituent in building material, but OPS is still not commercialised in the construction industry today. One of the reasons could be the lower mechanical properties of oil palm shell lightweight concrete (OPSLWC) as compared to that of other LWAC due to the weak bonding between OPS and cement paste. To enhance the performance of OPSLWC, two different types of synthetic PP fibres are added into OPSLWC. The two different fibres are singly, and hybrid reinforced respectively into OPSLWC. The mechanical and thermal properties of the

fibre-reinforced oil palm shell lightweight concrete (FROPSLWC) are investigated to study the effects of the reinforced fibres on OPSLWC.

1.3 Research Objectives

The objectives of this study are as below:

- a. To develop lightweight concrete with local agricultural waste oil palm shell as lightweight coarse aggregate with a 28-day cube compressive strength of not lesser than 25 MPa.
- b. To investigate the mechanical properties of control and fibre-reinforced oil palm shell lightweight concrete with oven-dried density of less than 2000 kg/m³.
- c. To compare the thermal conductivity, k value of the control and fibre-reinforced oil palm shell lightweight concrete.
- d. To study the thermal properties of the control and fibre-reinforced oil palm shell lightweight concrete by temperature gradient test.

1.4 Scope of Research

In this research, OPSLWC is reinforced with two different types of PP fibres, namely monofilament polypropylene straight (MPS) and barchip polypropylene straight (BPS). A new mixing method is introduced in this research and the outcome is compared with that of conventional mixing method. Chemical admixture (superplasticiser) is added to all mixes to enhance the workability. Several tests are carried out in accordance to

standards (BS EN, ASTM and etc) to determine the fresh, hardened, mechanical and thermal properties of FROPSLWC. This research is to study the effect of the incorporation of synthetic PP fibres on the mechanical and thermal properties of OPSLWC.

1.5 Significance of Research

The mechanical properties and thermal conductivity of OPSLWC reinforced with two different types of synthetic PP fibres are investigated in this study. The novelty of this research is defined by the types of PP fibres incorporated into OPSLWC and their hybridisation effect along with the new mixing method demonstrated in this research. The use of industrial by-product as a substituent in building material is trending globally due to the depletion of raw materials. Sustainable agricultural waste which is locally available OPS is a potential solution for the problem. The lightness of OPS is favourable in the reduction of construction cost in foundation design, formwork and installation. Good thermal resistance marks OPS as a good option for energy efficiency building material. Different types of PP fibres are discovered to enhance the properties of OPSLWC for building and construction. Therefore, the novelty is clearly elaborated and the contribution towards society is from the aspect of environmental friendliness.

1.6 Outline of Thesis

This thesis is presented in five chapters. Chapter 1 is the introduction of this research. It comprises of the research background, research objectives, scope of study and importance of research.

Chapter 2 is the review of literature related to the development of OPSLWC. The history background and the application of OPSLWC are presented. The development of fibres is described as well. All the related key findings from previous researches are summarised in this chapter.

In Chapter 3, the methodology implemented in this research is described. It includes properties of materials used, preparation of materials, test equipment and testing procedures. The steps to produce all specimens are described with all the mix designs. The relevant codes of practice and standards are also acknowledged in this chapter.

The experimental results are documented in Chapter 4. Fresh and hardened properties, mechanical properties and thermal properties of all mixes are compared and discussed with the aid of appropriate graphs, tables and relevant equations for better visual interpretation.

Chapter 5, which is the last chapter, concludes the findings of this research based on the experimental results. A list of recommendations for further research has been proposed in this chapter as well.

CHAPTER 2

LITERATURE REVIEW

2.1 Introduction

This chapter overviews the historical development of oil palm shell lightweight concrete (OPSLWC) with and without fibres. It includes the background of lightweight aggregate concrete (LWAC), oil palm shell (OPS) and fibres. From the previous researches, various effects of the inclusion of synthetic polypropylene fibres (PP) on OPSLWC were discussed, which included fresh and hardened concrete properties. The effect of the included fibres on the thermal properties of OPSLWC has no information. Therefore, the research gap was identified after reviewing the previous researches.

2.2 Lightweight Aggregate Concrete

Due to economic and practical considerations, the desirability of LWAC is increasing. The application of LWAC leads to green and sustainable construction with lower cost as the reduction of dead load results in the savings on reinforcement, formwork and scaffolding (Yap, et al., 2013). In fact, LWAC is not a new discovery of this decade; it has been used in building construction since ancient times. In the old days, natural aggregates of volcanic origin such as pumice, scoria, etc were used. Babylon built in the 3rd

millennium BC (before Christ) by Sumerians, St. Sofia Cathedral in Istanbul constructed in the 4th century AD (anno domini), Pantheon, Pont du Gard and Colosseum erected by the Romans in between the years of AD 14 to AD 128 are examples for the application of LWAC in ancient building construction (Chandra & Berntsson, 2002).

In fact, lightweight aggregate can be originated from natural resources or can be human made. Natural aggregates are mostly from volcanic origin and organic agricultural waste. For example, pumice, scoria, volcanic cinders, diatomite, OPS, coconut shell, corn cob, rice husk and etc (Chandra & Berntsson, 2002) (Shafigh, et al., 2014). Man-made aggregates are manufactured by thermal treatment. They include perlite, vermiculite, clay, shale, slate, fly ash, expanded clay and etc (Chandra & Berntsson, 2002) (Aslam, et al., 2016).

However, depletion of natural resource is arising with the inflating demand. Therefore, locally available and renewable agricultural waste OPS is a potential substituent for other depletable natural aggregates from volcanic origin.

2.3 Oil Palm Shell (OPS)

The tropical weather in Malaysia favours the plantation of palm oil trees, which makes Malaysia a major producer of palm oil. In 2018, Malaysia remained as the second major exporter of palm oil with approximately 20

million tonnes, which represented 27.7% of the global palm oil trade (Ling, 2019). The breakdown of palm oil exports by each country is illustrated in Figure 2.1. However, sustainability of the development of palm oil industry is always a concern. The biomass wastes generated from this sector had been accounted for 85.5% of the total production of biomass in Malaysia (Phang & Lau, 2017). The disposal of these wastes has become a major problem. In a fresh fruit bunch (FFB) of palm oil, OPS occupies 6.4% which is one of the wastes generated from the manufacturing of palm oil (Hambali & Rivai, 2017). According to Malaysian Palm Oil Board, the total production of FFB in 2018 is 98.42 million tonnes. At the same time, approximately 6.30 million tonnes of OPS waste are produced (Malaysian Palm Oil Board, 2018a). Hence, replacing OPS as coarse aggregate in concrete can help in relieving the solid waste disposal problem of palm oil industry. The development of LWAC with OPS as coarse aggregate had been initiated since 1984 in Malaysia (Abang, et al., 1984).

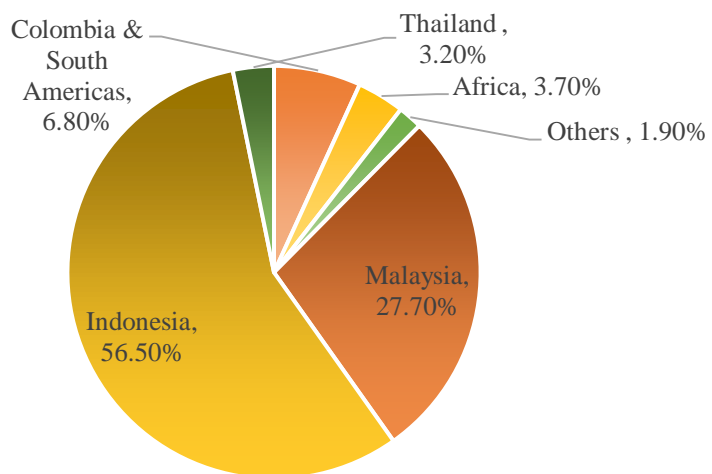





Figure 2.1: World Palm Oil Production by Country in 2018 (Ling, 2019)

The species of palm tree *Elaeis guineensis* Jacq was taken to Malaysia from Eastern Nigeria in 1961. There are three different species of palm oil fruits, namely *dura*, *tenera* and *pisifera*. *Dura* is a homozygous dominant with thick shells; while *pisifera* is a homozygous recessive without shells. *Tenera* is the cross-pollination of thick shelled *dura* and shell-less *pisifera*, which results in having shells with intermediate thickness. The specifications of each species are shown in Table 2.1. The shell thickness affects the mechanical properties of the OPSLWC (Yew, et al., 2014). In this research, the shell of *dura* and *tenera* were used as the coarse aggregate.

Table 2.1: Species of Oil Palm Fruits (Singh, et al., 2013)

	Species	Shell Thickness
	<i>dura</i>	2 mm – 5 mm
	<i>tenera</i>	1 mm – 2.5 mm
	<i>pisifera</i>	0 mm

In Malaysia, palm oil processing is separated into six stages: sterilisation, threshing, pressing, depericarping, separation of kernel and shell and clarification (Abdullah, 1996). Shells are the solid end-products of oil palm manufacturing process. The original shells have smooth surface on the outer convex side. The crushed shells are irregular in shape, it can be flaky,

polygonal, angular or circular depending on the breaking pattern of the nut as shown in Figure 2.2.



Figure 2.2: Crushed OPS of Different Shapes

2.3.1 Specification of OPS

The specific gravity of OPS is in the range of 1.17 to 1.37 and the bulk density is in between 510 to 600 kg/m³ (Shafigh, et al., 2014). Due to its lightweight properties, the density of OPS concrete is 20-25% lower than normal concrete (Shafigh, et al., 2010). From previous researches, the compressive strength of OPSSLWC with and without the addition of cementitious materials fell in the range of 20-35 MPa, which satisfied the specification of structural lightweight concrete (Shafigh, et al., 2014). However, the mechanical properties (splitting tensile strength, flexural strength and modulus of elasticity) of OPSSLWC are generally lower than other LWAC at the same compressive strength (Shafigh, et al., 2014). On the other hand, the thermal conductivity of OPS falls in the

range between 0.137-0.19 W/m°C (Okpala, 1990) (Serri, et al., 2014). The low thermal conductivity of OPS makes it a potential building material for energy efficiency building. Serri, et al. (2014) found that the lowest thermal conductivity of OPSLWC is 0.53 W/m°C. This fulfils the requirement of RILEM which states that thermal conductivity should be lower than 0.75 W/m°C for semi structured with thermal insulation characteristic (Newman & Owens, 2003).

2.3.2 Application of OPSLWC in Malaysia

Researches of investigating the structural performance of OPSLWC were initiated in Malaysia since 2001. A 125 mm thick with 3.1 m span length of floor slab constructed by OPS concrete reinforced with 10 mm diameter high yield steel was tested for a live load of 1.5 kN/m². The first crack was observed at a load of 8.25 kN/m² with a deflection of only 9.56 mm, which is lower than the allowable deflection of 12.4 mm (Mannan & Ganapathy, 2004). A footbridge of 125 mm thick and 2.0 m span constructed in May 2001 showed good performance when subjected to two-wheeler traffic (Teo, et al., 2007). Furthermore, a 58.68 m² area of model low-cost house was constructed in 2003 using 'OPS hollow blocks' for walls and 'OPS concrete' for footings, lintels and beams showed good structural performance without problem (Teo, et al., 2007). Figure 2.3 and Figure 2.4 illustrates the footbridge and model low-cost house constructed in Sabah respectively.



Figure 2.3: Footbridge Constructed with OPS Concrete (Teo, et al., 2006)



Figure 2.4: Model Low-cost House Built with OPS Concrete (Teo, et al., 2006)

2.4 Fibres

Fibres have been first introduced in construction materials 3500 years ago in the form of horsehair and straw (Brandt, 2008). Fibres are made up of various materials, which are suitable for concrete applications. Different types of fibres have been used in the production of fibre-reinforced concrete (FRC)

according to different application. The timeline for the evolution of FRC can be summarised as below (Nemati, 2015):

BC	Horsehair
1900	Asbestos fibres (Hatschek process)
1920	Griffith's theory of comparing theoretical and apparent strength
1950	Scientific concepts of composite materials developed
1960	Fibre-reinforced concrete
1970	New approach for asbestos cement replacement
1970	Introduction of steel fibres reinforced concrete (SFRC), glass fibres reinforced concrete (GFRC), polypropylene fibres reinforced concrete (PPFRC) and fibre shotcrete
1990	Development of micromechanics, hybrid systems, wood-based fibre systems manufacturing techniques, secondary reinforcement, high strength concrete ductility issues, shrinkage crack control
2000+	Introduction to structural applications, code integration and new products

Generally, fibres are categorised into synthetic fibres, steel fibres, glass fibres and natural or organic fibres (Bothma, 2013). For structural concrete, the basic groups of fibres are categorised by their material. They are steel fibres (different shapes and dimensions), glass fibres (only used as alkali-resistant (AR) fibres in cement matrices) and synthetic fibres (made from polypropylene, polyethylene and polyolefin, polyvinyl alcohol (PVA), etc.)

(Brandt, 2008). Table 2.2 summarises the basic material properties of some of the fibres from every category.

Table 2.2: Basic Properties of Various Fibres Type (Shah & Rangan, 1971) (Zollo, 1997)

Materials	Specific gravity	Tensile strength (MPa)	Elastic Modulus (GPa)
Acrylic	1.16-1.18	296-1000	14-19
Aramid I	1.44	2930	62
Aramid II	1.44	2344	117
Carbon I	1.9	1724	380
Carbon II	1.9	2620	230
Nylon	1.14	965	5
Polyester	1.34-1.39	228-1103	17
Polyethylene	0.92-0.96	76-586	5-117
Polypropylene	0.9-0.91	138-690	3.0-5.0
Alkali-resistant	2.7-2.74	2448-2482	79-80
Non-Alkali-resistant	2.46-2.54	3103-3447	65-72
Coconut	1.12-1.15	120-200	19-26
Sisal	-	276-568	13-26
Bagasse	1.2-1.3	184-290	15-19
Steel	7.8	1000-3000	200
Glass	2.6	2000-4000	80

To show effective improvement on the performance of mortars and concrete as reinforcement, the fibres must be easily dispersed in the mixture, equipped with adequate mechanical properties and durable in highly alkaline cement matrix (Silva, et al., 2005). The bonding between the fibres and the cement matrices is important for the transfer of tensile stresses across the concrete. Stiffness and the modulus of elasticity is essential for limiting cracking (Richardson, 2003).

2.4.1 Characteristics of Fibres

The geometrical properties and aspect ratio of fibres were reviewed in this section.

2.4.1.1 Geometrical Properties

The positive effects of inclusion of fibres in concrete are not only depend on the material properties of the fibres, but geometrical properties also play an influential role. Geometrical properties consist of the shape, longitudinal profile and dimensional properties (length, diameter and cross-sectional). Different geometrical profiles of steel fibres are illustrated in Figure 2.5.

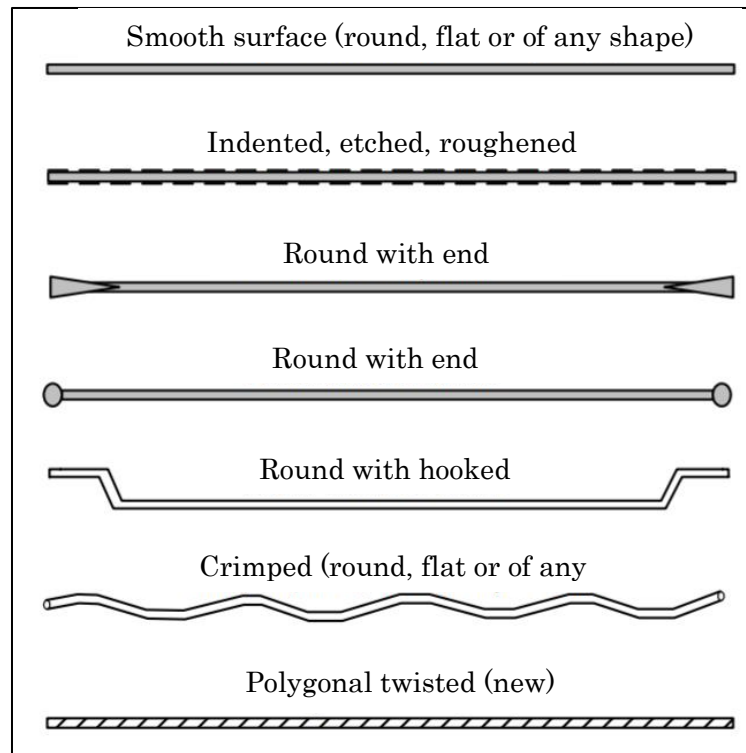


Figure 2.5: Typical Profiles of Steel Fibres Commonly Used in Concrete (Naaman, 2003)

The bond strength between fibres and cement matrices are provided by adhesion and friction. Additional mechanical bond is created by modifying the fibres into different geometries like crimped, indented, button ends, hooked and polygonal twisted as shown in Figure 2.5 (Naaman, 2003). The purpose of different geometrical forms is to enhance the fibre-matrix bond, promote interlocking, prevent bundling of fibres during blending and ensure the fibres are dispersed thoroughly in the concrete mix (Bothma, 2013). The bond in deformed fibres is much stronger than that of smooth fibres as experimented in the extensive pull-out tests (Sujivorakul & Naaman, 2003).

There are generally two categories of fibres according to dimensions, macro and micro fibres. Macro fibres have lengths between 19 mm and 60 mm, which are also known as structural fibres (Concrete Society, 2007a). Macro fibres are expected to arrest cracks and offer structural support to the concrete during hardened state upon their reinforcement (Won, et al., 2009). Micro fibres act as resistance to tensile forces developed by drying and plastic shrinkage. Micro fibre is classified by length of between 2 mm and 10 mm and nominal diameter of 0.1 mm to 1 mm (Concrete Society, 2007a). The inclusion of micro fibres aids in the enhancement of tensile and flexural strength of concrete during the fresh and early age (Pelisser, et al., 2010).

Moreover, British Standards (2006) separates polymer fibres into two different classes, which are as tabulated in Table 2.3. Class II fibres are effective in the enhancement of ductility, where they are usually used when an increase in post-crack flexural strength is needed (Concrete Society, 2007b).

The influences of fibres given vary with the length of fibres. Micro fibres control the opening and propagation of micro cracks; meanwhile fibres with length up to 50 mm or 80 mm restrain larger cracks and increase the final strength of fibres reinforced concrete (FRC) (Brandt, 2008). The mechanism of the cracking control and the influences on stress-strain relation are illustrated in Figure 2.6 and Figure 2.7.

Synthetic fibres have similar shapes as steel fibres with macro fibres are normally in the straight and crimped forms; while micro fibres for the both types are usually in short straight forms. Polypropylene is the most commonly used synthetic fibres for concrete due to their low specific gravity and relative cheaper in price (Manolis, et al., 1997) (Yap, et al., 2013),.

Table 2.3: Classifications of Fibres Made from Polymeric Materials (British Standards Institution, 2006)

Class	Name	Diameter (mm)	Remarks
Class I	Micro fibres	a) < 0.3	a) Monofilament
- Class Ia		b) < 0.3	b) Fibrillated
- Class Ib			
Class II	Macro fibres	> 0.3	

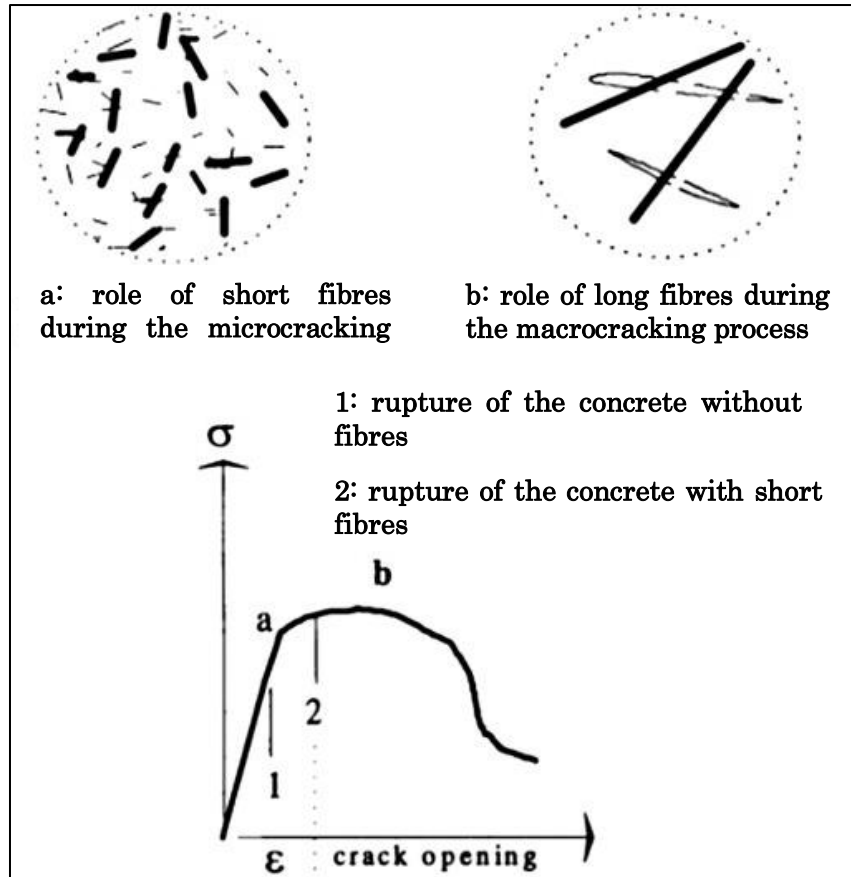


Figure 2.6: Illustration of the Role of Fibres during Cracking (Rossi, 1982)

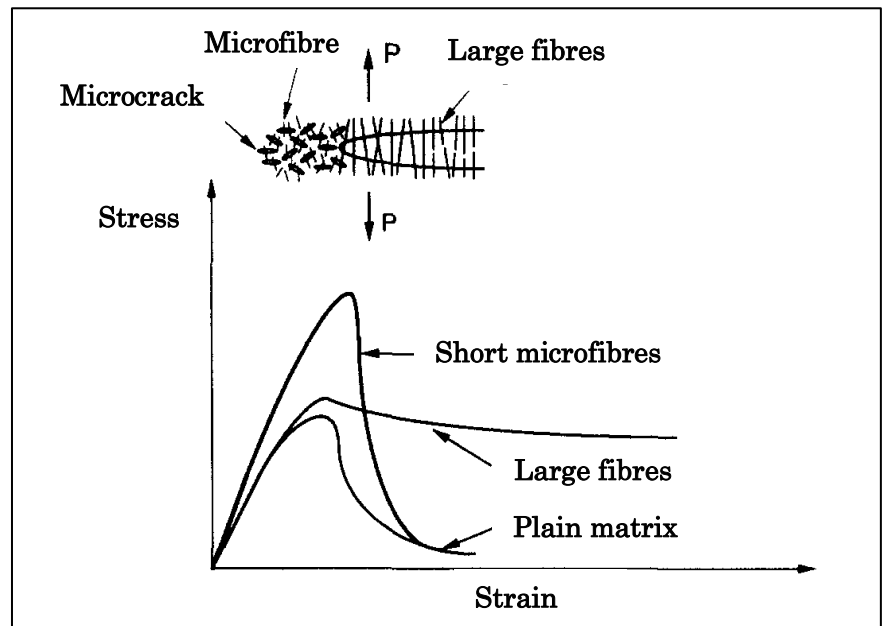


Figure 2.7: Mechanism of the Cracking Control by Large and Micro Fibres and the Effects on Stress-Strain Relation (Betterman, et al., 1995)

2.4.1.2 Aspect Ratio

Aspect ratio is defined as the ratio of fibre length to the diameter or equivalent diameter of the fibre. It can be explained in Equation 2.1.

$$a = \frac{l}{d_f} \quad (2.1)$$

where a = aspect ratio

l = length of fibre

d_f = Equivalent diameter of fibre

The aspect ratio of steel fibres with a round cross-sectional shape is usually in the range of 40 to 80, which is not more than 100 (Kim, et al., 2008). In other words, they have diameter of 0.4 mm to 0.8 mm and length of 25 mm to 60 mm. In concrete applications, the aspect ratio of very fine fibres is more than 100; however, it is less than 100 for courser fibres (Naaman, 2003).

2.4.1.3 Volume Fraction

Incorporation of fibre content in concrete mix is specified by the volume fraction (V_f) of the total composite. The range of volume fraction of fibres varies with the types of concrete of their application. Table 2.4 shows some example of the classification of different types of fibres and their volume fraction according to their application.

The same volume fraction of fibres with different densities will lead to different weight fraction of fibres. Therefore, precautions should be taken during addition of fibres as the volume fraction is the affecting parameter on the mechanical properties of the composites instead of the weight fraction.

Table 2.4: Volume Fractions of Fibres in Concrete Composites (Naaman, 2003)

Material	Range of Volume Fraction (V_f)
Fibre Reinforced Concrete (FRC)	$V_f \leq 2\%$
High Performance Fibre Reinforced Cement Composites (HPFRCC)	$V_f \geq (V_f)_{critical}$ $V_f \geq 1\%$
Shotcrete (steel fibre)	$V_f \leq 3\%$

2.4.2 Polypropylene Fibres

Polypropylene fibres (PP fibres) are one of the most common synthetic fibres used extensively in the construction industry today. They are manufactured from homopolymer polypropylene resin. Chemically, they are derived from organic polymer made up of a long chain of propene monomer. The chemical formula of propene monomer is expressed as $(C_3H_6)_n$.

Polypropylene fibres were first introduced in 1965 by Goldfein as reinforcement to concrete in the construction of blast-resistant buildings for the U.S. Corps of Engineers (Madhavi, et al., 2014). The advantages of polypropylene fibres include high alkaline resistance, lightweight and low-cost favour their usage in the industry. The micro-structure of polypropylene is in the arrangement that favours crystallisation gives its high chemical resistance

and heat stability (Bothma, 2013). The hydrophobic nature of polypropylene fibres does not affect the amount of water needed for concrete. The bonding between propylene fibres and cement matrices is mechanically instead of chemically. The properties of polypropylene fibres are tabulated in Table 2.5.

Table 2.5: Properties of Polypropylene Fibres (ACI Committee 544, 2002)

Property	Details
Specific Gravity	0.90-0.91
Tensile Strength (MPa)	138-690
Elastic Modulus (GPa)	3.45-4.83
Ultimate Elongation (%)	15
Ignition Temperature (°C)	593
Melt, Oxidation or Decomposition Temperature (°C)	165
Water Absorption (ASTM D 570)	Nil

2.4.3 Fibres Hybridisation

The properties of concrete and fibres are the key aspects that affect the performance of FRC. The influential fibres properties include fibre concentration, fibre geometry, fibre orientation and fibre distribution. However, the addition of single type of fibre has its limitation in enhancing the properties of FRC. Hence, the idea of adding two or more different types of fibres into concrete, which is also known as hybridisation, can offer better engineering properties as the presence of one fibre acts as an enhancer for the potential properties of the other fibres (Sahmaran, et al., 2005).

The combination of different kinds, types and sizes of fibres can optimise the mechanical and conductivity properties. The hybrid fibres

systems of Polypropylene fibres and steel fibres offer attractive advantages (Qian & Stroeven, 2000).

1. To provide a hybrid system, which consists of one type of stronger and stiffer fibre as to enhance the stress capacity for first cracking and the ultimate strength of the composite; while another type of fibre, which is more flexible and ductile and leads to improved toughness and strain capacity in the post-cracking zone.
2. To offer hybrid reinforcement of one type of smaller fibres for the bridging of micro-cracks to increase the tension capacity of the composite; while another type of larger fibres for resisting the propagation of macro-cracks and substantially enhancing the toughness of the composite.
3. To give a combined reinforcement of fibres with different durability. The durable fibres are more effective in strength enhancement and toughness retention after age; while another type is to ensure the temporary performance during transportation and installation of the composite elements.

“Synergy” is the term to describe the phenomena when the resulting hybrid performance of well-designed hybrid composites is better than the sum of individual fibre performances as there is positive interaction between the fibres. Some recognised examples of fibres combinations that may offer “Synergy” (Xu, et al., 1998):

1. Hybrids Based on Fibre Constitutive Response:

Adequate first crack strength and ultimate strength is offered by the presence of the stronger and stiffer type of fibres; while another type of fibres, which is relatively flexible, has positive effects on the toughness and the capacity of strain in the post-crack zone. These two types of fibres have significant difference in modulus of elasticity. Ideally, the load they carry is commensurate to the value of strain which the material is subjected to.

2. Hybrids Based on Fibre Dimensions:

The smaller fibres give bridging effect to hold micro-cracks and hence control their growth and delay coalescence. As a result, the composite has higher tensile strength. The second larger fibres intend to resist the propagation of macro-cracks. Therefore, the fracture toughness of the composite is enhanced substantially. This is agreed by Banthia and Shah in 1995 and 1991 respectively (Shah, 1991) (Banthia, et al., 1995)

3. Hybrids Based on Fibre Function:

One type of fibre is intended to enhance the fresh and early age properties such as resistance to plastic shrinkage, while the second fibre leads to the improvement of the hardened/mechanical properties. The hybridisation of these two fibres improves the fresh and hardened properties of the composites simultaneously.

2.4.4 Role of Fibres

The reinforcement of fibres in concrete is expected to improve the mechanical properties of the reinforced concrete. Their inclusion induces the inhibit of cracks propagation, which happens due to the low tensile capacity of concrete. The bridging effects offered by the fibres across the crack and the path followed by the crack can be clearly seen when the specimen is subjected to pure tension. Figure 2.8 shows the mechanisms of the energy absorption and crack controlling of fibres acted upon their reinforcement in concrete. Figure 2.9 illustrates the comparison of crack pattern between normal reinforced concrete (RC) and FRC under tension loading.

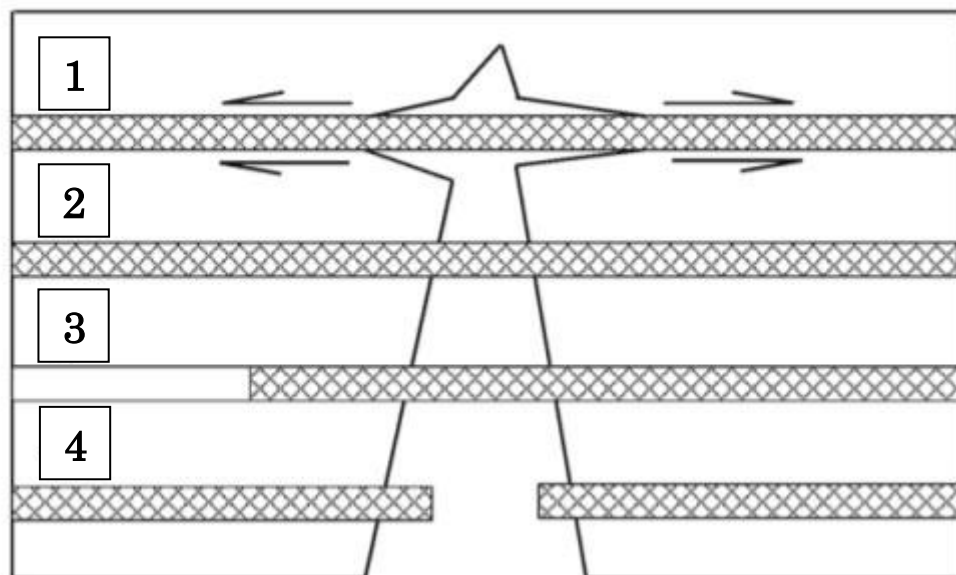


Figure 2.8: Mechanisms of Interactions between Fibres and Cement Matrix: (1) debonding (2) bridging (3) pull-out (4) failure (Abbas & Khan, 2016)

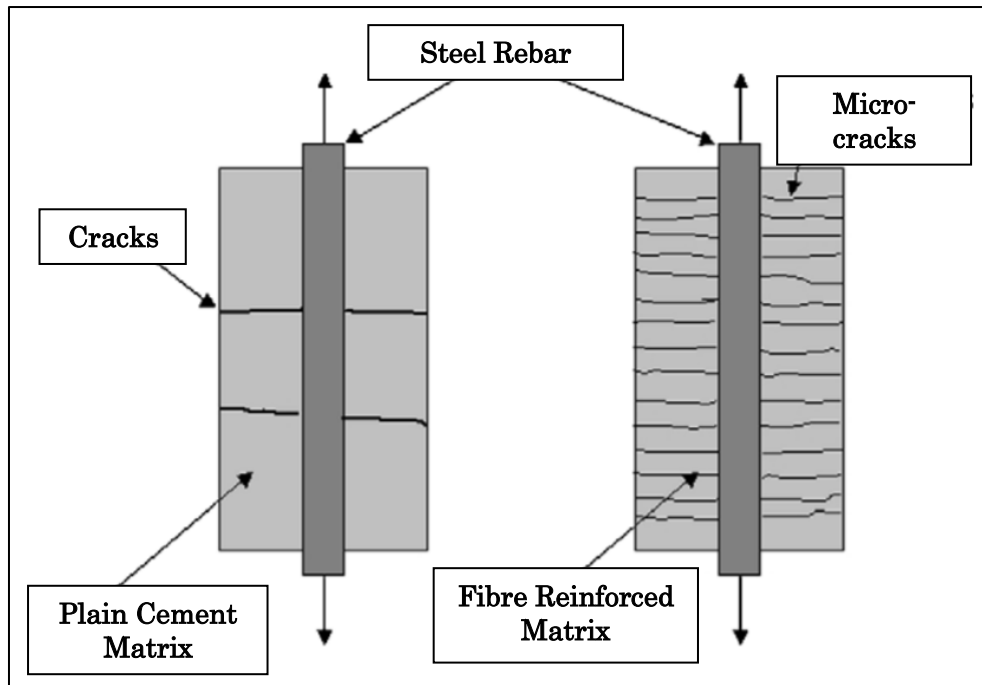


Figure 2.9: Crack Pattern in the Elements of RC and FRC Subjected to Tension Loading (Brandt, 2008)

2.5 Effects of Fibres on OPSLWC

The effects of fibres on the mechanical properties and thermal properties of OPSLWC of the previous researches were discussed in this section.

2.5.1 Compressive Strength

The compressive strength of OPSLWC with and without the addition of cementitious materials fell in the range of 20-35 MPa, which achieved the requirement for structural lightweight concrete (Shafigh, et al., 2014). From previous researches, the possibility of producing high strength OPSLWC with compressive strength of 53 and 56 MPa at 28 and 56-days had been ascertained (Shafigh, et al., 2011a) (Shafigh, et al., 2011b). However, the

mechanical properties of OPSLWC, which include splitting tensile strength and flexural strength, are lower than those of other LWA. Therefore, different types of fibres have been added to OPSLWC to enhance its mechanical properties. Table 2.6 summarises the compressive strength of fibres reinforced OPSLWC of previous researches.

Shafigh, et al. (2011c) and Mo, et al. (2014b) reported that the addition of steel fibres of volume fractions 0.25% to 1% improved the 28-days compressive strength by 6.2% to 37%. Incorporation of different types of polypropylene fibres of volume fractions 0.125% to 0.75% enhanced the compressive strength by 1.81% to 10.8% at 28-days (Yap, et al., 2013) (Yew, et al., 2015a) (Yew, et al., 2015c) (Yew, et al., 2018). Yew, et al. (2015a & 2018) reported that the addition of polyvinyl alcohol (PVA) fibres in the amount of 0.15% to 0.5% of volume fractions offered an increment in 28-days compressive strength up to 13.1%. Hybrid of polypropylene-steel fibres with appropriate volume fractions increased the 28-days compressive capacity up to 35.6% (Mo, et al., 2014a) (Yap, et al., 2014). Moreover, Yew, et al. (2018) demonstrated that hybrid of polypropylene-PVA fibres upgraded 5.69% of the 28 -days compressive strength.

2.5.2 Splitting Tensile Strength

For structural application, the splitting tensile strength of lightweight concrete must be at least 2.0 MPa in accordance to ASTM C330/ C330M-17a. Steel fibres added in volume fractions of 0.25%-1% gave 28-days splitting tensile

strength in the range of 2.49-6.94 MPa (Shafigh, et al., 2011c) (Mo, et al., 2014b). Yap, et al. (2013) and Yew, et al. (2015a & 2015c) reported that the splitting tensile strength of various types of polypropylene fibres with the volume fractions of 0.15%-0.75% was in the range of 2.23-4.12 MPa. In addition, hybrid of steel-polypropylene fibres gave splitting tensile strength of up to 5.81 MPa in a maximum volume fraction of 1% (Yap, et al., 2014). Table 2.6 shows the splitting tensile strength of OPSLWC incorporated with fibres in previous researches.

2.5.3 Flexural Strength

Shafigh, et al. (2011c) & Mo, et al. (2014b) outlined that the modulus of rupture of the addition of steel fibres up to 1% in volume fractions was in the range of 4.73-8.90 MPa. At the same time, incorporation of various polypropylene fibres with the amount of 0.125%-0.75% offered flexural strength of 2.50-7.64 MPa (Yap, et al., 2013) (Yew, et al., 2015a) (Yew, et al., 2015c) (Yew, et al., 2018). The combination of steel-polypropylene fibres with the amount not more than 1% in volume fractions resulted in flexural strength of 3.82-7.49 MPa (Yap, et al., 2014). Table 2.6 presents the modulus of rupture of previous researches of OPSLWC with addition of fibres.

Table 2.6: Mechanical Properties of OPSFRC of Previous Researches

Author (year)	W/C ratio	Mix proportions (Binder: Fine Aggregate: OPS)	Slump (mm)	Compressive Strength (MPa)	Splitting Tensile Strength (MPa)	Flexural strength (MPa)
(Shafigh, et al., 2011c)	0.38	1:1.74:0.72 (ST: 0 - 1% V_f)	45 - 195	39.34 - 44.95	2.83 - 5.55	5.42 - 7.09
(Yap, et al., 2013)	0.30	1:1.83:0.60 (PP1: 0 - 0.75% V_f)	40 - 75	36.3 - 23.9	2.23 - 2.48	2.50 - 3.79
		1:1.83:0.60 (PP2: 0 - 0.75% V_f)	20 - 75	34.8 - 36.0	2.23 - 3.23	2.50 - 4.54
		1:1.83:0.60 (Ny: 0 - 0.75% V_f)	15 - 75	34.8 - 36.8	2.23 - 3.49	2.50 - 4.37
(Yap, et al., 2014)	0.30	1:1.42:0.65 (ST-PP: 0 - 1% V_f)	15 - 75	26.6 - 49.9	2.90 - 5.81	3.82 - 7.49
(Mo, et al., 2014a)	0.30	1:1.42:0.65 (ST-PP: 0 - 1% V_f)	20 - 75	26.8 - 49.4	-	-
(Mo, et al., 2014b)	0.33	1:1.70:0.65 (ST: 0 - 1% V_f)	-	33.51 - 45.96	2.49 - 6.94	4.73 - 8.90
(Yew, et al., 2015a)	0.30	1:1.85:0.63 (PPTB 1: 0.25 - 0.5% V_f)	90 - 160	42.6 - 47.2	3.35 - 4.12	7.05 - 7.64
		1:1.85:0.63 (PPTB 2: 0.25 - 0.5% V_f)	75 - 155	42.2 - 46.8	3.42 - 3.95	6.43 - 7.09
		1:1.85:0.63 (PPS 1: 0.25 - 0.5% V_f)	65 - 150	42.4 - 46.6	3.49 - 3.74	5.75 - 6.52
(Yew, et al., 2015b)	0.29	1:1.74:0.64 (PVA: 0 - 0.5% V_f)	120 - 200	42.89 - 48.51	2.88 - 3.74	4.17 - 5.49
(Yew, et al., 2015c)	0.29	1:1.67:0.64 (PPTB: 0 - 0.5% V_f)	160 - 210	49.7 - 54.6	3.48 - 4.08	5.48 - 6.46
(Mo, et al., 2016)	0.30	1:1.80:0.63 (ST: 0 - 0.6% V_f)	-	28.0 - 38.0	3.00 - 5.80	-
(Yap, et al., 2016)	0.30	1:1.83:1.66 (ST: 0 - 0.75% V_f)	20 - 75	34.8 - 46.6	3.22 - 5.90	4.90 - 7.00
(Mo, et al., 2017b)	0.31	1:1.83:0.69 (ST: 0 - 1% V_f)	-	34.04 - 38.85	3.16 - 6.12	4.24 - 6.18
(Yew, et al., 2018)	0.32	1:1.73:0.74 (PVA: 0 - 0.285% V_f)	35 - 145	39.88 - 40.76	-	4.28 - 4.74
		1:1.73:0.74 (PP: 0 - 0.285% V_f)	25 - 145	39.88 - 38.18	-	4.28 - 4.49
		1:1.73:0.74 (PVA-PP: $V_f = 0.25\% + 0.035\%$)	20	42.15	-	5.17
(Yap, et al., 2019)	0.29	1:1.66:0.55 (ST: 0 - 1% V_f)	20-80	33.9 - 47.3	-	3.26 - 8.16

*Note: ST: steel, PP: polypropylene, Ny: nylon, PPTB: polypropylene twisted bundle, PVA: polyvinyl alcohol

2.5.4 Residual Strength

Residual compressive strength (RCS) is a simplified method to measure the post-failure toughness of the specimens. The specimens are further loaded for second and third time after they fail at first compressive loading to obtain the RCS. The incorporation of fibres is anticipated to improve the post-failure characteristics.

Yap et al. (2013) reported that the inclusion of polypropylene fibres produced about 8-14% higher RCS than OPSLWC without fibres. All FROPSLWC in Yew, et al. (2015a & 2015c) had achieved higher RCS values than the control mix. This indicates that various types of polypropylene fibres can enhance the post-failure properties. However, residual splitting tensile strength of FROPSLWC has not been studied in the previous researches.

2.5.5 Thermal Conductivity

Due to the high porosity of OPS, it is a poor thermal conductor with thermal conductivity of 0.137-0.19 W/m°C (Okpala, 1990) (Serri, et al., 2014). The utilisation of low thermal conductor, OPS as coarse aggregate decreases the overall thermal conductivity of the concrete. Okpala (1990) and Serri, et al. (2014) reported that the thermal conductivity of OPSLWC falls in the range of 0.45 – 1.05 W/m°C based on different mix proportions. However, there is no available information on the thermal conductivity of FROPSLWC.

The effect of fibres on thermal transferability in other types of concrete has been studied in previous researches. Polypropylene fibres have been found to improve the thermal resistance of lightweight foamed concrete (Jhatial, et al., 2018). The effect of different types of fibres (polypropylene, carbon, basalt and glass) on thermal conductivity of autoclaved aerated concrete has been studied (Phelivanli, et al., 2016). Furthermore, acrylic and polypropylene fibres have been discovered to be effective in upgrading the thermal resistance of palm oil fuel ash blended mortar (Mo, et al., 2017b).

2.5.6 Temperature Gradient

The measurement of the temperature gradient of two sides of a specimen, where one side is exposed to a heat source and another side is not, is a simplified method to evaluate the thermal insulation performance. A lab-developed setup as schematically shown in Figure 2.10 has been used to carry out the thermal insulation performance test of thermal insulation coatings (Zhang, et al., 2019).

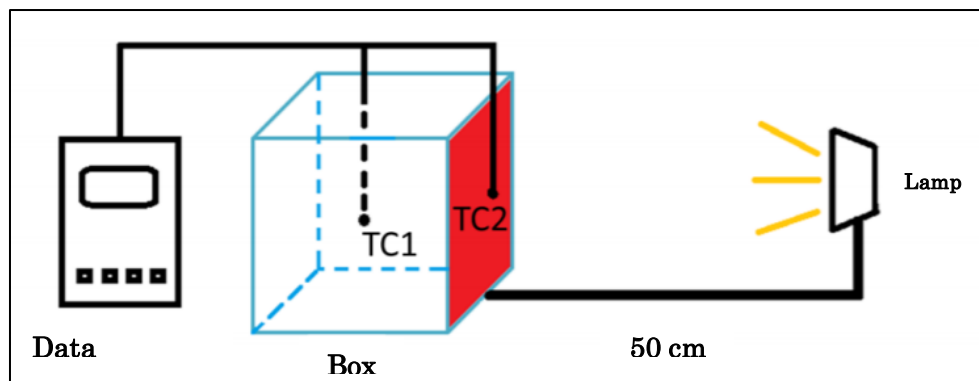


Figure 2.10: Schematic Diagram of the Thermal Insulation Performance Test Equipment (Zhang, et al., 2019)

2.6 Mixing Method

The process of mixing of concrete plays an important role in determining the quality of the final product. Hiremath, et al. (2017) had studied about the effect of mixing configuration on the fresh and hardened attributes of Reactive Powder Concrete. Two different mixing methods were compared, namely three stage mixing method and four stage mixing method. One of the main differences of these two methods is that three stage mixing method involves the blending of all ingredients and water; while the four stage mixing method initially blends the binders with water before adding the aggregates. The mixing stages of these two methods are tabulated in Table 2.7.

Table 2.7: Mixing Stages of Different Mixing Methods (Hiremath & Yaragal, 2017)

Mixing Stages	Three Stage Mixing	Four Stage Mixing
Stage 1	Dry mixing of all raw materials.	Dry mixing of cementitious materials (cement and silica fume)
Stage 2	Addition of 50% volume of water and 50% dosage of superplasticiser	Addition of 80% volume of water and full dosage of superplasticiser
Stage 3	Addition of the remaining water and superplasticiser.	Addition of aggregates (sand and Quartz powder)
Stage 4	-	Addition of the remaining water

A previous research concluded that the method of advance mixing of binders with water before adding aggregates showed 10-20% improvement in strength (Saeed, 1995). At the same time, the four stage mixing method had offered relatively higher flow and strength than that of the three stage mixing method. Hence, the blending of only binders with high percentage of water

and superplasticiser in full dosage enhanced the performance in workability and strength.

2.7 Summary

Utilising OPS as coarse aggregates in concrete had been researched since 1984 in Malaysia. Due to the lower mechanical properties of OPSLWC, the study has extended to the inclusion of different types of fibres, which includes steel fibres, PVA fibres, Nylon fibres and PP fibres to enhance the mechanical performance. The effect of different fibres on the mechanical performance of OPSLWC is one of the popular research interests in previous researches. However, the effect of the incorporation of fibres on the thermal performance of OPSLWC is also an interesting subject to study, which has limited knowledge from previous researches. With the availability of various types of fibres, the effect of some types of fibres has not been investigated before. Hence, the types of fibres which have not been studied before, is a fascinating topic to study. Moreover, the influence of fibres on the post-failure behaviour of OPSLWC is also a topic that is worth to look into.

CHAPTER 3

METHODOLOGY OF RESEARCH

3.1 Introduction

Preparation of materials, specifications of materials, design of mix, mixing procedures and test methods are elaborated in this chapter. The properties of raw materials (oil palm shell (OPS) coarse aggregate, sand, cement, water and superplasticisers) have been defined. The handling of raw materials and the process of mixing must be inspected carefully to minimise any discrepancies caused by human errors. The entire experimental work is segregated into two stages, which are trial mix and actual mix. The trial mix stage is to determine the optimum mix proportion of plain oil palm shell lightweight concrete (OPSLWC) to achieve compressive strength of greater than 25 MPa at 28-days. OPSLWC and fibre-reinforced oil palm shell lightweight concrete (FROPSLWC) with the optimum mix design obtained from trial mix are produced for further testing in the second stage, which is the actual mix stage. All the tests are categorised into three sections, which are fresh, hardened concrete tests and thermal conductivity test. The testing equipment required is also described in this chapter. The workflow of this research is summarised in a flowchart as shown in Figure 3.1.

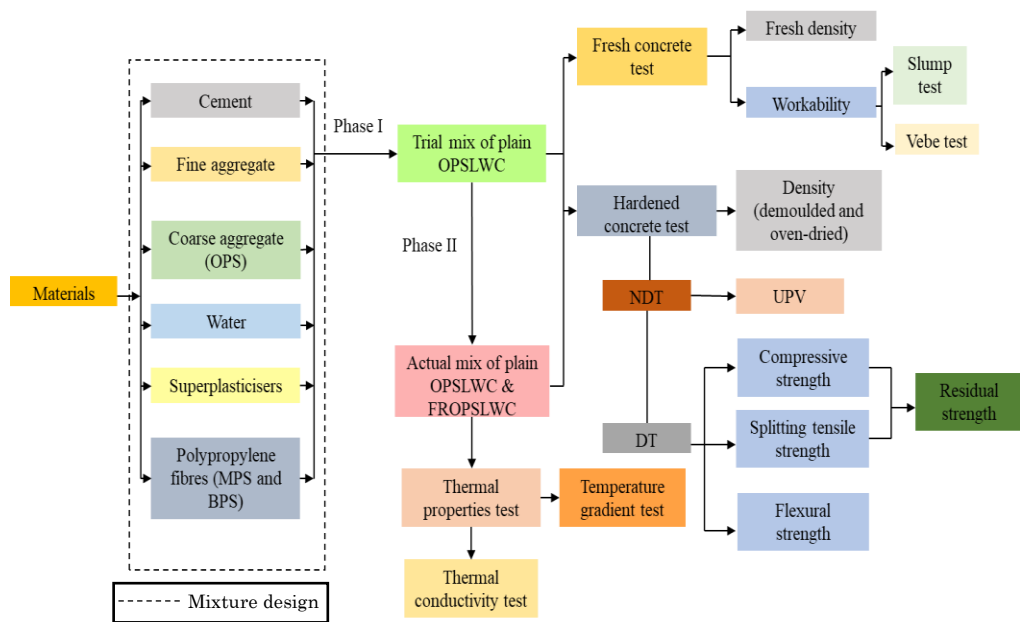


Figure 3.1: Flowchart of the Experimental Program

3.2 Materials

The specifications of the raw materials used in this study are described in this section. They include cement, OPS coarse aggregate, fine aggregate, water, superplasticiser and synthetic polypropylene (PP) fibres.

3.2.1 Cement

All the cement used in this study was Ordinary Portland Cement (OPC) branded “Cap Buaya”, which was manufactured by Tasek Corporation Berhad. For the assurance of the cement quality, the production of Tasek’s cement is in accordance to MS EN 197-2 (2007). To prevent the cement from contacting with the water vapour in the air, it was stored in air tight containers.

As the pre-hydrated cement prior usage will affect the quality of the final product. The typical specifications of OPC are shown in Table 3.1. The typical breakdown of the main compounds of OPC calculated by Bogue's equation in percentage is presented in Table 3.2.

Table 3.1: Specifications of OPC (Tasek Corporation Berhad, 2019)

Compositions and properties of cement	OPC
SiO ₂ (% by wt)	21.28
CaO (% by wt)	64.64
Al ₂ O ₃ (% by wt)	5.60
Fe ₂ O ₃ (% by wt)	3.36
MgO (% by wt)	2.06
SO ₃ (% by wt)	2.14
Total Alkalis	0.05
Insoluble Residue	0.22
Loss on Ignition	0.64
Specific gravity (g/cm ³)	3.14
Blaine's Specific Surface Area (cm ² /g)	3510
Modulus	
Lime Saturation Factor	0.92
Silica Modulus	2.38

**Table 3.2: Main Compounds of OPC (Neville & Brooks, 2010)
(Tasek Corporation Berhad, 2019)**

Compound	Symbol	Abbreviation	Composition
Tricalcium Silicate	3CaO.SiO ₂	C ₃ S	52.8%
Dicalcium Silicate	2CaO.SiO ₂	C ₂ S	21.2%
Tricalcium Aluminate	3CaO.Al ₂ O ₃	C ₃ A	9.2%
Tetracalcium Aluminoferrite	4CaO.Al ₂ O ₃ .Fe ₂ O ₃	C ₄ AF	10.2%

3.2.2 Fine Aggregates

Local mining sand was used as fine aggregates throughout this research. The sand was sieved through 4.75 mm sieve and was dried in the open air to achieve saturated surface dry (SSD) condition. The sieved sand was stored in covered plastic containers in shaded and sheltered area. The specific gravity of the sand is ranged from 2.5 -2.7 and the fineness modulus is 2.75 obtained from sieve analysis.

3.2.3 OPS Coarse Aggregates

Crushed OPS was used to substitute conventional coarse aggregates in this research. OPS was sieved through 10 mm sieve to segregate and remove those of size greater than 10 mm. Before mixing, OPS were immersed in the water for 24 hours. Owing to the high-water retention property, OPS were dried in air for approximately 3 hours to achieve SSD state after removal from water as to prevent the addition or reduction of free water to the mix. The specifications of OPS are presented in Table 3.3. Crushed OPS coarse aggregates are shown in Figure 3.2.

Table 3.3: Specifications of OPS

Attributes	OPS
Maximum size (mm)	10
Specific gravity (SSD state)	1.30
Aggregate impact value (%)	2.33
Compacted bulk density (kg/m ³)	632
Water absorption (%)	2.34

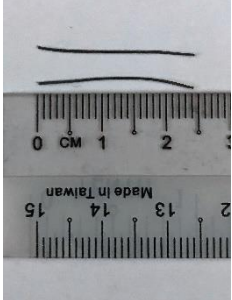
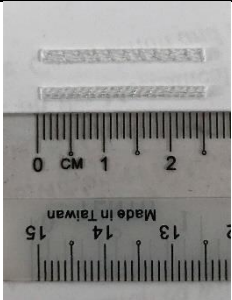


Figure 3.2: Crushed OPS Coarse Aggregates

3.2.4 Polypropylene (PP) Fibres

PP is derived from monomeric hydrocarbon C_3H_6 . PP has low specific gravity of 0.91, which favours to be included into lightweight concrete. PP has good mechanical properties with tensile strength of 600 MPa and Young's Modulus of 4.11 GPa. The mode of polymerisation gives PP a sterically regular atomic arrangement, which results for its chemical inertness. Hence, it can be added into highly alkaline matrix without any adverse effects on its properties. PP is also a good thermal insulator, which has a low thermal conductivity of 0.1-0.22 W/mK. The melting point of PP is approximately 165°C. In this research, two different types of PP fibres (Monofilament polypropylene straight - MPS, Barchip polypropylene straight - BPS) were introduced into OPSLWC. In accordance to ASTM C1609/C1609M – 10 (2010), the maximum fibre length shall be 1/3 of the width and depth of the test specimens. The properties of these PP fibres are presented in Table 3.4.

Table 3.4: Specifications of PP Fibres

Fibres	Fibre type	Length (mm)	Diameter (mm)	Aspect ratio
	Monofilament polypropylene straight (MPS)	25	0.5	50
	Barchip polypropylene straight (BPS)	25	1.5	17

3.2.5 Water

Potable water from the water tap supplied by Syarikat Bekalan Air Selangor Sdn. Bhd. (SYABAS) was used as mixing water and curing water for this research. The water was utilised at room temperature, which ranged from 27-29°C for both mixing and curing process. Excessive impurities in the mixing water can adversely affect the hydration of cement and the properties of fresh and hardened concrete. The specific gravity of the mixing water was taken to be 1.0 g/cm³.

3.2.6 Superplasticiser

MasterGlenium SKY 8808, manufactured by BASF, was the high-performance superplasticiser used in this study. The addition of

superplasticiser can reduce the water to cement ratio without the compensation of workability to enhance the concrete strength. From the manufacturer's data sheet, the standard recommended dosage of this water reducer is 1.5% of the binder weight.

3.3 Mix Design

Mix design is the process of determining the correct proportion of each ingredient to achieve the minimum properties mechanically and economically with an adequate uniformity. The plain OPSLWC was designed to achieve targeted compressive strength of greater than 25 MPa at 28-days. Superplasticiser was added in small amount to enhance the workability without increasing the water to cement ratio.

3.3.1 Absolute Volume Method

Absolute volume is defined as the actual volume of solid matters in the particles, excluding spaces between particles. Hence, the volume of concrete is equal to the total absolute volumes of all the concrete constituents, which include cement, fine aggregates, OPS, superplasticiser, water and air. The absolute volume of each constituent is calculated from the mass of a material and its specific gravity. It can be expressed in the following equation:

$$\text{Absolute volume} = \frac{\text{Mass of loose material}}{SG \times \text{Density of water}} \quad (3.1)$$

3.3.1.1 Sample Calculation of the Mix

The sample calculation of the absolute volumes of all the constituents in the designed mix is demonstrated in Table 3.5.

Table 3.5: Sample Calculation of Absolute Volume Method

Material	kg/m³	SG	Absolute volume
Cement	515	3.15	$\frac{515}{3.15 \times 1000} = 0.163$
Fine Aggregates	1000	2.63	$\frac{1000}{2.63 \times 1000} = 0.380$
OPS	290	1.22	$\frac{290}{1.22 \times 1000} = 0.238$
Water	170	1.00	$\frac{170}{1.00 \times 1000} = 0.170$
Superplasticiser	10.3	1.00	$\frac{10.3}{1.00 \times 1000} = 0.010$
Air content (%)	4.5		$\frac{4.5}{100} = 0.045$
		Total	1.01 \approx 1.00

3.3.1.2 Sample Calculation of the Fibre Volume

The mass of fibres incorporated into the concrete is calculated according to their volume fraction to the volume of concrete. The computation is demonstrated in Equation 3.2. The sample calculation is shown in Table 3.6.

$$\text{Mass of Fibre} = V_f \times SG \times \text{Density of water} \quad (3.2)$$

where,

V_f = volume fraction of fibre (%)

SG = specific gravity of the fibres

Table 3.6: Sample Calculation of the Mass of PP Fibres

Material	V_f (%)	SG	Mass (kg/m ³)
PP fibres	0.3	0.91	$\frac{0.3}{100} \times 0.91 \times 1000 = 2.73$

3.4 Mixing Method

Mixing method is an influential factor to the quality of concrete produced. In this study, two different mixing methods were implemented. At the same time, their outcomes were compared to identify the best option. At first, OPSLWC was produced with conventional mixing method (CMM), which comprises of dry and wet mix. However, inconsistency in the workability of OPSLWC was observed. Eventually, a new mixing method (NMM) was proposed to counter the problem.

3.4.1 Conventional Mixing Method (CMM)

This method was separated into two stages, which were dry mix and wet mix. Dry mix is the mixing process without the presence of water; it is vice-versa for wet mix. Firstly, cement and fine aggregates were poured into the mixing

bowl and were blended for 1 min. Then, OPS were added and were mixed for another 1 min. The total mixing time for dry mix was 2 mins. Superplasticiser was pre-mixed with 70% of the mixing water before being added into the dry mix. Then, the blending continued for 3 mins before adding the remaining 30% of mixing water. Before the concrete was ready to be placed, it was blended for another 2 mins. Hence, the blending time for wet mix was 5 mins. In overall, the total mixing time was 7 mins. The whole process is summarised in Figure 3.3.

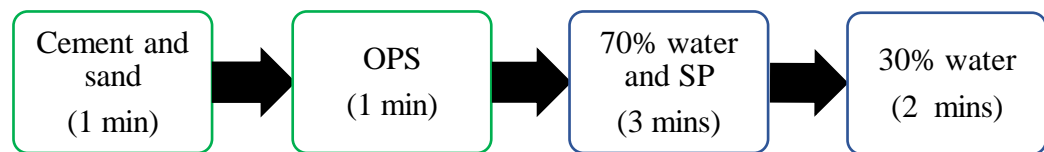


Figure 3.3: Flowchart of the Conventional Mixing Method (CMM)

3.4.2 New Mixing Method (NMM)

This method was developed by modifying a mixing method of a previous research of Hiremath & Yaragal (2017), which involves the initial blending of binders with water before the addition of other solid constituents. This technique of mixing was also referred to one of the mix design methods of self-compacting concrete (SCC), which consists of two phases, the liquid phase (paste) and the solid phase (coarse and fine aggregates) (Shi, et al., 2015). SCC is a type of special highly workable concrete, which can consolidate by self-weight without external vibration and has enough cohesiveness to be handled without bleeding or segregation. Initially, cement

was placed into the mixing bowl and 70% of the mixing water pre-mixed with water reducer was added. The slurry was blended for 1 min. After that, both OPS and fine aggregates were added and mixed for 3 mins. The last step was to add the remaining water and blended for another 2 mins. The total blending time was 6 mins, 1 min for liquid phase and 5 mins for solid phase. The entire process is illustrated comprehensively in Figure 3.4.

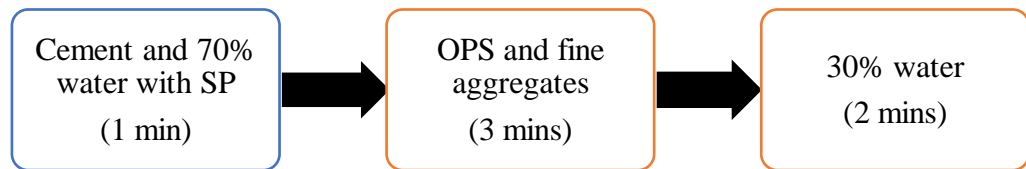


Figure 3.4: Flowchart of the New Mixing Method (NMM)

3.5 Water Curing

Curing method is an influential factor to the growth of concrete strength resulted from the hydration process of cement paste. In this research, water curing method was used to provide continuous hydration process. After demoulding, the concrete samples were measured for their demoulded densities and were labelled accordingly. Then, they were put into water tank for water curing until their desired testing age. Clean tap water from the municipal water supply was used as the curing water at room temperature (approximately 26 – 29°C). The water tank was placed under trees for shade from direct sunlight to maintain its ambient temperature. Figure 3.5 shows specimens in the water tank for water curing.



Figure 3.5: Specimens in the Water Tank for curing

Prior testing, the samples were removed from curing tank and were then placed into oven at temperature of 100 – 110°C for 24 hours (with 2 hours tolerance) to eliminate the moisture content and to achieve oven-dried condition. The oven-dried densities were measured and recorded. After 1- 2 hours of cooling down, the dimensions of the samples were measured to avoid discrepancies caused by thermal expansion.

3.6 Fresh Concrete Tests

Fresh concrete tests were carried out to identify the fresh properties of plain OPSLWC and FROPSLWC. Slump test and Vebe test were conducted to

measure the workability of concrete. The fresh density was obtained by using a digital balance.

3.6.1 Fresh Density of Concrete

The fresh density of concrete is measured by digital balance and a standard container with known volume and mass as referred to BS EN: 12390 - Part 7 (2009). Fresh concrete was put into the standard container. Before weighing, the fresh concrete was well compacted and excessive concrete was cleaned from the top and sides of the container. Figure 3.6 shows the measurement of fresh density. The density of fresh concrete is expressed as in Equation 3.3.

$$\rho = \frac{m}{V} \quad (3.3)$$

where,

ρ = density of fresh concrete, kg/m³

m = mass of fresh concrete, kg

V = volume of container, m³



Figure 3.6: Measurement of Fresh Density

3.6.2 Slump Test

Slump test is suitable in measuring the flow property of concrete with medium to high workability. However, it cannot be used in determining the flowability of concrete with low workability. It is very easy, fast and cost effective to conduct on site. It is a commonly used in construction sites to ensure the quality of concrete before placing. In this research, the test was carried out in accordance to BS EN: 12350 - Part 2 (2009).

The test must be carried out in a smooth, horizontal, rigid and non-absorbent surface. A flat steel plate was used as the base for testing in this study. A cone mould with bottom diameter of 200 mm and with height of 300 mm and a tamping rod of 600 mm long are required for this test. Before starting the test, the steel plate and the internal surface of the mould were

cleaned and damped adequately. The steel plate was placed on a smooth and flat ground. Then, the cone was held tightly to the steel plate base while filling up in three equal layers where each layer was compacted with 25 strokes of the tamping rod. The surplus concrete was struck off from the top of the mould before it was raised up cautiously in vertical direction and the concrete could slump by its own weight. The slump was measured by using ruler with the overturned cone and the tamping rod as a guide. The slump was measured to the highest point of the concrete as shown in Figure 3.7.



Figure 3.7: Measurement of Slump Value.

3.6.3 Vebe Test

Vebe test is applicable for the measurement of flowability of stiff, dry mixes (less than 20 mm slump or zero slump), especially for fibre-reinforced

concrete (FRC). It shows greater relation with concrete placing conditions as compared to slump. However, it is more complex as it requires standard vibrating equipment and the identification of the end-point is difficult. The workability is defined by the Vebe time, which is the time at constant vibration to achieve full compaction. Full compaction is when the concrete shape is compressed from a frustum cone to a cylinder. The Vebe time is recorded up to the nearest 0.5 s. The test is greatly influenced by the consistency, flow and compactable changes of the concrete.

The procedures of this test are described in BS EN: 12350 - Part 3 (2009). A standard set of Vebe test apparatus is equipped with a container on a standard vibrating table, a slump cone mould, a clear plastic disc connected to a moving vertical rod, a funnel and a tamping rod of 600 mm long and 16 mm diameter. Firstly, the slump cone was held firmly on the container with the funnel while the concrete was added into it in three equal layers. Tamping rod was used to compact each layer with 25 strokes in a way of gravity falling to remove air bubbles. Extra concrete was removed from the top of the mould just as in slump test. Before lifting the slump mould, any concrete leaked from gaps between the mould and the container or fell from the top was cleaned. Then, the mould was removed just as in slump test and the clear plastic disc was placed on the top surface of slumped concrete without disturbing it. Next, the vibration table was switched on and the concrete was vibrated at constant amplitude and frequency. The vibration was stopped when the lower surface of the transparent disc was completely covered with grout. The time taken for the concrete to completely cover the lower surface of the disc was recorded

with a stopwatch and was taken as the Vebe time. The details of the apparatus are illustrated in Figure 3.8.



Figure 3.8: Vebe Test Apparatus

3.7 Hardened Concrete Tests

Hardened concrete tests are carried out at least one day after placing when the concrete is set. Hardened concrete tests can be categorised into two types, which are destructive tests (DT) and non-destructive tests (NDT). DTs are carried out to evaluate certain properties of specimens at their failure point where the specimens are broken permanently after testing. In contrary, NDTs are not causing damage or causing only minor damage that will not affect the performance of specimens after testing. In this study, DTs such as mechanical

properties tests (compression test, splitting tension test and flexure test) were carried out; NDTs such as Ultrasonic Pulse Velocity (UPV) test was conducted to identify the uniformity of all the mixes.

3.7.1 UPV Test (Non-Destructive Test)

The procedures of conducting this test are as stated in BS EN: 12504 - Part 4 (2004). The outcome of this test is affected by the speed of propagation of a sound wave from the transmitter to the receiver through the specimen. The density of the specimen is also one of the factors that will alter the results. The speed of an ultrasonic pulse propagating in a solid material is dependent on its elastic properties and density. It is important to tare the reading to zero before commencing the test to avoid discrepancies in the results. The reading is often influenced by a delay of time caused by the transmission of pulse through the transducers and the transmission of electrical signal along the cables. Concrete cubes of dimension 100 mm x 100 mm x 100 mm are tested at 1, 7, 28, 56, 90 and 180-days. Figure 3.9 illustrates the equipment for UPV test.

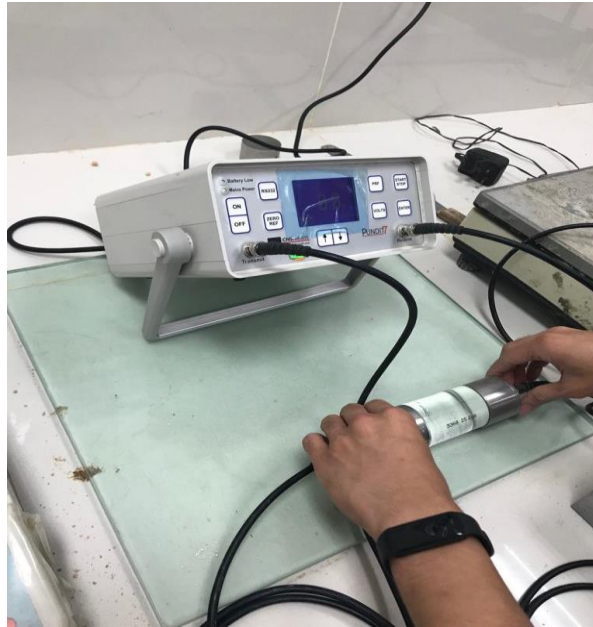


Figure 3.9: UPV Test Apparatus

Before testing, the transducers were coupled to the both ends of a reference bar with an accurately defined transit time to reset the time delay adjustment. In this study, reference bar of $25.2 \mu\text{s}$ was used. The transducers were connected in the arrangement of direct transmission as this arrangement offered the maximum energy transfer between the transducers. Hence, the accuracy of path length measurement became the principal factor to govern the accuracy of velocity identification. Adequate acoustical coupling is essential in between concrete surfaces to ensure the detection of ultrasonic pulses from the transmitting transducer to the receiving transducer after passing through the concrete. Therefore, smooth surfaces of concrete were chosen as the contact surface for the transducers. A good acoustical contact can be guaranteed by the application of coupling medium and the application of adequate pressure on the transducers to the concrete surfaces by hands. High viscosity grease was used as the coupling medium.

In a nutshell, a pulse of longitudinal vibrations is generated by an electroacoustic transducer attached to one of the surfaces of the specimen, which is known as the transmitter. The pulse of vibrations is transformed into electrical signal by the receiver, which is coupled at the opposite surface of the specimen after traversing through the specimen with a known path length, L . The transit time, T , of the pulse is measured by the electronic timing circuits. Therefore, the UPV, V , in the unit of km/s can be computed in the formula below:

$$v = \frac{l}{t} \quad (3.6)$$

where,

v = velocity of pulse, km/s

l = length of specimen, mm

t = transit time from the transmitter to the receiver, μ s

3.7.2 Compression Test (Destructive Test)

The compression test was carried out on cube specimens of 100 mm \times 100 mm \times 100 mm at 1, 7, 28, 56, 90 and 180-days in accordance to BS EN 12390 – Part 3 (2019) with a loading rate of 0.2 to 1 MPa/s. Hence, the loading rate for 100 mm cube is 2 to 10 kN/s. The testing machine was manufactured by Unit Test Scientific Sdn. Bhd. (UTS) with a load capacity of 3000 kN. It is essential to ensure that the rough surface (the top surface exposed to the air in the mould) is not the contact surface with the testing plates. The uneven distribution of load on the rough surface will lead to inaccurate results

obtained. In this research, the loading rate was set to a constant rate of 3.0 kN/s until reaching the failure point. The compression test is illustrated in Figure 3.10.



Figure 3.10: Compression Test

The stress-strain relation of concrete is non-linear as the strain increases gradually at high stress rate. Upon reaching the failure state, the movement of the pressure plate of the testing machine will increase. The loading rate decreases when the testing specimen fails. The peak loading applied on the sample is determined as the failing point and is recorded. The compressive strength is then calculated with the formula as below:

$$f_{cu} = \frac{P}{A} \quad (3.7)$$

where,

f_c = compressive strength, N/mm²

P = peak load recorded, N

A = surface area of specimen, mm²

3.7.3 Splitting Tension Test (Destructive Test)

This test was conducted by following all the guidelines stated in BS EN 12390 - Part 6 (2009). Cylinders with diameter of 100 mm and length of 200 mm at 7, 28 and 90-days were prepared for this test. The same machine for compression test was used. According to BS EN 12390 – Part 6 (2009), the loading rate is in the range of 0.04 – 0.06 MPa/s, which is 1.257 to 1.885 kN/s for the dimension of specimens used. This test promises more consistent results as compared to other tensile strength test and it is easy to carry out. The apparatus set-up is shown in Figure 3.11.



Figure 3.11: Splitting Tension Test

The cylinder specimen was placed into a steel jig before it was put into the platen of the machine. Plywood strips were inserted on the top and bottom of the specimen in the jig for even load distribution and for the prevention of concentrated local compressive stresses at the load lines. The loading rate was set to 1.5 kN/s in compliance with the range mentioned above and was maintained until failure point of the testing specimen. The ultimate load at the failure point was recorded. At the failure point, splitting occurred along the vertical diameter of the specimen because of the indirect tension from the load applied. The tensile splitting strength can be expressed as below:

$$f_{ct} = \frac{2P}{\pi l D} \quad (3.8)$$

where,

f_{ct} = tensile splitting strength, N/mm²

P = ultimate load applied, N

l = length of specimen, mm

D = diameter of specimen, mm

3.7.4 Flexure Test (Destructive Test)

Flexural strength, also known as the Modulus of Rupture (MOR) is examined abiding to BS EN 12390 – Part 5 (2019). In this study, 100 mm × 100 mm × 500 mm beam blocks at 7 and 28-days were used to test for flexural strength under the configuration of two-points loading. Motorised Digital Concrete Beam Flexural Test Machine of 100 kN capacity with DHR 2000 manufactured by UTS was used to test all the research specimens. ASTM C78/C78M – 18 (2018) states that the loading rate ranges from 0.040 – 0.056 kN/s for flexural strength test. Figure 3.12 shows the equipment for this test.



Figure 3.12: Flexure Test

Before placing the specimen on the machine, the machine surfaces were wiped to ensure that they were free from any concrete debris and the contact surfaces of specimen with the rollers were ensured to be free from any grit. Then, the sample was put on the lower rollers and was centred accordingly with the longitudinal axis of the specimen is perpendicular to the longitudinal axis of the upper and lower rollers. The loading shall be applied perpendicularly to the direction of casting. When all the supporting and loading rollers rested evenly on the specimen, an initial load, which did not exceed 20% of the failure load, was applied in a constant rate of 0.05 kN/s and was increased gradually until the specimen failed. The application of vertical load on the specimen induced a symmetrical triangular stress distribution along the vertical section with compression above the neutral axis at the mid-

point and tension below the neutral axis. The ultimate tensile stress at the bottom of the specimen was taken as the MOR. The flexural strength of the specimen can be expressed as below:

$$f_{cr} = \frac{PL}{bd^2} \quad (3.9)$$

where,

f_{cr} = flexural strength, N/mm²

P = ultimate load, N

L = distance between the supporting rollers, mm

b = breadth of the specimen, mm

d = depth of the specimen, mm

3.8 Thermal Properties Tests

Two different types of tests were conducted in this research to identify the effect of PP fibres on the thermal properties of OPSLWC. Thermal conductivity test and temperature gradient test were conducted to evaluate the thermal properties of FROPSLWC. Thermal conductivity test determines the thermal conductivity, k value of the specimens. Temperature gradient test is a self-fabricated test to simulate the performance of OPSLWC and FROPSLWC under the sun in laboratory scale.

3.8.1 Thermal Conductivity Test

In this research, thermal conductivity test is abided with BS EN 12664 (2001), which is the guarded hot plate and heat flow meter method. The test equipment is shown in Figure 3.13. It is made up of four main components, which are the electric control box, chiller, data logger and specimen compartment. Slab panels of dimension 300 mm × 300 mm × 50 mm were casted for this test. They were tested at 7 and 28-days. Rubber foams were used to insulate the sample inside the specimen compartment from losing heat to the surrounding.



Figure 3.13: Test Equipment for Thermal Conductivity

In the specimen compartment, there are two plates, hot and cold plates. The concrete sample was sandwiched in between the hot and cold plates when conducting the test. These plates were lightly compressed to ensure the close contact between the plates and the surface of the sample. Gaps on the four sides of the plates were filled with rubber foams tightly to prevent heat loss to the surrounding. The hot plate was set to heat up and maintain at 40°C; while the cold plate was set to maintain at 20°C. According to the principle of thermal equilibrium, heat tends to flow from higher temperature to lower temperature; the heat generated from the hot plate was transferred to the cold plate through the sample. The hot plate temperature dropped eventually when heat was being transferred to the cold plate. Current was supplied to heat up the hot plate at the stipulated temperature and was measured by using CS15-L CR Magnetics Current Transformer supplied by Campbell Scientific Limited. Thermocouples were attached on the both surfaces of the specimen. All the thermocouples and the current transformer were connected to AM25T Solid State Multiplexer, which was connected to CR800 series Data logger supplied by Campbell Scientific Limited. The test was set to run with duration of 20 hours. A laptop was required for data collection. The thermal conductivity, k value can be expressed in equation 3.10.

$$k = \frac{\phi d}{A} (T_1 - T_2) \quad (3.10)$$

where,

ϕ = average power supplied to the heating unit, W

d = average specimen thickness, m

A = contact surface area of the specimen, m²

T_1 = average hot side temperature of the specimen, °C

T_2 = average cold side temperature of the specimen, °C

3.8.2 Temperature Gradient Test

Temperature gradient test was carried out in this study to evaluate the thermal performance of OPSLWC and FROPSLWC as wall panels under the sun in laboratory scale. The test equipment was self-fabricated with acrylic boards. Slab panels of dimension 300 mm × 300 mm × 50 mm were used for this test at 7 and 28-days. Spot R80 100W Reflector Incandescent Lamp manufactured by General Electric was attached at the acrylic box and was used as the virtual sun.

The first step was to place the sample into the acrylic box. The spacing between the sample and the light source was set to 15 cm. Thermal sensors were contacted to the surface of the specimen which was not exposed directly to the light source. A digital thermometer was connected to the thermal sensors to record the temperature of the sample in an interval of 15 minutes for 2 hours, where the light was switched on for the first hour for heating; while

cooling on the second hour with the light switched off. The schematic diagram for the apparatus is shown in Figure 3.14. The setup of the apparatus is illustrated in Figure 3.15.

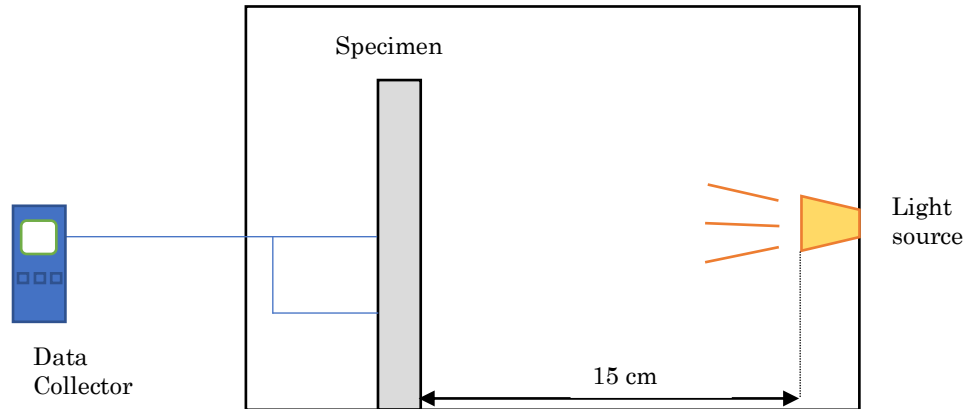


Figure 3.14: Schematic Diagram of the Test Apparatus.



Figure 3.15: Setup of the Test Apparatus.

3.9 Summary

Various types of tests were conducted in this study. These tests were grouped into three categories; which are fresh concrete tests, hardened concrete tests and thermal properties tests. Fresh concrete tests were conducted right after the mixing of concrete and the test results were obtained immediately. Hardened concrete tests and thermal properties tests were conducted at specific age after curing. The types of specimens and the age of testing for hardened concrete tests and thermal properties tests were summarised in Table 3.7.

Table 3.7: Types of Specimens and Age of Testing of Different Tests

Test	Types of Specimens	Age of Testing (days)
Hardened concrete tests		
Compressive Strength	Cubes (Dimension: 100 mm x 100 mm x 100 mm)	1,7,28,56, 90 and 180
Splitting tensile strength	Cylinders (Dimension: ϕ =100 mm; L = 200 mm)	7, 28 and 90
Flexural strength	Prisms (Dimension: 100 mm x 100 mm x 500 mm)	7 and 28
UPV	Cubes (Dimension: 100 mm x 100 mm x 100 mm)	1,7,28,56, 90 and 180
Thermal properties tests		
Thermal conductivity	Panels (Dimension: 300 mm x 300 mm x 50 mm)	7 and 28
Temperature gradient	Panels (Dimension: 300 mm x 300 mm x 50 mm)	7 and 28

CHAPTER 4

RESULTS AND DISCUSSIONS

4.1 Introduction

The results collected from the experimental work were discussed and justified in this chapter. The experimental work was separated into two main sections, which were trial mix and actual mix. In the subsections, fresh and hardened concrete properties, performance index and thermal properties were discussed. Workability, uniformity, compressive strength, splitting tensile strength, flexural strength and thermal conductivity were included in the discussion. Comprehensive and appropriate graphs, diagrams and tables were used for better visual interpretation of the results.

4.2 Trial Mix

The preliminary stage of this research was to develop plain oil palm shell lightweight concrete (OPSLWC) with 28-days compressive strength of greater than 25 MPa and adequate workability with tolerance for deterioration after the addition of fibres at the later stage. The trial mixes were mixed by two different mixing methods. Initially, Conventional Mixing Method (CMM) was implemented to produce OPSLWC. Then, a New Mixing Method (NMM) was proposed to enhance the performance of OPSLWC. The mix design,

workability and compressive strength of the trial mixes will be explained in this section. The design of mix was varied by the proportions of constituents. The flowability of the trial mixes were tested during their fresh state. Simultaneously, the 28-days compressive strength after water curing were obtained.

4.2.1 Mix Design

The quantity of cement, fine aggregates, oil palm shell (OPS) coarse aggregates and water used was within the range of 500 – 515 kg/m³, 900 – 1000 kg/m³, 290 – 320 kg/m³ and 155 – 190 kg/m³ respectively. The different mix proportions of all the trial mixes were summarised in Table 4.1.

Table 4.1: Mix Proportions of Trial Mixes

Mix	Trial Mix 1	Trial Mix 2	Trial Mix 3	Trial Mix 4	Trial Mix 5
Cement (kg/m ³)	500	500	515	515	515
Fine Aggregate (kg/m ³)	900	900	1000	1000	1000
OPS (kg/m ³)	320	320	290	290	290
Water (kg/m ³)	190	190	180	170	155
Water/Cement Ratio	0.38	0.38	0.35	0.33	0.30
Superplasticiser (% of the total binder weight)	1.0%	1.5%	1.5%	2.0%	2.0%

4.2.2 Workability

The flowability of each trial mix was determined by carrying out slump test during fresh concrete state. Same amount of mixing water (190 kg/m^3) was designated in Trial Mix 1 and 2, which was the most amount of water added among all trial mixes. The proportion of water added in Trial Mix 3 and 4 was 180 kg/m^3 and 170 kg/m^3 respectively. Meanwhile, the amount of water used in Trial Mix 5 was the least, 155 kg/m^3 . The dosage of superplasticiser (SP) was varied from 1.0 % to 2.0 % of the binder weight in the trial mixes. This was to determine the optimum dosage and the optimum water-cement ratio to achieve the targeted strength. The slump values of all the trial mixes are illustrated in Figure 4.1.

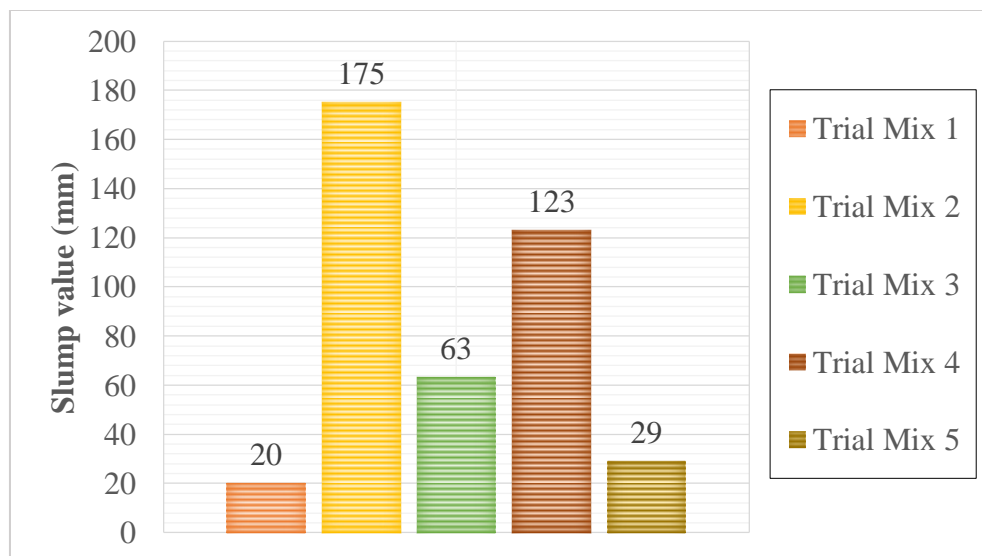


Figure 4.1: Workability of Trial Mixes

From Figure 4.1, Trial Mix 2 had the highest slump value of 175 mm. It was then followed by Trial Mix 4 with the slump value of 123 mm. The

slump values for Trial Mix 3, 5 and 1 were 63 mm, 29 mm and 20 mm respectively. Although the workability of Trial Mix 2 is better than Trial Mix 4, but the water content in Trial Mix 2 is higher than that of Trial Mix 4, which may compromise its strength. Therefore, the compressive strength of all the trial mixes was tested to identify the most suitable mix design for the actual mix.

4.2.3 Compressive Strength

All the 100 mm x 100 mm x 100 mm trial cubes were placed into the water tank for curing until their desired ages for compression test. Water-cement ratio plays an influential role to the compressive strength. According to Abrams' Law, lower water-cement ratio should be accompanied by higher compressive strength (Nagaraj & Banu, 1996). Pores are developed after the added water is consumed for hydration in the cement paste and cause reduction in strength (Kim, et al., 2014). Higher water content produces more pores, which results in lower strength. Figure 4.2 illustrates the compressive strength of the trial mixes.

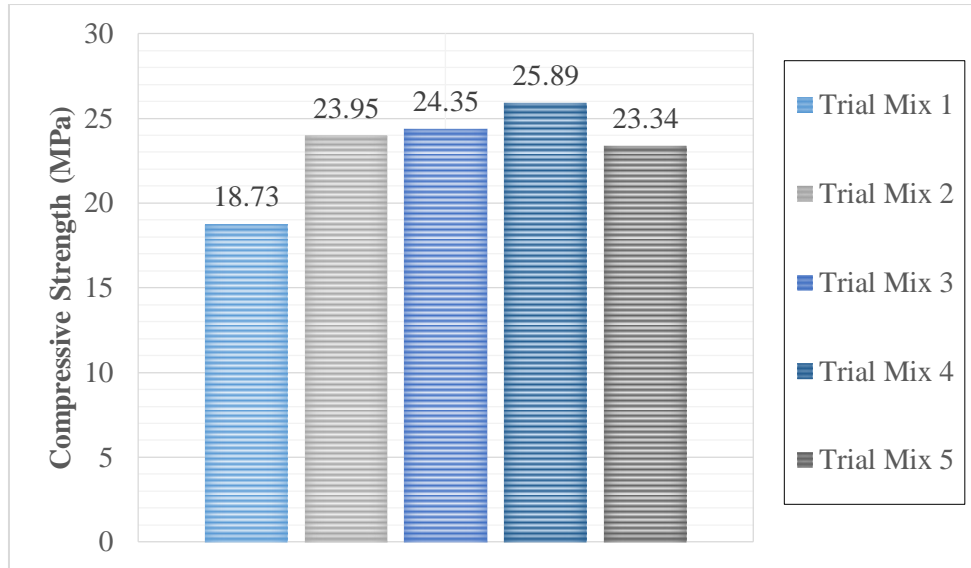


Figure 4.2: Compressive Strength of Trial Mixes at 28-days

From Figure 4.2, Trial Mix 4 had the highest 28-days compressive strength with a value of 25.89 MPa. Meanwhile, the 28-days compressive strength of Trial Mix 3, 2, 5 and 1 were 24.35 MPa, 23.95 MPa, 23.34 MPa and 18.73 MPa respectively. Trial Mix 4 had fulfilled the objective of producing OPSLWC with the 28-days compressive strength exceeding 25 MPa. In order to enhance the performance of OPSLWC, the author proposed an innovative mixing method, namely NMM, which was modified from one of the mix design methods of self-compacting concrete (SCC) where SCC is highly workable concrete (Shi, et al., 2015). It was expected to offer better outcome in terms of workability and compressive strength.

4.2.4 Comparison of Workability between CMM and NMM

Trial Mix 4 and 5 were casted in both methods to study the effect of different mixing methods on the workability of mixes with different water-cement ratio. The comparison of the obtained data is presented in Figure 4.3.

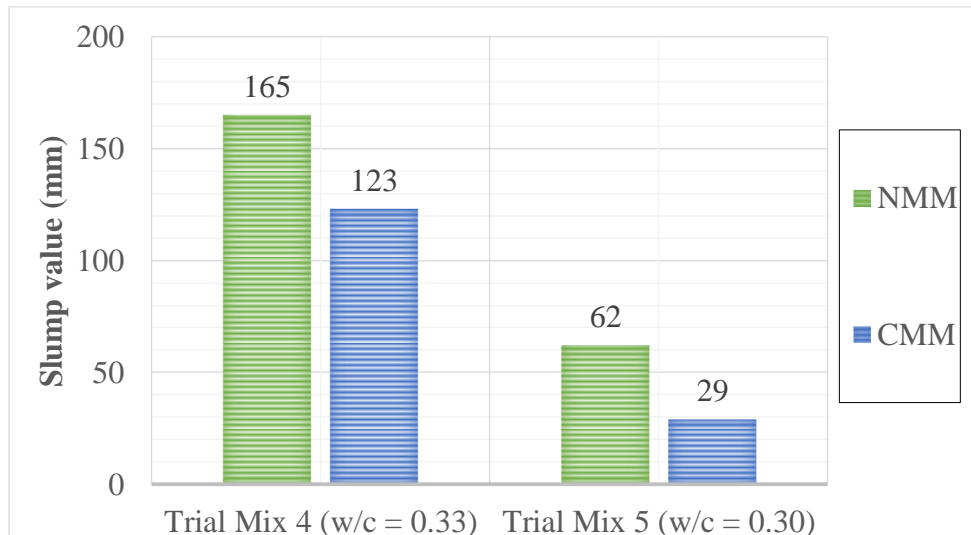


Figure 4.3: Workability of Trial Mixes by Different Mixing Methods

From Figure 4.3, NMM showed better workability in both mixes as compared to the workability of CMM. The slump value of Trial Mix 4 was improved by 34.1% with NMM. For Trial Mix 5, the slump value increased by 113.8% in the implementation of NMM. The time of adding SP during mixing affects the workability of the concrete (Anagnostopoulos, 2014). SP was added in the first stage of mixing (liquid phase) with cement and water in NMM. The early addition of SP without the presence of aggregates expedited the absorption of molecules on cement particles, which caused electrostatic repulsion and steric hindrance between the cement particles (Ezzat, et al., 2019). Hence, better slump value was resulted with NMM. The mixing sequence of blending only cement slurry with superplasticiser improved the workability and strength (Hiremath & Yaragal, 2017).

4.2.5 Comparison of 28-days Compressive Strength between CMM and NMM

Compressive strength is the most important attribute for concrete. The specimens were tested for 28-days compressive strength after water curing to study the effect of two different mixing methods on the compressive strength. The comparison between the 28-days compressive strength of different mixing methods is shown in Figure 4.4.

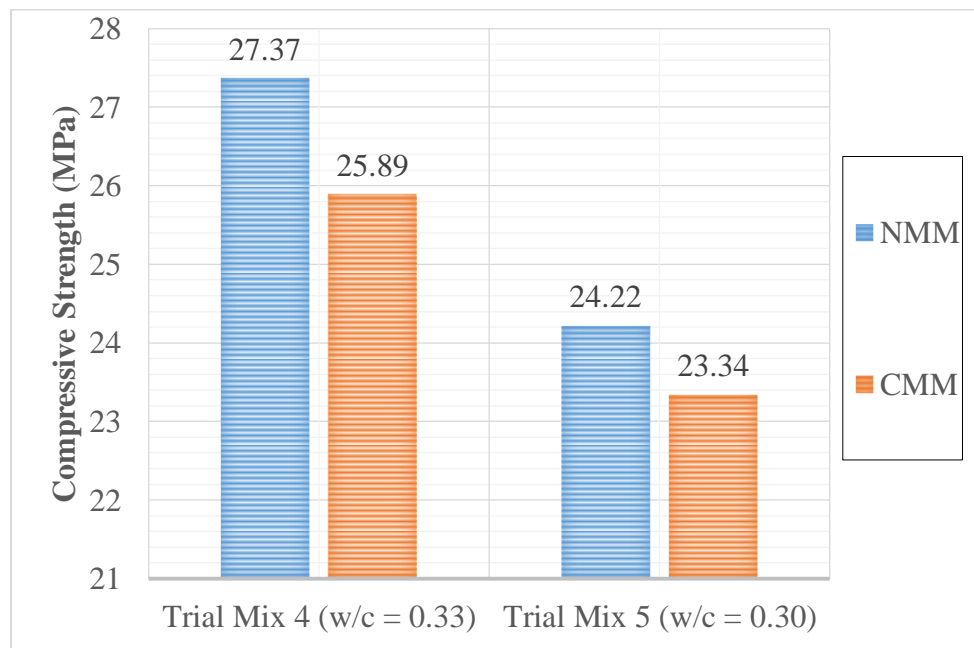


Figure 4.4: Compressive Strength of Trial Mixes by Different Mixing Methods at 28-days

From Figure 4.4, NMM offered a higher 28-days compressive strength than that of CMM. The 28-days compressive strength of NMM (27.37 MPa) was 5.72% better than that of CMM (25.89 MPa) in Trial Mix 4. While, the 28-days compressive strength of Trial Mix 5 was enhanced by 3.77% with

NMM (from 23.34 MPa to 24.22 MPa). Hence, NMM was implemented to produce all the specimens in this research.

4.3 Actual Mix

After obtaining the base mix design from the previous phase, the next step would be the casting of the actual mix with NMM. Two types of different polypropylene (PP) fibres, namely monofilament polypropylene straight (MPS) and barchip polypropylene straight (BPS), were incorporated into the mixes with the designated volume fractions. All types of specimens, which include cubes, cylinders, prisms and slabs, were casted. Then, the respective specimens were tested for their respective tests as mentioned in the previous chapter (UPV test, compression test, splitting tension test, flexure test, thermal conductivity test and temperature gradient test). All the results collected were analysed and justified in this section.

4.3.1 Mix Design

All the mixes were designed to the same proportions of water, cement, OPS, sand and SP as Trial Mix 4. The types and the volume fractions of PP fibres added were varied in all mixes. Each mix was given a mix code for the ease of identification. The mix codes for each mix were presented in Table 4.2.

Table 4.2: Mix Codes for All Mixes

Mix Code	Types of Fibres added	Volume Fractions (%)
OPSLWC ¹ -CTR ² -0% ³	-	0
OPSLWC-MPS-0.1%	MPS	0.1
OPSLWC-BPS-0.1%	BPS	0.1
OPSLWC-MPS-0.3%	MPS	0.3
OPSLWC-BPS-0.3%	BPS	0.3
OPSLWC-HYB-0.4%	MPS + BPS	0.1+0.3

Note:

¹ “OPSLWC” denotes oil palm shell lightweight concrete

² Types of Fibres added into the mix; “CTR” refers to “control”, which means no fibres added; “HYB” defines as “hybrid”, which means both types of fibres are added.

³ Volume fractions of fibres added.

4.3.2 Fresh Properties

The fresh properties, fresh density and workability of the concrete were investigated in this study. Slump test and Vebe test were carried out to examine the workability of all the mixes.

4.3.2.1 Fresh Density

From Table 4.3, the fresh density ranged from 2101.6 kg/m³ to 2148 kg/m³. The control mix, OPSLWC-CTR-0% had the highest density, 2148 kg/m³; while OPSLWC-HYB-0.4% had the lowest density of 2101.6 kg/m³. Generally, the fresh density decreased with increasing volume fractions of fibres included due to the lower density of PP fibres (910 kg/m³). The relative low density of PP fibres decreases the overall mass of the mixture in a fixed volume. At the same volume fraction, the inclusion of BPS reduced the fresh

density more than MPS. The reason could be attributed to the larger geometry of BPS, which has higher volume at the same mass as compared to MPS.

Table 4.3: Fresh Density of All Mixes

Mix Code	Fresh Density (kg/m³)
OPSLWC-CTR-0%	2148.0
OPSLWC-MPS-0.1%	2138.8
OPSLWC-BPS-0.1%	2127.6
OPSLWC-MPS-0.3%	2123.9
OPSLWC-BPS-0.3%	2104.6
OPSLWC-HYB-0.4%	2101.6

4.3.2.2 Workability

The workability of concrete plays an important role in determining the homogeneity of the concrete to be blended, placed, compacted and finished. In this research, slump test and Vebe test were carried out to measure the workability. The results collected from the both tests were tabulated in Table 4.4.

Table 4.4: Workability of All Mixes

Mix Code	Workability	
	Slump Value (mm)	Vebe Time (s)
OPSLWC-CTR-0%	165	9.46
OPSLWC-MPS-0.1%	146	10.55
OPSLWC-BPS-0.1%	138	10.86
OPSLWC-MPS-0.3%	122	10.92
OPSLWC-BPS-0.3%	110	11.09
OPSLWC-HYB-0.4%	96	12.26

From Table 4.4, the slump value fell between 96 mm to 165 mm; while the Vebe time was in the range of 9.46 s to 12.26 s. A higher slump value indicates better workability; while shorter Vebe time defines better flowability. Therefore, the Vebe time should be shorter at higher slump value. In fact, BPS contributed to lower slump value at the same volume fraction as compared to MPS. This phenomenon might be attributed to the stiffer nature of BPS, which acted like “holding” the fresh concrete mixture and causing the mixture to be more viscous (Mo, et al., 2017b).

The slump value can be correlated to the Vebe time as shown in Figure 4.5, with a R^2 value of 0.873. Hence, Equation 4.1 was proposed to predict the slump value with given Vebe time.

$$S = 24491(V_e)^{-2.208} \quad (4.1)$$

where S denotes the slump value in mm and V_e indicates the Vebe time in s.

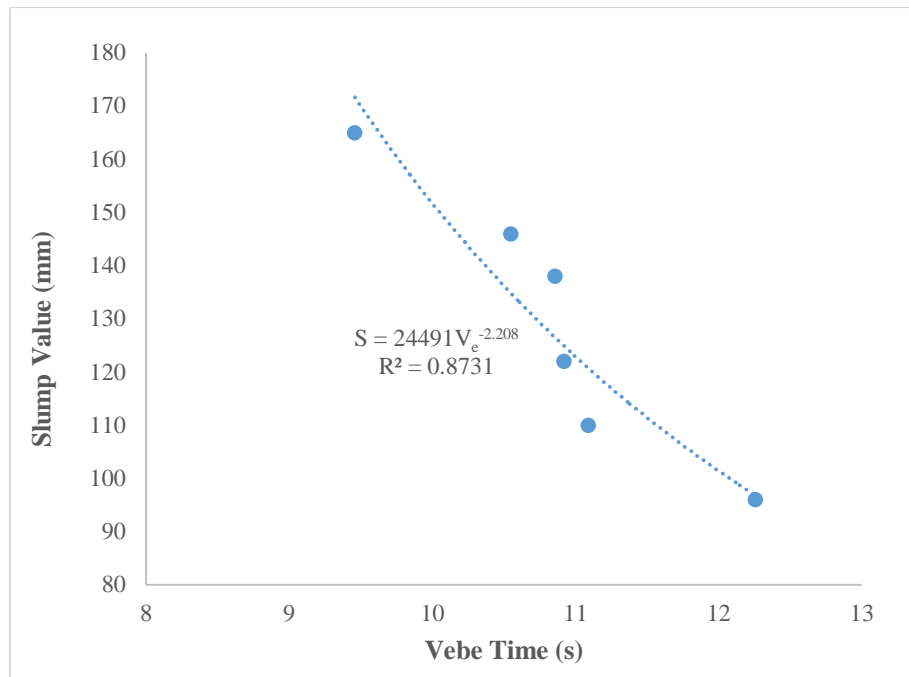


Figure 4.5: Relationship between Slump Value (mm) and Vebe Time (s)

4.3.3 Hardened Properties

In this research, hardened properties (density, uniformity) and mechanical properties (compressive strength, splitting tensile strength and flexural strength) of the mixes were investigated. Uniformity was measured with Ultrasonic Pulse Velocity (UPV) test. The mechanical properties were defined by compression test, splitting tension test and flexure test.

4.3.3.1 Density

Demoulded density (DD) and oven-dried density (ODD), were measured for all mixes. DD is calculated with the weight of the specimens measured after demoulding; while ODD is calculated with the weight of the specimens measured after being oven dried for 24 hours. All specimens in this study were

attributed with DD and ODD in the range of 2047.4- 2095.0 kg/m³ and 1936.7 – 1976.5 kg/m³, respectively. Hence, the outcome fulfilled the objective of obtaining OPSLWC with ODD lesser than 2000 kg/m³. At the same time, they also met the requirement for structural application as structural lightweight concrete (SLWC) is defined as concrete with ODD of not greater than 2000 kg/m³ (Newman & Owens, 2003). The DD and ODD of each mix were summarised in Table 4.5.

Table 4.5: Densities of All Mixes

Mix Code	DD (kg/m³)	ODD (kg/m³)
OPSLWC-CTR-0%	2095.0	1976.5
OPSLWC-MPS-0.1%	2088.6	1963.8
OPSLWC-BPS-0.1%	2082.4	1959.6
OPSLWC-MPS-0.3%	2075.5	1958.2
OPSLWC-BPS-0.3%	2062.8	1952.4
OPSLWC-HYB-0.4%	2047.4	1936.7

4.3.3.2 UPV Test (Uniformity)

UPV test is the measure of the time taken for an ultrasonic pulse to propagate through a known distance in the tested concrete, from which the velocity is calculated. UPV test can be applied to predict the concrete strength, which is applicable on-site where destructive strength test is not able to conduct. Moreover, detection of internal cracking, voids and inhomogeneity of concrete can also be done by UPV test. Higher velocity defines better concrete quality in terms of density, uniformity and homogeneity. The quality of concrete is categorised by UPV as shown in Table 4.6.

Table 4.6: Category of Concrete Quality Based on UPV (Neville, 2011)

UPV (km/s)	Concrete Quality (Grading)
Above 4.5	Excellent
3.5-4.5	Good
3.0-3.5	Medium
Below 3.0	Doubtful

UPV test was conducted at 1-day, 7-days, 28-days, 56-days, 90-days and 180-days. Generally, the UPV increases with their age in all concrete mixes. The increment of UPV with age is due to the ratio of gel to space. After hydration, gel is produced and eventually fills up the void within the concrete. The ratio of gel to void increases as hydration proceeds. As the pulse propagates slower in solid matter than in void, thus the UPV increases with the increasing of solid matter.

Figure 4.6 illustrates the development of UPV with mixes of different volume fractions of fibres. In general, it can be observed that UPV of all mixes increased with the increase of compressive strength. The UPV values for all specimens were in the range of 3.29 km/s to 4.39 km/s. From the results, the addition of different PP fibres provided positive effects on the UPV values of fibre-reinforced oil palm shell lightweight concrete (FROPSLWC).

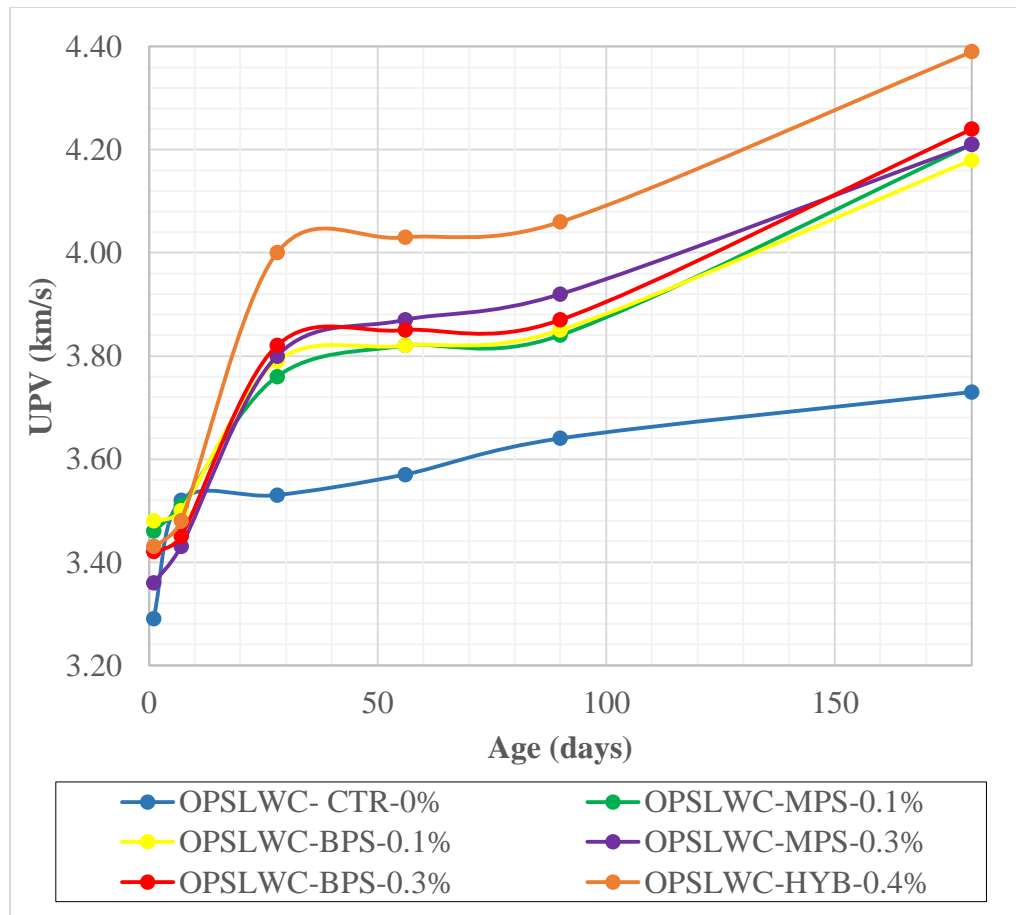


Figure 4.6: UPV of Different Percentage of Fibres Content

4.3.3.3 Compressive Strength

Compression test is the most common hardened concrete test because compressive strength is the most important attribute to be considered in structural design. The compressive strength is an overview of the quality of concrete. Compressive strength was investigated at 1-day, 7-days, 28-days, 56-days, 90-days and 180-days. Water curing was applied to all mixes until the desired age for testing. Compressive strength of all mixes increases along with the age of concrete due to the continuous hydration of cement. Table 4.7 summarises the compressive strength of each mix at different ages.

Table 4.7: Compressive Strength of All Mixes at Different Ages

Mix Code	Compressive Strength (MPa)					
	1-day	7-days	28-days	56-days	90-days	180-days
OPSLWC-CTR-0%	18.66 74.6%	24.23 96.8%	25.02 100.0%	25.95 103.7%	25.99 103.9%	26.88 107.4%
OPSLWC-MPS-0.1%	23.09 88.1%	24.68 94.1%	26.22 100.0%	26.80 102.2%	27.00 103.0%	30.07 114.7%
OPSLWC-BPS-0.1%	20.22 76.1%	24.47 92.1%	26.57 100.0%	27.04 101.8%	27.16 102.2%	30.11 113.3%
OPSLWC-MPS-0.3%	23.47 87.5%	25.21 94.0%	26.83 100.0%	26.90 100.3%	27.23 101.5%	30.24 112.7%
OPSLWC-BPS-0.3%	20.45 75.6%	23.53 87.0%	27.04 100.0%	27.30 101.0%	27.70 102.4%	30.39 112.4%
OPSLWC-HYB-0.4%	21.05 71.6%	24.19 82.3%	29.38 100.0%	29.88 101.7%	29.92 101.8%	31.45 107.0%

*The data in bold and italic are percentage of 28-days compressive strength.

From Table 4.7, the 28-days compressive strength of all mixes is in the range of 25 to 30 MPa, which met the minimum requirement of 17 MPa for structural lightweight concrete (SLWC) (ACI Committee 213, 2014). The inclusion of PP fibres enhanced the compressive strength by 4.8% - 17.4% at 28-days and 11.9% - 17.0% at 180-days. OPSLWC-HYB-0.4% had the highest compressive strength (29.38 MPa at 28-days, 31.45 MPa at 180-days) with the highest volume fractions of fibres added. At the same volume fraction of 0.3%, BPS enhanced the compressive strength by 8.1% and 13.1% at 28-days and 180-days respectively; while MPS improved the compression capacity by 7.2% and 12.5% at 28-days and 180-days, respectively. With the inclusion of 0.1%, BPS showed improvement of 6.2% and 12.0% in the 28-days and 180-days compressive strength; while MPS upgraded the compression capacity at 28-days and 180-days with 4.8% and 11.9%,

respectively. The hybridised fibres improved the compressive strength by 17.4% at 28-days and 17.0% at 180-days. Hence, BPS is more effective than MPS in improving the compressive strength. The control mix, OPSLWC-CTR-0% had the lowest compressive strength of 25.02 MPa at 28-days and 26.88 MPa at 180-days.

When compressive load is applied on the specimen, lateral tension is produced randomly throughout the sample. Then, minor cracks will start to develop due to the heterogeneous of different constituents in the concrete. Minor cracking will continue to occur; eventually major cracks will form when the advancing minor cracks meet each other. The cracking will take place in the direction parallel to the applied load. The presence of PP fibres blocks the propagation of the crack and acts as a resistance to the lateral tension. As a result, additional compressive loading can be withstood, thus the capacity to withstand compression of concrete is upgraded. This proves the ability of fibres in arresting cracks and creating bridging effect in concrete (Song, et al., 2005) (Yew, et al., 2011) (Kakooei, et al., 2012) (Smarzewski, 2019).

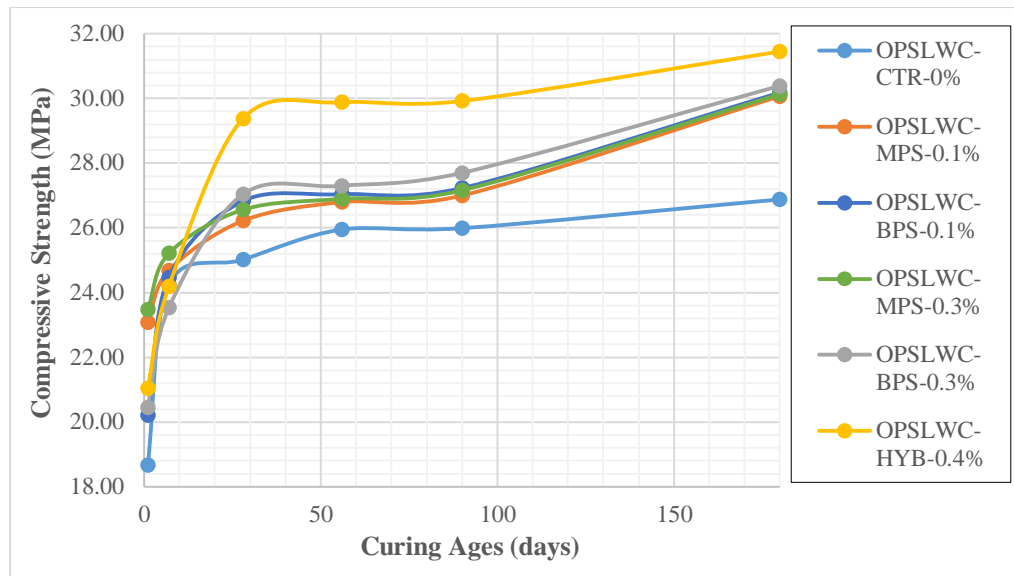


Figure 4.7: Development of Compressive Strength at Different Ages

Figure 4.7 illustrates the growth of compressive strength in respect to the ages of the mixes. In general, the compressive strength of all mixes increased with the age. The compressive strength of all mixes increased gradually from 28-days to 90-days and slightly shot up at 180-days. This phenomenon could be due to the NMM as the expedited integration of SP molecules on the cement particles, which could result a more thorough dispersion of cement particles (Peng, et al., 2015). Therefore, a longer period is needed to fully hydrate the dispersed cement particles.

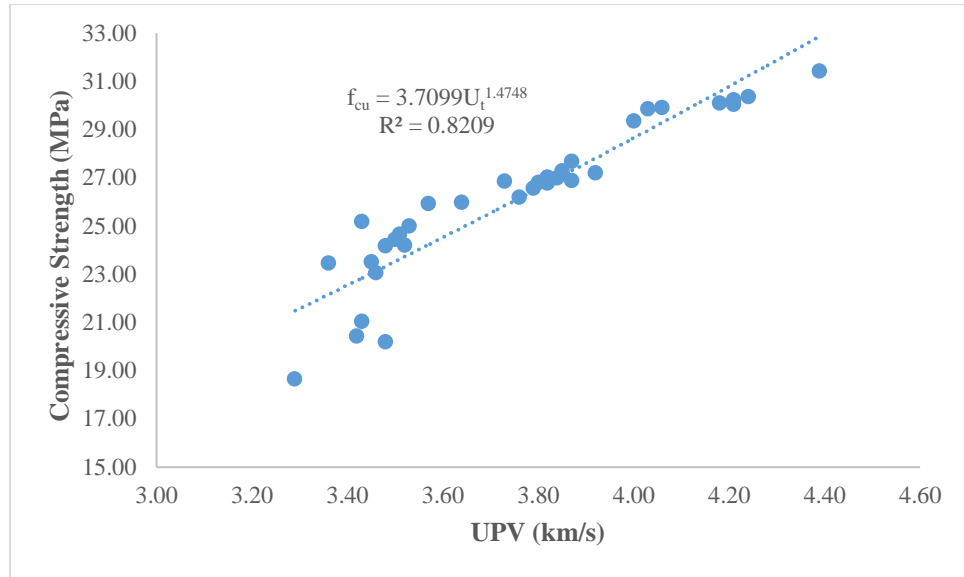


Figure 4.8: Correlation between Cube Compressive Strength and UPV

Furthermore, the correlation between UPV and the corresponding cube compressive strength is shown in Figure 4.8 with a R^2 value of 0.82. The compressive strength can be estimated based on the UPV values by using the proposed equation 4.2.

$$f_{cu} = 3.7099(U_t)^{1.4748} \quad (4.2)$$

where f_{cu} denotes the cube compressive strength in MPa; while U_t represents the transverse UPV in km/s.

4.3.3.4 Residual Compressive Strength

The residual compressive strength (RCS) is a simplified method to evaluate the effects of fibres on the toughness of concrete. This test was conducted by further loading the specimens for second time and third time at 28-days. The

RCS shows a clearer comparison of the favourable effects of different types of PP fibres on the post-cracking of fibre reinforced oil palm shell lightweight concrete (FROPSLWC). The first loading compressive strength (FLCS), second loading compressive strength (SLCS) and third loading compressive strength (TLCS) were tabulated in Table 4.8.

Table 4.8: Residual Compressive Strength of All Mixes at 28-days

Mix Code	FLCS (MPa)	SLCS (MPa)	TLCS (MPa)
OPSLWC-CTR-0%	25.02 (100.0%)	16.22 (64.8%)	10.24 (40.9%)
OPSLWC-MPS-0.1%	26.22 (100.0%)	21.66 (82.6%)	19.5 (74.4%)
OPSLWC-BPS-0.1%	26.57 (100.0%)	22.91 (86.2%)	19.78 (74.4%)
OPSLWC-MPS-0.3%	26.83 (100.0%)	21.87 (81.5%)	19.85 (74.0%)
OPSLWC-BPS-0.3%	27.04 (100.0%)	23.53 (87.0%)	20.21 (74.7%)
OPSLWC-HYB-0.4%	29.38 (100.0%)	26.14 (89.0%)	24.47 (83.3%)

*The data in parentheses are percentage of the FLCS.

Without the incorporation of fibres, OPSLWC-CTR-0% failed at 64.8% of FLCS and 40.9% of FLCS for second loading and third loading respectively. The inclusion of fibres showed remarkable improvement of 17.8% to 24.2% for SLCS and 33.5% to 42.4% for TLCS. Comparing OPSLWC-BPS-0.3% and OPSLWC-MPS-0.3%, the mix with BPS produced higher SLCS and TLCS of 87.0% and 74.7%, respectively. While the mix with MPS showed SLCS of 81.5% and TLCS of 74.0%. Furthermore, the same outcome can be observed with 0.1% of fibres added. The addition of BPS remained 86.2% and 74.4% during second and third loading; whereas the

inclusion of MPS retained 82.6% and 74.4% during second and third loading. The mix with hybrid fibres, OPSLWC-HYB-0.4% had the highest RCS values of 89.0% and 83.3% for SLCS and TLCS, respectively. This could be due to the synergy effect of the two different fibres. From the aspect of geometry, MPS is smaller and is more effective in arresting minor cracks; while BPS is bigger and stiffer, which is more effective in arresting major cracks. The comparison of the post-failure compressive strength of mixes with different types and different volume fractions of fibres is illustrated in Figure 4.9.

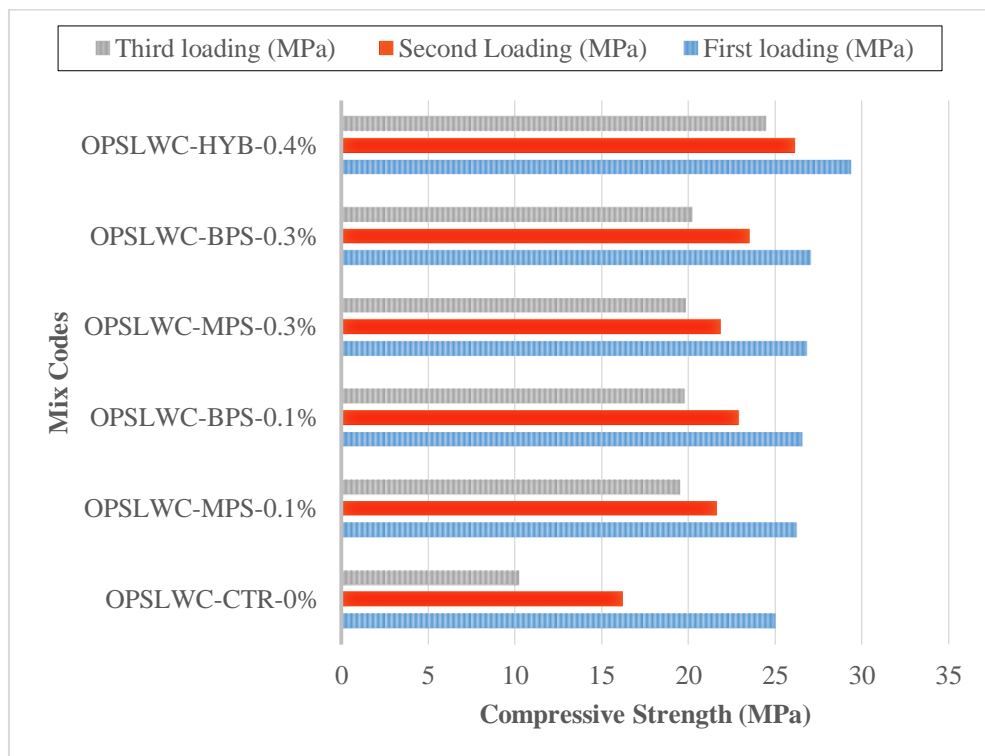


Figure 4.9: Comparison of RCS of All Mixes

The failure pattern of OPSLWC with fibres and without fibres was illustrated in Figure 4.10. The cube specimen without fibres underwent semi-explosive failure; while the cube specimen with fibres underwent non-explosive failure (Mo, et al., 2014a) (Yahaghi, et al., 2016). The linking bridge

between fibres and cement matrices (Figure 4.11) prevented spalling caused by the lateral tension induced by the compressive loading applied (Yew, et al., 2015a). The holding effect of fibres contributed to the improvement of RCS.

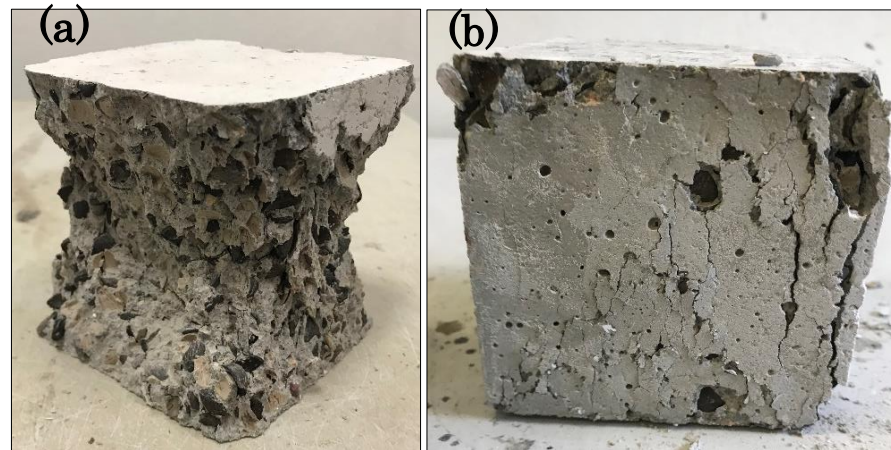


Figure 4.10: Failure Pattern of OPSLWC (a) without Fibres (b) with Fibres after Third Loading



Figure 4.11: Linking Bridge between Fibres and Cement Matrices

4.3.3.5 Splitting Tensile Strength

Splitting tensile strength is a measurement of the performance of fibres incorporated in concrete. Concrete is weak in tensile strength and is prone to fail at tension. One of the significant beneficial effects of fibres reinforcement in concrete is to strengthen the tension capacity of concrete. In this research, splitting tensile strength was evaluated at 7-days, 28-days and 90-days for all mixes.

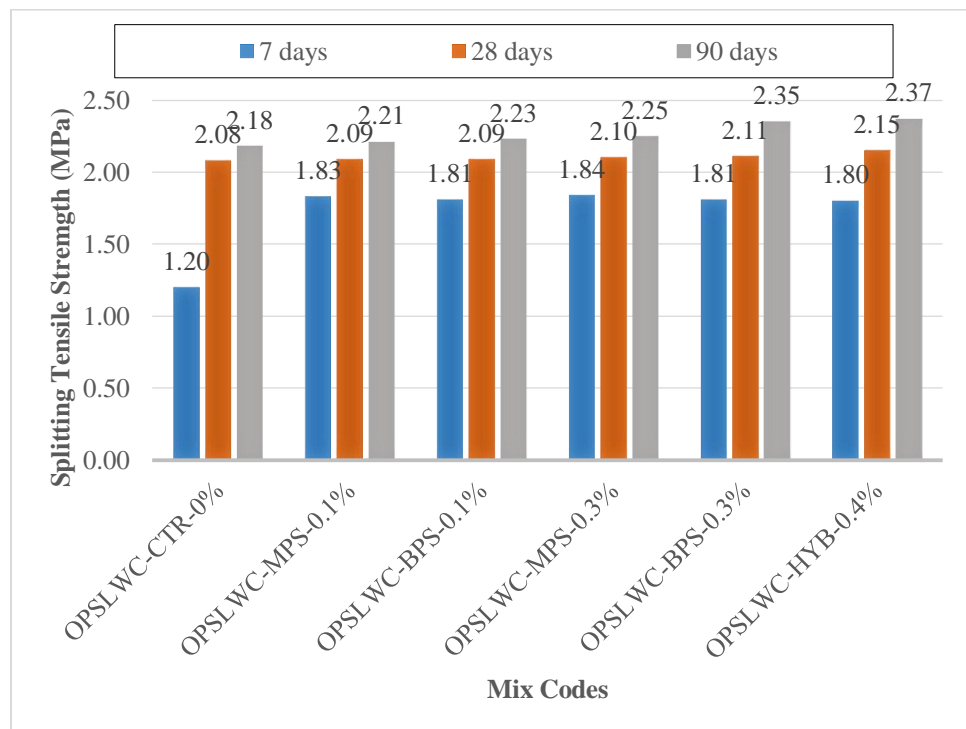


Figure 4.12: Development of Splitting Tensile Strength of All Mixes

From Figure 4.12, the splitting tensile strength increased with the ages of concrete. Inclusion of 0.1% of BPS and MPS improved 28-days splitting tensile strength by the same amount of 0.5%. Meanwhile, BPS gave 2.3% of improvement at 90-days, whilst MPS only offered 1.4% of increment at the

same age. Simultaneously, addition of 0.3% of BPS upgraded 28-days-splitting tensile strength by 1.4% and 90-days-splitting tensile strength by 7.8%; the same volume fraction of MPS raised the splitting tensile strength by 1.0% and 3.2% at 28-days and 90-days, respectively. Incorporation of hybrid MPS and BPS with a total volume fraction of 0.4% enhanced splitting tensile strength by 3.4% and 8.7% at 28-days and 90-days respectively, as compared to the control mix.

Splitting tensile strength of OPSLWC is comparatively lower than concrete with normal aggregate because of the weak bonding between the OPS and cement matrix (Shafigh, et al., 2011a). Therefore, the addition of PP fibres was to enhance the capacity of withstanding tension. From Figure 4.12, the trend of the development of splitting tensile strength was clearly presented, which showed that the strength increased with the volume fractions of fibres added. Upon loading, the cylindrical specimen tended to split by the tensile stress induced by the load. The presence of fibres held the cylindrical specimen from splitting. With the high tensile strength of PP fibres, the fibres stretched upon splitting to hold the cement matrix with the strong interface bonding. Consequently, higher splitting load was required to separate the specimen into half. The stretching of fibres upon splitting is illustrated in Figure 4.13.

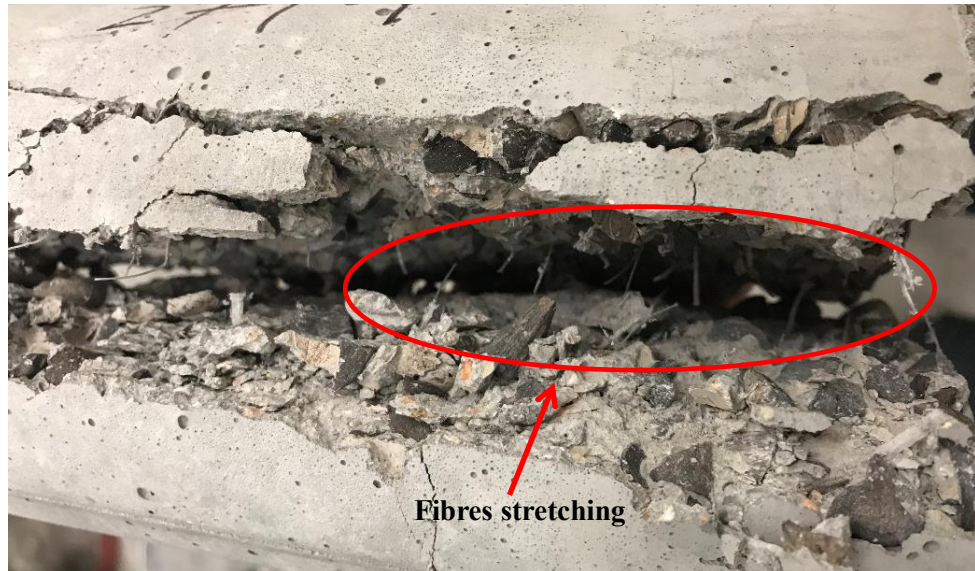


Figure 4.13: Stretching of Reinforced Fibres upon Splitting

4.3.3.6 Residual Splitting Tensile Strength

Residual splitting tensile strength (RSTS) is another method to investigate the effect of fibres on the integrity of concrete. This test was conducted in similar way as RCS, where the specimens were further loaded for another two times after initial failure. This test highlighted the positive effects of fibres in the improvement of the mechanical performance of concrete. Without the presence of fibres, OPSLWC-CTR-0% split into half after first loading as shown in Figure 4.14.



Figure 4.14: Failure Mode of OPSLWC-CTR-0% after First Loading

However, the other fibres-reinforced mixes (OPSLWC-MPS-0.1%, OPSLWC-BPS-0.1%, OPSLWC-MPS-0.3%, OPSLWC-BPS-0.3% and OPSLWC-HYB-0.4%) were not split into half after first loading. Thus, all the fibres-reinforced mixes were advanced to second loading and third loading to determine the residual strength at 28-days. The first loading splitting tensile strength (FLSTS), second loading splitting tensile strength (SLSTS) and third loading splitting tensile strength (TLSTS) of all mixes at 28-days are tabulated in Table 4.9.

Table 4.9: Residual Splitting Tensile Strength of All Mixes at 28-days

Mix Code	FLSTS (MPa)	SLSTS (MPa)	TLSTS (MPa)
OPSLWC-CTR-0%	2.08	-	-
OPSLWC-MPS-0.1%	2.09	1.06 (50.7%)	0.61 (29.2%)
OPSLWC-BPS-0.1%	2.09	1.23 (58.9%)	0.96 (45.9%)
OPSLWC-MPS-0.3%	2.10	1.10 (52.4%)	0.64 (30.5%)
OPSLWC-BPS-0.3%	2.11	1.32 (62.6%)	1.02 (48.3%)
OPSLWC-HYB-0.4%	2.15	1.74 (80.9%)	1.43 (66.5%)

*The data in parentheses are percentage of the FLSTS.

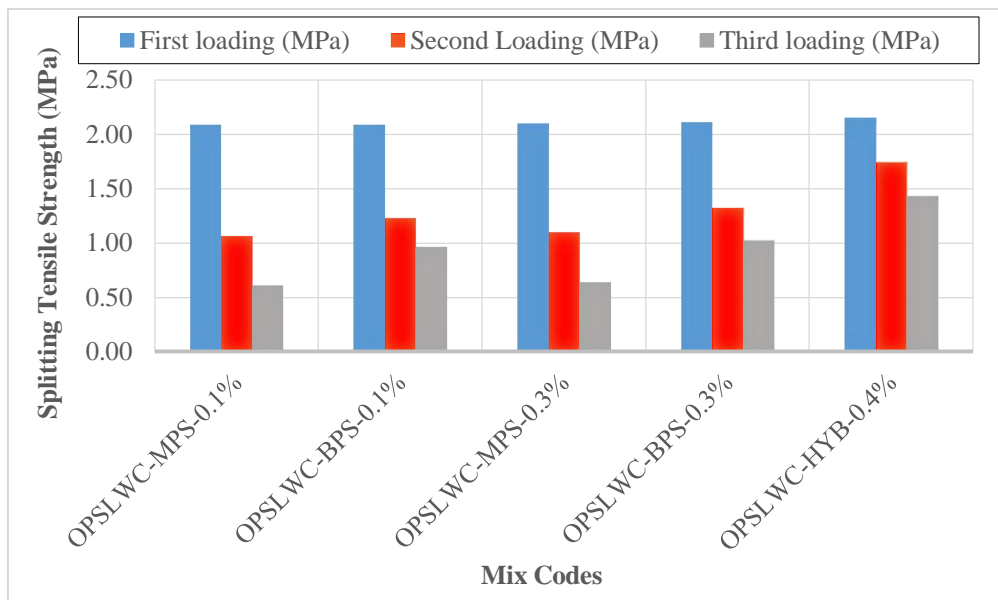


Figure 4.15: Comparison of 28-days RSTS of All Mixes

From Figure 4.15, OPSLWC-MPS-0.1% reserved 50.7% of its strength at second loading and 29.2% at third loading. Higher strength was retained for OPSLWC-BPS-0.1% (58.9% at second loading and 45.9% at third loading) as the geometry of BPS provided better bridging effect compared to MPS. The increase of the volume fractions of fibres also increased the residual strength of the concrete. The reinforcement of MPS with volume fraction of 0.3% preserved 52.4% and 30.5% of strength at second and third loading, respectively. The performance of the same amount of BPS was even better

with 62.6% and 48.3% of residual strength during second and third loading. OPSLWC-HYB-0.4% had the highest residual strength of preserving 80.9% at second loading and 66.5% at third loading. This highlighted the combined effect of two different types of fibres on OPSLWC. Although the improvement of FLSTS was not very significant, but the enhancement in SLSTS and TLSTS was very pronounced with the increment of residual strength within the range of 18.3% - 30.2% in the second loading and 18.2% - 37.3% in the third loading as compared to that of the mixes reinforced by single type fibres.

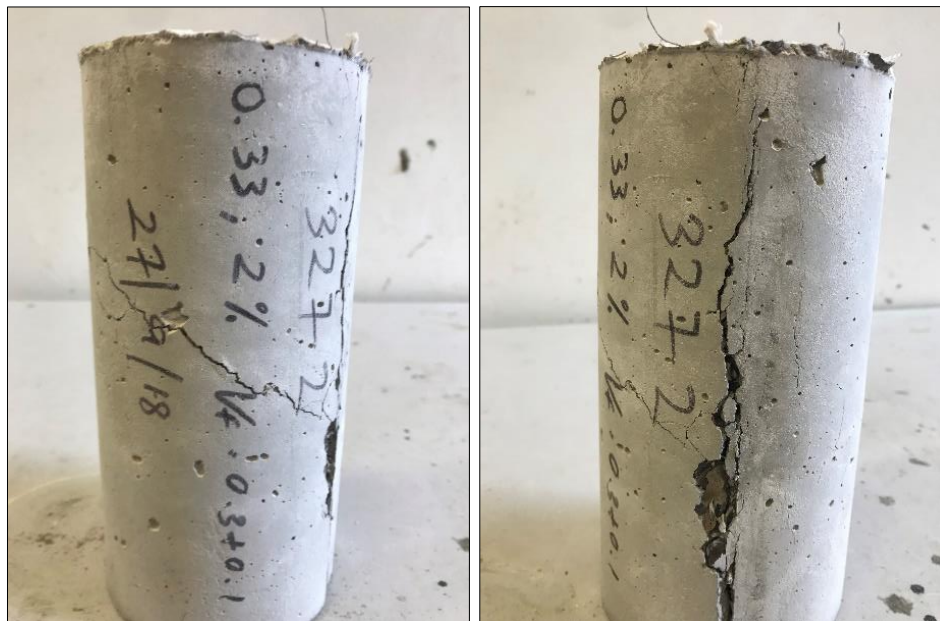


Figure 4.16: Failure Mode of OPSLWC-HYB-0.4% after Third Loading

The failure mode of the fibres reinforced specimens differed from the control mix, as shown in Figure 4.16. Apart from splitting failure, shear failure was occurred as well. This could be the reason explaining the enhancement of RSTS by the fibres. The bridging effect of the fibres was strong enough to

hold the specimen from splitting completely (Behfarnia & Behravan, 2014). This phenomenon provided extra capacity for stress transfer until the occurrence of shear failure.

4.3.3.7 Flexural Strength

Flexural strength, also known as the Modulus of Rapture (MOR) is to test the bending capacity of concrete in terms of tensile strength. As when a beam is under bending, the bottom part of the beam is subjected to tensile stress. Therefore, the tensile strength of the concrete will govern its flexural strength. The flexural strength at 7 and 28-days was investigated in this research.

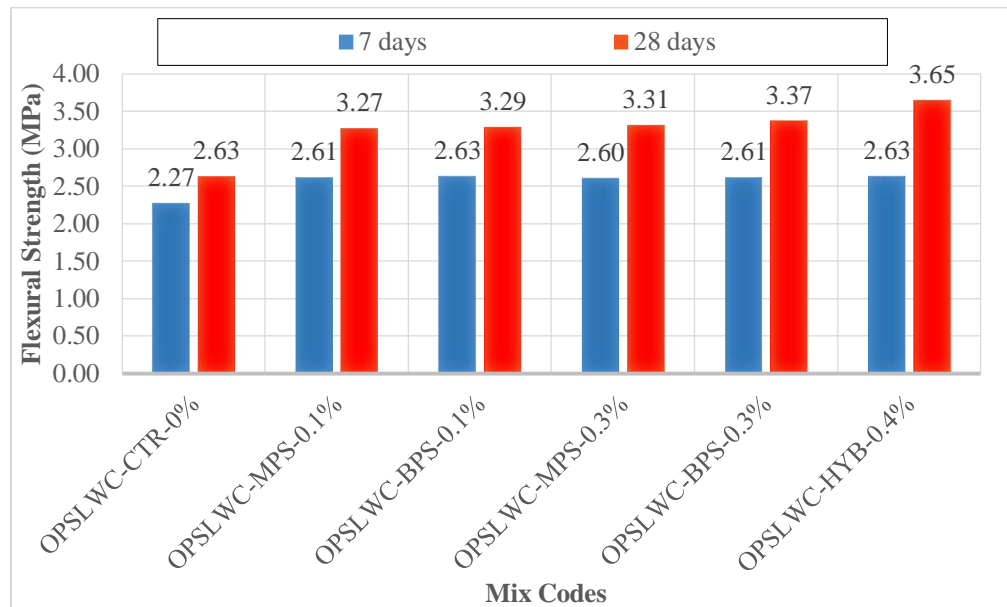


Figure 4.17: Flexural Strength of Different Mixes at 7 and 28-days

From Figure 4.17, the flexural strength increased with the volume fractions of fibres along with concrete age. The inclusion of fibres increased the 7-days flexural strength from 15.0% to 15.9% (2.27 MPa to 2.63 MPa). On

the other hand, the flexural strength at 28-days was enhanced by the fibres within the range of 24.3% to 38.8% (2.63 MPa to 3.65 MPa). The results showed that the incorporation of 0.4% of the hybrid BPS and MPS fibres had the highest improvement of about 38.8% at 28-days.

As the prism specimen is under bending, the tensile behaviour is critical in defining the strength as concrete is brittle and poor in tension. Upon bending, tensile stress will be induced at the bottom of the prism and will cause cracking to start in micro scale. These micro cracks propagated rapidly in parallel direction to the load applied. Without the presence of fibres, the prism split into pieces immediately. Concrete is prone to sudden failure when subjected to bending. Therefore, steel reinforcement is used to compensate the low tensile resistance of concrete in the practical application to prevent sudden structural failure. The presence of fibres acted as an inhibitor to the propagation of cracks. The integration of the cement matrices by the incorporated fibres deteriorated the propagation of cracks. Upon the application of continuous loading, minor cracks started to develop. As these micro cracks propagated and joined together to form macro cracks, the fibres stretched themselves to accommodate the crack face separation. This incident induced the formation of linking bridge to hold the openings by displacing minor cracks. The stretching of fibres allowed stress distribution and additional energy-absorbing mechanism. Eventually, the failure was delayed with greater tolerance of deformation. Thus, the MOR was improved as the consequence of additional load capacity.

The rupture mode of OPSLWC prisms with fibres and without fibres is shown in Figure 4.18. Without fibres, the prism broke into two pieces in a sudden failure. However, the cracking of prism reinforced with fibres was slower and it did not break into two pieces after the test as the fibres inhibited the propagation of cracks and was able to hold it. This explained the improvement in MOR contributed by the fibres.

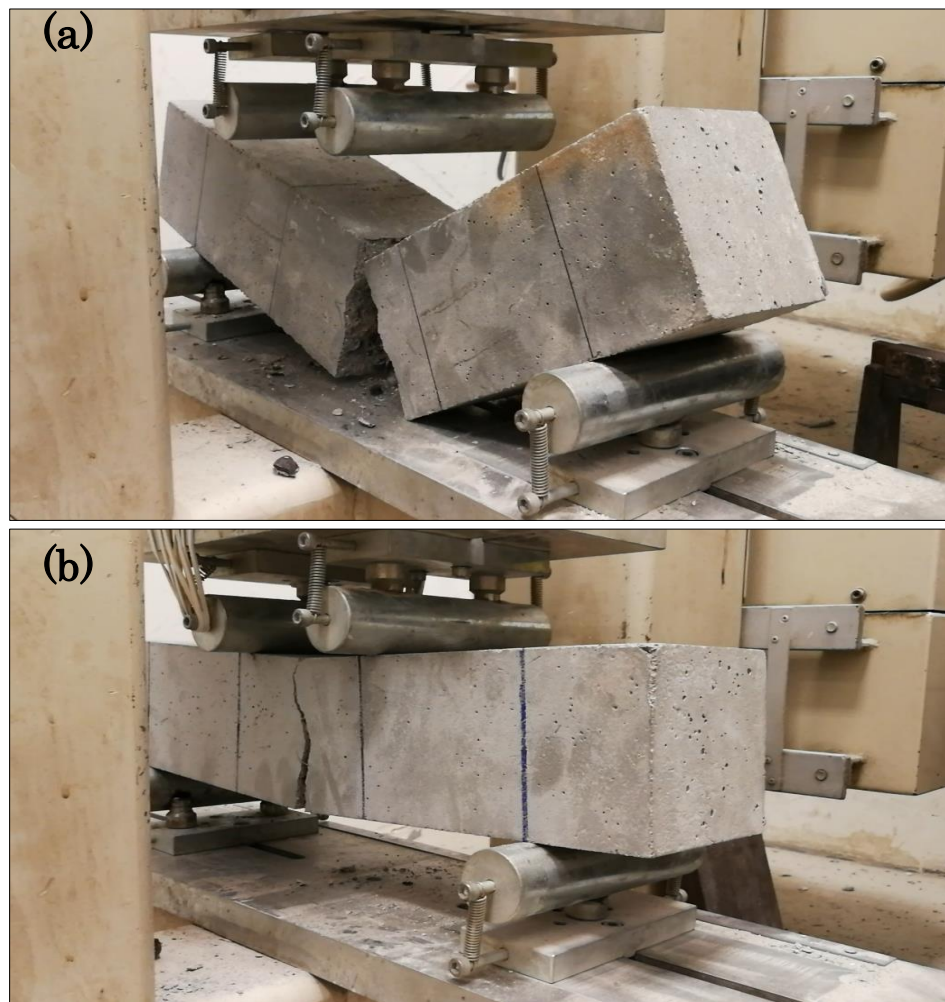


Figure 4.18: Rupture Mode of Prisms (a) without Fibres and (b) with Fibres

4.3.4 Performance Index

Performance index is the measurement of the performance of a material which is characterised by the combination of different material properties in a given application. The performance indices of compressive strength, splitting tensile strength and flexural strength were discussed in this study.

4.3.4.1 Performance Index of Compressive Strength

The average performance index of compressive strength of OPSLWC reinforced with different types of PP fibres of different volume fractions at different ages is presented in Figure 4.19.

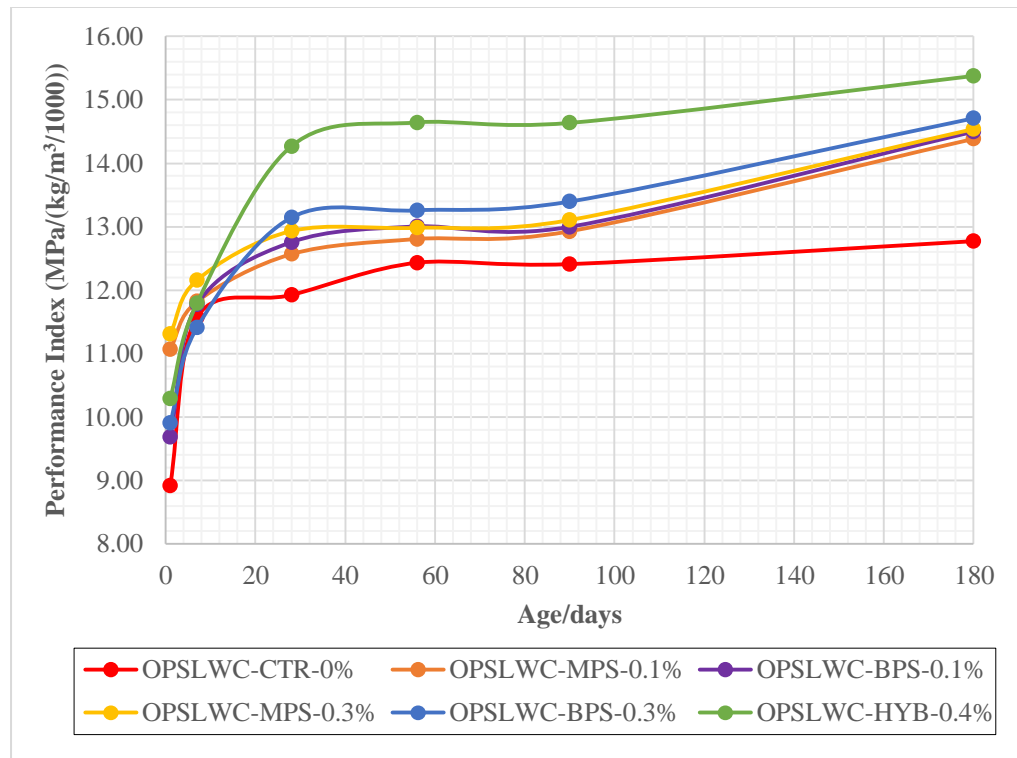


Figure 4.19: Performance Index of Compressive Strength of OPSLWC Reinforced with PP Fibres of Various Volume Fractions at Different Ages

From Figure 4.19, the performance index implied that the compressive strength increased with curing age. From 28-days onwards, the increment of performance index was observed with increasing of volume fractions of fibres added. For 1-day and 7-days, fluctuation of performance index occurred in an irregular trend with the increasing amount of fibres included. This could be due to the instable strength gain in the early age as 28-days strength is the benchmark for mature strength growth. Hence, this minor error can be omitted and declared that the performance index increased with amount of fibres incorporated as referred to the performance index at 28-days, 56-days, 90-days and 180-days.

4.3.4.2 Performance Index of Splitting Tensile Strength

Generally, the performance index of splitting tensile strength increased as the curing ages of the specimens increased. However, the improvement in performance index was insignificant with the reinforcement of fibres. This was explained by the slight enhancement of splitting tensile strength by the added fibres. The reinforcement of fibres was more effective in the upgrade of residual strength. The average performance index of splitting tensile strength of OPSLWC with different volume fractions of PP fibres incorporated at 7-days, 28-days and 90-days is illustrated in Figure 4.20.

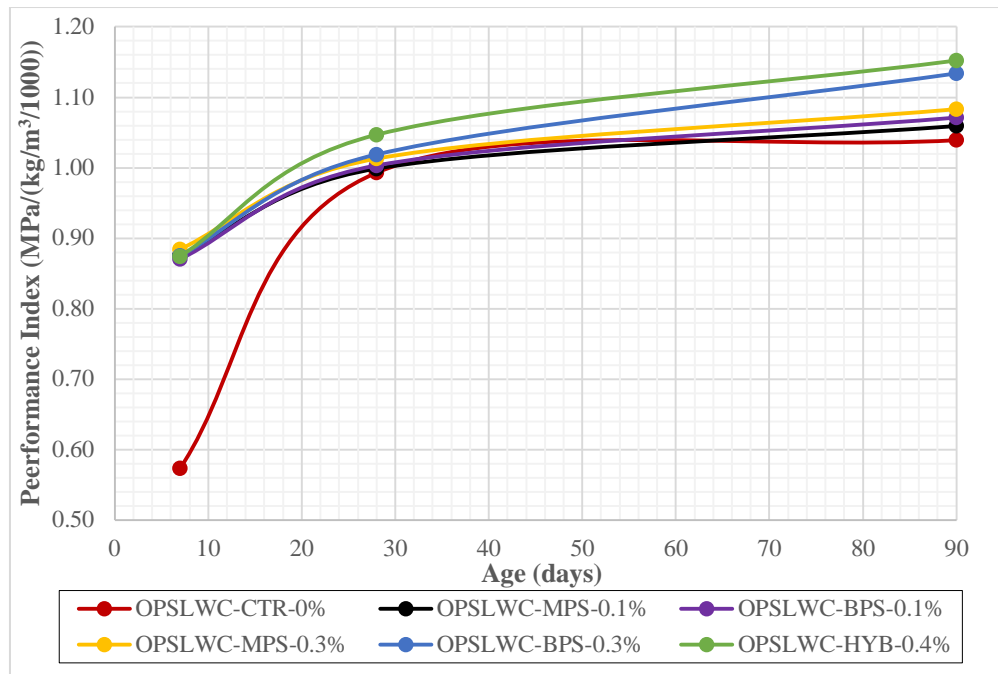


Figure 4.20: Performance Index of Splitting Tensile Strength of OPSSLWC Reinforced with PP Fibres of Various Volume Fractions at Different Ages

4.3.4.3 Performance Index of Flexural Strength

The average performance index of flexural strength of OPSSLWC with different volume fractions of PP fibres incorporated at 7-days and 28-days is presented in Figure 4.21.

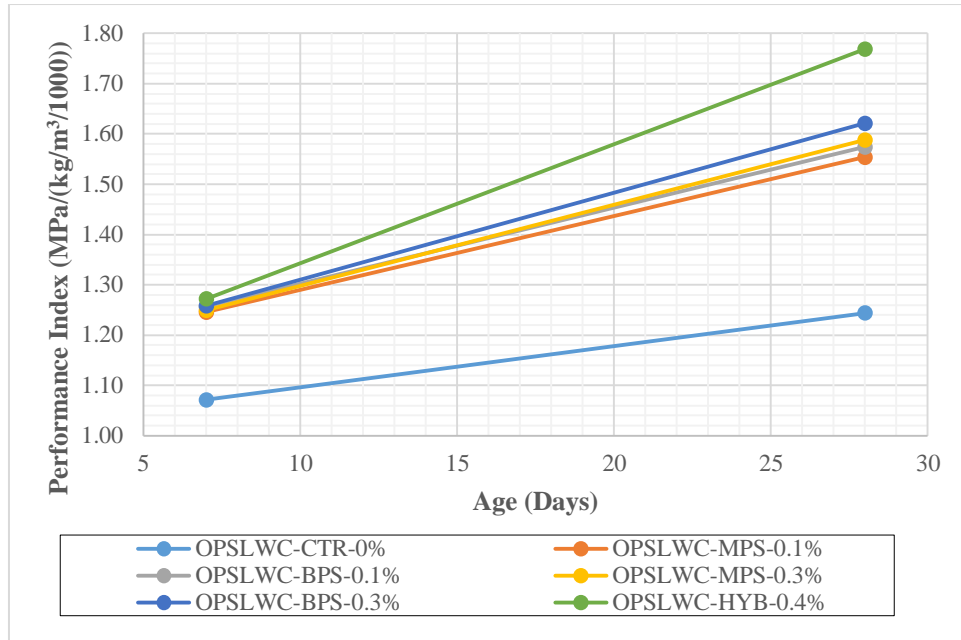


Figure 4.21: Performance Index of Flexural Strength of OPSLWC Reinforced with PP Fibres of Various Volume Fractions at Different Ages

The performance index of flexural strength possessed similar relationship as that of compressive strength and splitting tensile strength just as displayed in Figure 4.21. Higher performance index was obtained in later ages and with higher content of fibres. Referring to the performance index of 28-days, a huge inflation from 1.24 MPa/(kg/m³/1000) to 1.76 MPa/(kg/m³/1000) was found. This implied that the effect of fibres on flexural strength was more significant at higher percentage.

4.3.4 Thermal Properties

Thermal conductivity and temperature gradient were discussed in this section.

4.3.4.1 Thermal Conductivity

The thermal conductivity of OPSLWC with different percentage of fibres is indicated in Figure 4.22. The thermal conductivity inflated with the curing age as the thermal conductivity of 28-days was higher than the thermal conductivity of 7-days of similar mix. This was because voids were present in the mix at the age of 7-days due to the partial hydration of cement (Benmansour, et al., 2014). The further hydration of cement in the mix at 28-days produced calcium silica hydrate to fill up the voids in the mix. Therefore, it resulted in higher thermal conductivity. 28-days thermal conductivity should be discussed instead of 7-days thermal conductivity.

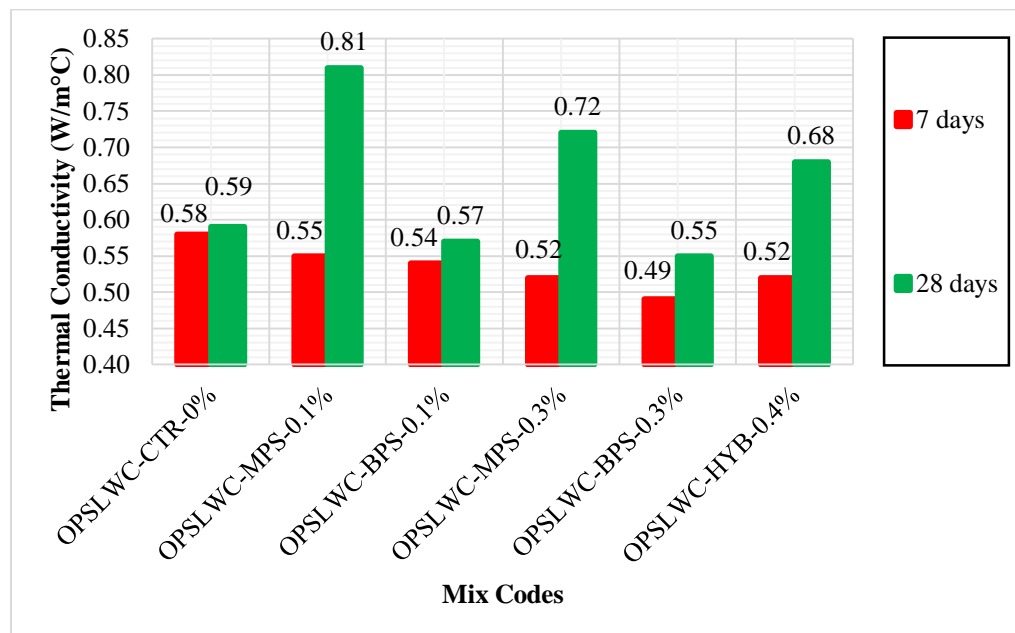


Figure 4.22: Thermal Conductivity of OPSLWC Incorporated with Various Percentage of Fibres at 7-days and 28-days

As displayed in Figure 4.22, the thermal transferability of the control mix at 28-days was 0.59 W/m°C. The 28-days thermal conductivity of

OPSLWC-MPS-0.1% showed the highest at 0.81 W/m°C. Although the fibres incorporated was low in thermal conductivity, but due to the micro geometry and low amount of MPS fibres, their addition could have filled up the voids of the binder matrix and caused the increment of thermal conductivity (Benmansour, et al., 2014) (Mo, et al., 2017b). Meanwhile, the 28-days thermal conductivity of OPSLWC-MPS-0.3% dropped to 0.72 W/m°C. This occurrence could be explained by the filling of the matrix voids exceeded the optimum level due to the increase amount of MPS fibres (Mo, et al., 2017b). The presence of the randomly dispersed extra fibres of low thermal conductivity then decreased the overall thermal conductivity of the specimen (Phelivanli, et al., 2016). However, OPSLWC-BPS-0.1% showed decrement in its 28-days thermal conductivity with a value of 0.57 W/m°C. By increasing the volume fraction of BPS to 0.3%, the 28-days thermal conductivity was further reduced to 0.55 W/m°C. This was because the presence of lower thermal conductivity of BPS fibres randomly distributed in the concrete panel, resulting in lowering the overall thermal conductivity of the panel (Phelivanli, et al., 2016). However, the thermal conductivity of OPSLWC-HYB-0.4% increased to 0.68 W/m°C. This was because the presence of both MPS and BPS fibres, where MPS filled up the voids and caused the rise of the thermal transferability. In contrast, BPS contributed to lower the overall thermal transferability. Thus, the thermal transferability of OPSLWC-HYB-0.4% lied between that of OPSLWC-MPS-0.1% and OPSLWC-BPS-0.3%. In a nutshell, BPS is effective in lowering thermal conductivity with its incorporation; while it is vice versa for the inclusion of MPS at low volume fractions.

4.3.4.2 Temperature Gradient

The temperature gradient test was carried out to test the thermal performance of the specimens under a simulated sun. The results obtained can be taken as an indirect measurement of the thermal conductivity of the specimen. The temperature gradient of OPSLWC with various percentages of fibres is illustrated in Figure 4.23.

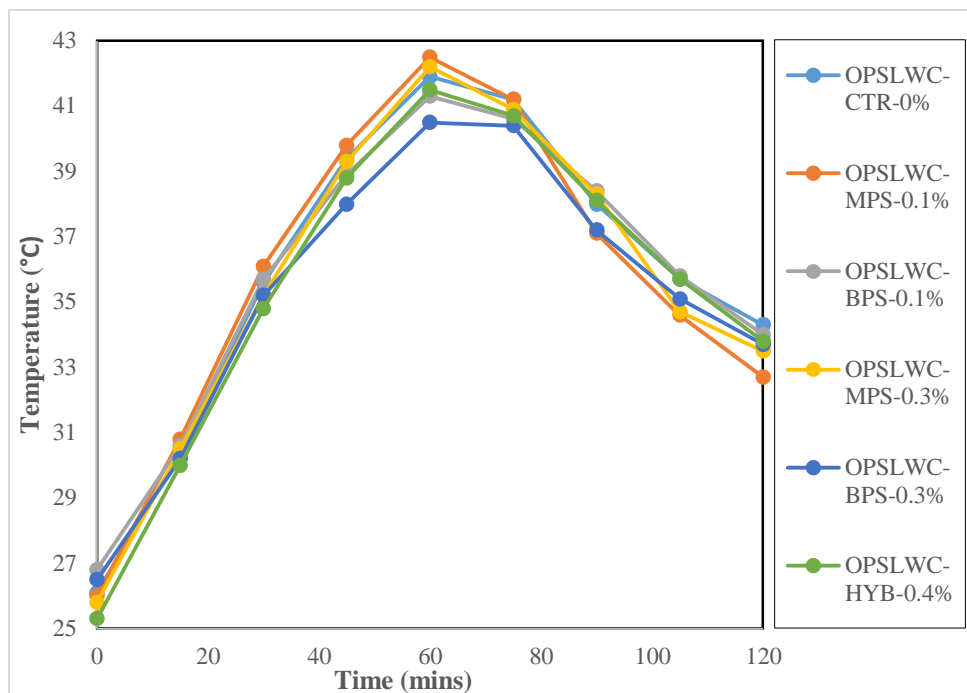


Figure 4.23: Temperature Gradient of OPSLWC with Various Percentages of Fibres

Thermal conductivity is the measure of the ability of a substance to transfer heat. The temperature gained during heating and the temperature loss during cooling are calculated as a measurement for the thermal conductivity of the specimens and are tabulated in Table 4.10. Temperature rise is calculated by subtracting the temperature at 60 minutes by the initial temperature at 0

minutes; the difference between the final temperature at 120 minutes and the temperature at 60 minutes defines the temperature loss.

Table 4.10: Temperature Changes of All Specimens

Mix Code	Temperature Rise, ΔT_H (°C)	Temperature Loss, ΔT_C (°C)
OPSLWC-CTR-0%	15.8	-7.6
OPSLWC-MPS-0.1%	16.5	-9.8
OPSLWC-BPS-0.1%	14.5	-7.3
OPSLWC-MPS-0.3%	16.4	-8.7
OPSLWC-BPS-0.3%	14.0	-6.8
OPSLWC-HYB-0.4%	16.2	-7.7

Based on the temperature changes of the specimens, OPSLWC-MPS-0.1% had the highest temperature changes (gained 16.5°C and lost -9.8°C). The result implied that the heat transfer within OPSLWC-MPS-0.1% is the fastest. It was then followed by OPSLWC-MPS-0.3% with temperature rise of 16.4°C and temperature loss of 8.7°C. The hybrid fibres mix gained 16.2°C after being exposed to the stimulated sun for 60 minutes and lost 7.7°C after being allowed to cool down for the next 60 minutes. Next, the temperature of control mix (OPSLWC-CTR-0%) was increased by 15.8°C and reduced by 7.6°C. Meanwhile, the incorporation of BPS showed the least temperature changes. With the addition of 0.1%, it contributed to 14.5°C of temperature increment and 7.3°C of temperature decrement. The increase in volume fraction of the fibres further reduced the changes of temperature. The

temperature raised 14°C and dropped 6.8°C when 0.3% of BPS was incorporated. It was observed that the trend is similar as the trend in thermal conductivity.

As the surface of the concrete panel was exposed to the bulb, the surface temperature increased because of the heat dissipated by the bulb. As heat transfers from higher temperature region to lower temperature region, the heat will transfer through the body of the concrete panel to the colder opposite surface of the panel, where the thermal probes are placed to record the temperature changes. As heat transports through the body of the panel, it must pass through different types of constituents in the concrete of different thermal properties. When the advancing heat encounters the relatively low thermal conductor incorporated in the concrete, the heat transfer is slowed down. Thus, it explained the lower temperature of the concrete panel with the presence of fibres. Figure 4.24 shows the cross-section of OPSLWC-HYB-0.4% with fibres randomly distributed in the panel.



Figure 4.24: Cross-Section of OPSLWC-HYB-0.4% with Randomly Distributed Fibres

4.4 Summary

During the initial stage, the water-cement ratio of 0.33 was found to be optimum to achieve the required 28-days compressive strength of not lesser than 25 MPa. Due to the inconsistent slump obtained in the initial stage, NMM was proposed and the outcome was compared with the outcome from CMM. The workability and 28-days compressive strength were improved by using the NMM. Thus, all the actual mixes were produced with NMM.

Two different types of PP fibres, MPS and BPS were added singly and hybrid with the designated volume fractions (0.1%, 0.3% and 0.4%) in the second phase. With the increasing volume fractions of fibres incorporated, the fresh density and the workability (slump value and Vebe time) of the mixes was reduced.

The mechanical properties (compressive strength, splitting tensile strength and flexural strength) were enhanced with higher volume fractions of fibres added. The enhancement effect of fibres was more prominent in the flexural strength (24.3% to 38.8% at 28-days). Another remarkable improvement offered by the inclusion of fibres is the post-failure performance. The improvement in residual compressive and splitting tensile strength was significant. Moreover, the combined effect of the hybrid fibres was more pronounced in enhancing the post-failure behaviour. The modification in the failure pattern was also observed with the presence of fibres in the mixes.

The geometrical properties of the fibres administered the effect on the thermal properties of OPSLWC. MPS increased the thermal conductivity of OPSLWC panels; while BPS decreased the thermal conductivity of OPSLWC panels. The micro geometry of MPS filled up the matrix voids; while the macro geometry of BPS did not fill up the matrix voids. As the volume fractions of fibres increases, the thermal conductivity decreases. This is due to the lower thermal conductivity of PP fibres. The presence of the randomly distributed PP fibres decreases the overall thermal conductivity of the panel. This explained the reason of the lower thermal conductivity of OPSLWC-MPS-0.3% than that of OPSLWC-MPS-0.1%. After all the matrix voids had been filled up, the additional randomly distributed MPS fibres decreased the overall thermal conductivity of the panel.

CHAPTER 5

CONCLUSIONS AND RECOMMENDATIONS

5.1 Conclusions

Lightweight aggregate concrete (LWAC) by using renewable oil palm shell (OPS) as coarse aggregate with 28-days cube compressive strength of minimum 25 MPa and with oven-dried density of less than 2000 kg/m³ was developed . With the addition of different types of synthetic polypropylene (PP) fibres, the 28-days cube compressive strength was further improved and the oven-dried density was further reduced. At the same time, the other mechanical properties of oil palm shell lightweight concrete (OPSLWC) and fibre-reinforced oil palm shell lightweight concrete (FROPSLWC) were investigated. The thermal properties, thermal conductivity, k value of OPSLWC and FROPSLWC were compared and were studied by temperature gradient test.

Based on the results obtained from laboratory experimental work, the prescribed objectives were achieved and the following conclusions can be drawn:

1. The oven-dried densities of all plain OPSLWC and fibres reinforced OPSLWC were lower than 2000 kg/m^3 , which fell in the range of 1936.7 kg/m^3 to 1976.5 kg/m^3 .
2. The compressive strengths at 28-days of all mixes were greater than 25 MPa, which fell in the range of 25.02 MPa to 29.38 MPa.
3. The NMM had showed improvement on the workability and the compressive strength in comparison with the CMM. The increment in the range of 3.77% - 5.72% on the 28-days compressive strength was observed.
4. The inclusion of synthetic polypropylene fibres deteriorated the workability. The workability decreases with increasing amount of fibres added. The slump value decreased from 165 cm to 96 cm and the Vebe time increased from 9.46 s to 12.26 s.
5. Incorporation of synthetic polypropylene fibres in OPSLWC offered positive effect on the mechanical properties. The presence of the fibres had modified the failure mode of OPSLWC under compression, splitting tension and flexure.
6. The addition of synthetic polypropylene fibres with the volume fraction of 0.1% to 0.4% had enhanced the compressive strength of OPSLWC in the range of 4.8% - 17.4% and 11.9% - 17.0% on 28-days and 180-days, respectively.
7. The splitting tensile strength of FROPSLWC with the volume fraction of synthetic polypropylene fibres from 0.1% to 0.4% had increased in the range of 0.5% - 3.4% at 28-days and 1.4%-8.7% at 90-days as compared to the splitting tensile strength of control OPSLWC.

8. The reinforcement of synthetic polypropylene fibres with the volume fraction of 0.1%-0.4% had improved the Modulus of Rapture at 28-days by 24.3% to 38.8% as compared to that of the control OPSLWC.
9. The improvement of residual compressive strength of OPSLWC with synthetic polypropylene fibres was more pronounced as compared to the control OPSLWC. The effect on the residual strength was more significant than the effect on the compressive strength.
10. The control OPSLWC had failed completely upon splitting tension. The addition of synthetic polypropylene fibres provided the capacity for residual splitting tensile strength for OPSLWC. The enhancement of residual splitting tensile was most significant in the mix reinforced with hybrid fibres.
11. The thermal conductivity, k values of OPSLWC and FROPSLWC were in the range of 0.49 – 0.58 W/m°C at 7-days; 0.55 – 0.81 W/m°C at 28-days.
12. The effect of the fibres on thermal conductivity varied with the types of fibres added. The thermal conductivity of the panel consisting of Monofilament Polypropylene Straight (MPS) was higher than the control mix panel. Meanwhile, the thermal conductivity of the panel comprising of Barchip Polypropylene Straight (BPS) was lower than the control mix panel. Simultaneously, the thermal conductivity of the panel incorporated with hybrid fibres was lower than that of the control mix panel, but was higher than that of the panel incorporated with BPS. The similar trend was observed from the temperature gradient test.

5.2 Recommendations for Future Research Work

The outcome of this research showed that synthetic polypropylene fibres did contribute positive effects on the mechanical and thermal properties of OPSLWC. However, further study is needed to assure the behaviour of the fibres. Therefore, several recommendations are proposed for future research work in this area:

1. Different volume fractions and different aspect ratio of fibres shall be introduced into OPSLWC.
2. Effects of the incorporation of fibres on the durability of OPSLWC shall be investigated.
3. Influences of the addition of the fibres on the impact resistance of OPSLWC shall be studied.
4. Scanning Electron Microscopy (SEM) shall be carried out to study the effects of fibres on OPSLWC based on the microstructure of the concrete.
5. The parameters for the comparison of CMM and NMM shall be increased to further investigate the advantages of NMM.
6. The effect of different curing methods shall be investigated.
7. The numbers of thermal sensors in temperature gradient test shall be increased to obtain more data for more precise results.
8. Temperature gradient test shall be carried out on actual scale specimens and under real sun condition. The actual scale results shall be compared with the results from laboratory scale.

REFERENCES

- Abang, A., Abang, A., Abdus Salam, S. & Abang, A. R., 1984. Basic Strength Properties of Lightweight Concrete Using Agricultural Wastes as Aggregates. *International Conference on Low Cost Housing for Developing Countries*, pp. 143-146.
- Abbas, Y. M. & Khan, M. I., 2016. Fiber-matrix interactions in fiber-reinforced concrete: a review. *Arabian Journal for Science and Engineering*, 41(4), pp. 1183-1198.
- Abdullah, A., 1996. 10 - Palm Oil Shell Aggregate for Lightweight Concrete. In: S. Chandra, ed. *Waste Materials Used in Concrete Manufacturing*. Westwood, NJ: William Andrew Publishing, pp. 624-636.
- ACI Committee 213, 2014. *Guide for Structural Lightweight-Aggregate Concrete*, Michigan: American Concrete Institute.
- ACI Committee 544, 2002. *Report on Fiber Reinforced Concrete*, s.l.: American Concrete Institute.
- Anagnostopoulos, C. A., 2014. Effect of different superplasticisers on the physical and mechanical properties of cement grouts. *Construction and Building Materials*, Volume 50, pp. 162-168.
- Aslam, M., Shafiqh, P. & Jumaat, M., 2016. Oil-palm by-produces as lightweight aggregate in concrete mixture - A review. *Journal of Cleaner Production*, Volume 126, pp. 56-73.
- ASTM C1609/C1609M-10, 2010. *Standard Test Method for Flexural Performance of Fiber-Reinforced Concrete (Using Beam with Third-Point Loading)*, Pennsylvania: ASTM International.
- ASTM C330/C330M-17a, 2017. *Standard Specification for Lightweight Aggregates for Structural Concrete*, Pennsylvania: ASTM International.
- ASTM C78/C78M -18, 2018. *Standard Test Method for Flexural Strength of Concrete (Using Simple Beam with Third-Point Loading)*, Pennsylvania: ASTM International.
- Banthia, N., Moncef, A., Chokri, K. & Sheng, J., 1995. Uniaxial tensile response of microfibre reinforcement cement composites. *Journal of Materials and Structures RILEM*, 183(28), pp. 507-517.
- Behfarnia, K. & Behravan, A., 2014. Application of high performance polypropylene fibers in concrete lining of water tunnels. *Materials and Design*, Volume 55, pp. 274-279.

Benmansour, N. et al., 2014. Thermal and mechanical performance of natural mortar reinforced with date palm fibers for use as insulating materials in building. *Energy and Buildings*, Volume 81, pp. 98-104.

Betterman, L. R., Ouyang, C. & Shah, S. P., 1995. Fiber-matrix interaction in microfiber-reinforced mortar. *Advanced Cement Based Materials*, 2(53-61), p. 2.

Bothma, J., 2013. *ISI2013-15 - Literature Review on Macro Synthetic Fibres in Concrete*, Stellenbosch: Institute of Structural Engineering, University of Stellenbosch.

Brandt, A., 2008. Fibre reinforced cement-based (FRC) composites after over 40 years of development in building and civil engineering. *Composite Structures*, Volume 86, pp. 3-9.

British Standards Institution, 2001. *BS EN 12664: Thermal Performance of Building Materials and Products. Determination of Thermal Resistance by Means of Guarded Hot Plate and Heat Flow Meter Methods. Dry and Moist Products of Medium and Low Thermal Resistance*. London: British Standards Institution.

British Standards Institution, 2004. *BS EN 12504 - 4: Testing Concrete - Part 4: Determination of Ultrasonic Pulse Velocity*. London: British Standards Institution.

British Standards Institution, 2009. *BS EN 12390 - 6: Testing Hardened Concrete - Part 6: Tensile Splitting Strength of Test Specimens*. London: British Standards Institution.

British Standards Institution, 2019a. *BS EN 12350 - 2 : Testing Fresh Concrete - Part 2: Slump Test*. London: British Standards Institution.

British Standards Institution, 2019b. *BS EN 12350 - 3: Testing Fresh Concrete - Part 3: Vebe Test*. London: British Standards Institution.

British Standards Institution, 2019c. *BS EN 12390 - 3: Testing Hardened Concrete - Part 3: Compressive Strength of Test Specimens*. London: British Standards Institution.

British Standards Institution, 2019d. *BS EN 12390 - 5: Testing Hardened Concrete - Part 5: Flexural Strength of Test Specimens*. London: British Standards Institution.

British Standards Institution, 2019e. *BS EN 12390 - 7: Testing Hardened Concrete - Part 7: Density of Hardened Concrete*. London: British Standards Institution.

British Standards Institution, 2006. *BS EN 14889: Fibres for concrete - Part 2: Polymer fibres - Definitions, specifications and conformity*. United Kingdom: British Standards Institution.

Chandra, S. & Berntsson, L., 2002. *Lightweight Aggregate Concrete*. New York: Noyes Publications.

Concrete Society, 2007a. *TR 63 Guidance for the design of steel-fibre-reinforced concrete*, United Kingdom: Concrete Society.

Concrete Society, 2007b. *TR 65 Guidance on the use of macro-synthetic fibre reinforced concrete*, UK: Concrete Society.

Department of Standards Malaysia, 2007. *Malaysian Standard: Cement - Part 2: Conformity Evaluation*. Putrajaya: Department of Standards Malaysia.

Ezzat, M. et al., 2019. Structure-property relationships for polycarboxylate ether superplasticizers by means of RAFT polymerization. *Journal of Colloid and Interface Science*, Volume 553, pp. 788-797.

Hambali, E. & Rivai, M., 2017. The potential of palm oil waste biomass in Indonesia in 2020 and 2030. *IOP Conference Series: Earth and Environment Science*, Volume 65, pp. 1-9.

Hiremath, P. & Yaragal, S., 2017. Influence of mixing method, speed and duration on the fresh and hardened properties of Reactive Powder Concrete. *Construction and Building Materials*, Volume 141, pp. 271-288.

Jhatial, A. A. et al., 2018. *Effect of polypropylene fibres on the thermal conductivity of lightweight foamed concrete*. s.l., EDP Sciences.

Kakooei, S., Akil, H., Jamshidi, M. & Rouhi, J., 2012. The effects of polypropylene fibres on the properties of reinforced concrete structures. *Construction and Building Materials*, 27(1), pp. 73-77.

Kim, D. J., Naaman, A. E. & El-Tawil, S., 2008. Comparative flexural behaviour of four fibre reinforced cementitious composites. *Cement and Concrete Composites*, 30(10), pp. 917-928.

Kim, Y., Lee, K., Bang, J. & Kwon, S., 2014. Effect of W/C Ration on Durability and Porosity in Cement Mortar with Constant Cement Amount. *Advances in Materials Science and Engineering*, Volume 2014.

Ling, A., 2019. *Global Palm Oil Trade - Prospects and Outlook*. [Online] Available at: http://www.mpob.gov.my/images/stories/pdf/2019/2019_1Palm%20Oil%20Global%20Trade.pdf [Accessed 23 July 2019].

Madhavi, T. C., Raju, L. S. & Mathur, D., 2014. Polypropylene fiber reinforced concrete - a review. *International Journal of Emerging Technology and Advanced Engineering*, 4(4), pp. 114-119.

Malaysian Palm Oil Board, 2018a. *Fresh fruit bunch (FFB) received by mill for the month of December 2018*. [Online] Available at: <http://bepi.mpob.gov.my/index.php/en/statistics/sectoral-status/190-sectoral-status-2018/862-ffb-received-by-mill-2018.html> [Accessed 23 July 2019].

Malaysian Palm Oil Board, 2018b. *Production of Crude Palm Oil for the Month of December 2018*. [Online] Available at: <http://bepi.mpob.gov.my/index.php/en/statistics/production/186-production-2018/850-production-of-crude-oil-palm-2018.html> [Accessed 23 July 2019].

Mannan, M. A. & Ganapathy, C., 2004. Concrete from an agricultural waste-oil palm shell (OPS). *Building and Environment*, 39(4), pp. 441-448.

Manolis, G. D., Gareis, P. J. & Tsonos, A. D. N. J. A., 1997. Dynamic properties of polypropylene-fiber-reinforced concrete slabs. *Cement and Concrete Composites*, 19(4), pp. 341-349.

Mo, K. H. et al., 2014a. Impact resistance of hybrid fibre-reinforced oil palm shell concrete. *Construction and Building Materials*, 50(0), pp. 499-507.

Mo, K. H., Yap, K. K. Q., Alengaram, U. J. & Jumaat, M. Z., 2014b. The effect of steel fibres on the enhancement of flexural and compressive toughness and fracture characteristics of oil palm shell concrete. *Construction and Building Materials*, Volume 55, pp. 20-28.

Mo, K. H., Chin, T. S., Alengaram, U. J. & Jumaat, M. Z., 2016. Material and structural properties of waste-oil palm shell concrete incorporating ground granulated blast-furnace slag reinforced with low-volume steel fibres. *Journal of Cleaner Production*, Volume 133, pp. 414-426.

Mo, K. H. et al., 2017a. Shear behaviour and mechanical properties of steel fibre-reinforced cement-based and geopolymer oil palm shell lightweight aggregate concrete. *Construction and Building Materials*, Volume 148, pp. 369-375.

Mo, K. H. et al., 2017b. Thermal conductivity, compressive and residual strength evaluation of polymer fibre-reinforced high volume palm oil fuel ash blended mortar. *Construction and Building Materials*, Volume 130, pp. 113-121.

Naaman, A., 2003. Engineered Steel Fibers with Optimal Properties for Reinforcement of Cement Composites. *Journal of Advanced Concrete Technology*, 1(3), pp. 241-252.

Nagaraj, T. & Banu, Z., 1996. Generalization of Abrams' Law. *Cement and Concrete Research*, 26(6), pp. 933-942.

Nemati, K. M., 2015. *Progress in Concrete Technology - Fiber Reinforced Concrete (FRC)*. [Online] Available at: <http://courses.washington.edu/cm425/frc.pdf> [Accessed 23 July 2019].

Neville, A., 2011. *Properties of concrete*. 5th ed. London: Pearson Education Limited.

Neville, A. M. & Brooks, J. J., 2010. *Concrete Technology*. 2nd ed. Harlow: Pearson Education Limited.

Newman, J. & Owens, P., 2003. Properties of Lightweight Concrete. In: J. Newman & B. Choo, eds. *Advanced Concrete Technology. Processes*. Oxford: Butterworth - Heinemann, pp. 3-29.

Nurhayati, A. & Fauziah, S., 2013. The Oil Palm Wastes in Malaysia. In: M. D. Matovic, ed. *Biomass Now - Sustainable Growth and Use*. Rijeka: InTech, pp. 75-100.

Okpala, D. C., 1990. Palm kernel shell as a lightweight aggregate in concrete. *Building and Environment*, 25(4), pp. 291-296.

Pelisser, F., Neto, A. B. D. S. S., Rovere, H. L. L. & Pinto, R. C. D. A., 2010. Effect of the addition of synthetic fibers to concrete thin slabs on plastic shrinkage cracking. *Construction and Building Materials*, 24(11), pp. 2171-2176.

Peng, J. et al., 2015. Influence of superplasticizer on the rheology of fresh cement asphalt paste. *Case Studies in Construction Materials*, Volume 3, pp. 9-18.

Phang, K. & Lau, S., 2017. A Survey on the Usage of Biomass Wastes from Palm Oil Mills on Sustainable Development of Oil Palm Plantations in Sarawak. *IOP Conference Series: Materials Science and Engineering*, Volume 206, p. 15.

Phelivanli, Z. O., Uzun, I., Yucel, Z. P. & Demir, I., 2016. The effect of different fiber reinforcement on the thermal and mechanical properties of autoclaved aerated concrete. *Construction and Building Materials*, Volume 112, pp. 325-330.

Qian, C. X. & Stroeven, P., 2000. Development of hybrid polypropylene-steel fibre-reinforced concrete. *Cement and Concrete Research*, 30(1), pp. 63-69.

Richardson, J., 2003. Precast concrete structural elements . In: J. Newman & B. S. Choo, eds. *Advanced Concrete Technology Set*. Oxford: Butterworth-Heinemann, pp. 3-46.

Rossi, P., 1982. Ultra-high performance fibre-reinforced concretes. In: *Concrete international*. s.l.:s.n., pp. 46-52.

- Saeed, K., 1995. Technique of multi-step concrete mixing. *Materials and Structures*, 28(4), pp. 230-234.
- Sahmaran, M., Yurtseven, A. & Ozgur Yaman, I., 2005. Workability of hybrid fibre reinforced self-compacting concrete. *Building and Environment*, 40(12), pp. 1672-1677.
- Serri, E., Mydin, M. A. O. & Suleiman, M. Z., 2014. Thermal properties of oil palm shell lightweight concrete with different mix designs. *Jurnal Teknologi*, 70(1), pp. 155-159.
- Shafigh, P., Jumaat, M. & Mahmud, H., 2010. Mix design and mechanical properties of oil palm shell lightweight aggregate concrete: A review. *International Journal of the Physical Sciences*, 5(14), pp. 2127-2134.
- Shafigh, P., Jumaat, M. Z. & Mahmud, H., 2011a. Oil palm shell as a lightweight aggregate for production high strength lightweight concrete. *Construction Building Material*, Volume 25, pp. 1848-1853.
- Shafigh, P., Jumaat, M. Z., Mahmud, H. & Alengaram, U. J., 2011b. A new method of producing high strength oil palm shell lightweight concrete. *Materials & Design*, 32(10), pp. 4839-4843.
- Shafigh, P., Mahmud, H. & Jumaat, M. Z., 2011c. Effect of steel fibre on the mechanical properties of oil palm shell lightweight concrete. *Materials & Design*, 32(7), pp. 3926-3932.
- Shafigh, P., Mahmud, H., Jumaat, M. Z. & Zargar, M., 2014. Agricultural wastes as aggregate in concrete mixtures - A review. *Construction and Building Materials*, Volume 53, pp. 110-117.
- Shah, S. P., 1991. Do fibres increase the tensile strength of cement-based matrixes. *ACI Materials Journal*, 88(6), pp. 595-602.
- Shah, S. P. & Rangan, B. V., 1971. Fiber reinforced concrete properties. *ACI Journal Proceedings*, 68(2), pp. 126-135.
- Shi, C., Wu, Z., Lv, K. & Wu, L., 2015. A Review on Mixture Design Methods for Self-compacting Concrete. *Construction and Building Materials*, Volume 84, pp. 387-398.
- Silva, D. A. et al., 2005. Degradation of recycled PET fibres in Portland cement-based materials. *Cement and Concrete Research*, 35(9), pp. 1741-1746.
- Singh, R. et al., 2013. Oil palm genome sequence reveals divergence of interfertile species in Old and New worlds. *Nature*, Volume 500, pp. 335-339.

Smarzewski, P., 2019. Analysis of Failure Mechanics in Hybrid Fibre-Reinforced High-Performance Concrete Deep Beams with and without Openings. *Materials*, 12(1), p. 101.

Song, P., Hwang, S. & Sheu, B., 2005. Strength properties of nylon- and polypropylene-fiber-reinforced concretes. *Cement and Concrete Research*, Volume 35, pp. 1546-1550.

Sujivorakul, C. & Naaman, A., 2003. Modelling bond components of deformed steel fibres in FRC composites. In: A. Naaman & H. Reinhardt, eds. *PRO 30: 4th International RILEM Workshop on High Performance Fiber Reinforced Cement Composites (HPFRCC 4)*. USA: RILEM Publications, pp. 35-48.

Tasek Corporation Berhad, 2019. *Cement Quality*. [Online] Available at: http://www.tasekcement.com/index/cement_facts/cement_quality.html [Accessed 23 July 2019].

Teo, D. C. L., Mannan, M. A. & Kurian, V. J., 2006. Structural concrete using oil palm shell (OPS) as lightweight aggregate. *Turkish Journal of Engineering and Environmental Sciences*, 30(4), pp. 251-257.

Teo, D. C. L., Mannan, M. A., Kurian, V. J. & Ganapathy, C., 2007. Lightweight concrete made from oil palm shell (OPS): Structural bond and durability properties. *Building and Environment*, 42(7), pp. 2614-2621.

The Freedonia Group, 2016. *World Construction Aggregates - Industry Study 3389*, United States: The Freedonia Group .

Won, J. P. et al., 2009. Performance of synthetic macrofibres in reinforced concrete for tunnel linings. *Magazine of Concrete Research*, 61(3), pp. 165-172.

Xu, G., Magnani, S. & Hannant, D. J., 1998. Durability of hybrid polypropylene-glass fibre cement corrugated sheets. *Cement and Concrete Composites*, 20(1), pp. 79-84.

Yahaghi, J., Muda, Z. C. & Beddu, S., 2016. Impact resistance of oil palm shells reinforced with polypropylene fibre. *Construction and Building Materials*, Volume 123, pp. 394-403.

Yap, S. P., Alengaram, U. J. & Jumaat, M. Z., 2013. Enhancement of mechanical properties in polypropylene- and nylon- fibre reinforced oil palm shell concrete. *Materials and Design*, Volume 49, pp. 1034-1041.

Yap, S. P. et al., 2014. Flexural toughness characteristics of steel-polypropylene hybrid fibre reinforced oil palm shell concrete. *Materials & Design*, Volume 57, pp. 652-659.

- Yap, S. P., Alengaram, U. & Jumaat, M. Z., 2016. The effect of aspect ratio and volume fraction on mechanical properties of steel fibre-reinforced oil palm shell concrete. *Journal of Civil Engineering and Management*, 22(2), pp. 168-177.
- Yap, S. P., Alengaram, U. J., Mo, K. H. & Jumaat, M. Z., 2019. Ductility behaviours of oil palm shell steel fibre-reinforced concrete beams under flexural loading. *European Journal of Environmental and Civil Engineering*, 23(7), pp. 866-878.
- Yew, M. K., Mahmud, H., Ang, B. C. & Yew, M. C., 2015a. Influence of different types of polypropylene fibre on the mechanical properties of high-strength oil palm shell lightweight concrete. *Construction and Building Materials*, Volume 90, pp. 36-43.
- Yew, M. K., Mahmud, H., Ang, B. C. & Yew, M. C., 2015b. Effects of low volume fraction of polyvinyl alcohol fibers on the mechanical properties of oil palm shell lightweight concrete. *Advances in Materials Science and Engineering*, Volume 2015, pp. 1-11.
- Yew, M. K. et al., 2015c. Effects of polypropylene twisted bundle fibers on the mechanical properties of high-strength oil palm shell lightweight. *Materials and Structures*, 49(4), pp. 1221-1233.
- Yew, M. K. et al., 2018. Influence of high performance hybrid polyvinyl alcohol-polypropylene fibres on mechanical properties of oil palm shell lightweight concrete. *Journal of Advanced Research in Applied Mechanics*, 49(1), pp. 1-11.
- Yew, M. K., Mahmud, H., Ang, B. C. & Yew, M. C., 2014. Effects of Oil Palm Shell Coarse Aggregate Species on High Strength Lightweight Concrete. *The Scientific World Journal*, Volume 2014, p. 12.
- Yew, M. K. et al., 2011. Strength properties of hybrid nylon-steel and polypropylene-steel Fibre reinforced high strength concrete at low volume fraction. *International Journal of Physical Sciences*, 6(33), pp. 7584-7588.
- Zhang, P. et al., 2019. Shell powder as a novel bio-filler for thermal insulation coatings. *Chinese Journal of Chemical Engineering*, 27(2), pp. 452-458.
- Zollo, R. F., 1997. Fiber-reinforced concrete: an overview after 30 years of development. *Cement and Concrete Composites*, 19(2), pp. 107-122.

APPENDICES

APPENDIX A

CALCULATIONS FOR THERMAL CONDUCTIVITY

Table A1: Thermal Conductivity for OPSLWC-CTR-0% Panel at 7-days

Hours	Heat Flow, Q (W)	Avg Hot Plate Temp	Avg Cold Plate Temp	Avg Temp Different, ΔT (K)	Area, A (m ²)	Thickness, L (m)	Thermal Conductivity, K (W·K ⁻¹ ·m ⁻¹)
1	20.00	38.22	22.55	15.67	0.09	0.05	0.71
2	14.82	38.12	22.67	15.45	0.09	0.05	0.53
3	10.14	38.10	22.77	15.34	0.09	0.05	0.37
4	15.26	38.10	22.55	15.55	0.09	0.05	0.54
5	20.07	38.12	22.67	15.45	0.09	0.05	0.72
6	14.79	38.09	22.76	15.33	0.09	0.05	0.54
7	15.00	38.09	22.55	15.54	0.09	0.05	0.54

8	15.02	38.10	22.71	15.39	0.09	0.05	0.54
9	14.90	38.11	22.74	15.37	0.09	0.05	0.54
10	14.97	38.12	22.57	15.55	0.09	0.05	0.53
11	20.29	38.12	22.65	15.46	0.09	0.05	0.73
12	10.23	38.13	22.68	15.45	0.09	0.05	0.37
13	9.94	38.11	22.52	15.59	0.09	0.05	0.35
14	19.90	38.11	22.61	15.49	0.09	0.05	0.71
15	24.78	38.15	22.60	15.56	0.09	0.05	0.88
16	19.94	38.16	22.50	15.66	0.09	0.05	0.71
17	19.57	38.14	22.60	15.54	0.09	0.05	0.70
18	15.12	38.14	22.42	15.72	0.09	0.05	0.53
19	14.77	38.11	22.58	15.54	0.09	0.05	0.53
20	14.72	38.10	22.39	15.71	0.09	0.05	0.52
AVG		38.12	22.60				0.58

Table A2: Thermal Conductivity for OPSLWC-MPS-0.1% Panel at 7-days

Hours	Heat Flow, Q (W)	Avg Hot Plate Temp	Avg Cold Plate Temp	Avg Temp Different, ΔT (K)	Area, A (m ²)	Thickness, L (m)	Thermal Conductivity, K (W·K ⁻¹ ·m ⁻¹)
1	19.96	38.10	21.43	16.67	0.09	0.05	0.67
2	15.17	38.13	21.64	16.49	0.09	0.05	0.51
3	20.16	38.15	21.46	16.69	0.09	0.05	0.67
4	15.11	38.14	21.55	16.59	0.09	0.05	0.51
5	15.02	38.13	21.61	16.52	0.09	0.05	0.51
6	19.92	38.14	21.44	16.70	0.09	0.05	0.66
7	20.21	38.14	21.66	16.48	0.09	0.05	0.68
8	10.21	38.15	21.49	16.66	0.09	0.05	0.34
9	20.08	38.13	21.62	16.50	0.09	0.05	0.68
10	15.09	38.13	21.75	16.39	0.09	0.05	0.51
11	20.08	38.15	21.54	16.61	0.09	0.05	0.67
12	19.93	38.18	21.71	16.47	0.09	0.05	0.67
13	14.88	38.19	21.65	16.54	0.09	0.05	0.50
14	9.97	38.22	21.61	16.60	0.09	0.05	0.33
15	14.64	38.18	21.70	16.48	0.09	0.05	0.49

16	14.75	38.15	21.63	16.53	0.09	0.05	0.50
17	14.84	38.18	21.72	16.46	0.09	0.05	0.50
18	10.10	38.18	21.70	16.49	0.09	0.05	0.34
19	15.14	38.17	21.65	16.52	0.09	0.05	0.51
20	19.76	38.15	21.77	16.38	0.09	0.05	0.67
AVG		38.16	21.62				0.55

Table A3: Thermal Conductivity for OPSLWC-BPS-0.1% Panel at 7-days

Hours	Heat Flow, Q (W)	Avg Hot Plate Temp	AvgCold Plate Temp	Avg Temp Different, ΔT (K)	Area, A (m ²)	Thickness, L (m)	Thermal Conductivity, K (W·K ⁻¹ ·m ⁻¹)
1	14.72	38.01	21.99	16.02	0.09	0.05	0.51
2	19.12	38.03	22.21	15.82	0.09	0.05	0.67
3	14.88	38.05	22.03	16.03	0.09	0.05	0.52
4	19.84	38.04	22.11	15.92	0.09	0.05	0.69
5	10.08	38.03	22.17	15.85	0.09	0.05	0.35
6	14.98	38.04	22.01	16.03	0.09	0.05	0.52

7	19.95	38.04	22.22	15.82	0.09	0.05	0.70
8	10.02	38.05	22.06	15.99	0.09	0.05	0.35
9	15.10	38.03	22.19	15.84	0.09	0.05	0.53
10	20.00	38.03	22.31	15.72	0.09	0.05	0.71
11	25.14	38.05	22.10	15.95	0.09	0.05	0.88
12	19.72	38.08	22.28	15.81	0.09	0.05	0.69
13	15.16	38.09	22.22	15.87	0.09	0.05	0.53
14	14.83	38.12	22.18	15.94	0.09	0.05	0.52
15	9.99	38.08	22.27	15.82	0.09	0.05	0.35
16	14.78	38.05	22.19	15.86	0.09	0.05	0.52
17	15.21	38.08	22.29	15.79	0.09	0.05	0.54
18	10.19	38.08	22.26	15.82	0.09	0.05	0.36
19	9.94	38.07	22.22	15.85	0.09	0.05	0.35
20	15.08	38.05	22.34	15.71	0.09	0.05	0.53
AVG		38.06	22.18				0.54

Table A4: Thermal Conductivity for OPSLWC-MPS-0.3% Panel at 7-days

Hours	Heat Flow, Q (W)	Avg Hot Plate Temp	AvgCold Plate Temp	Avg Temp Different, ΔT (K)	Area, A (m ²)	Thickness, L (m)	Thermal Conductivity, K (W·K ⁻¹ ·m ⁻¹)
1	15.08	37.93	22.82	15.11	0.09	0.05	0.55
2	10.12	38.08	22.84	15.23	0.09	0.05	0.37
3	19.82	38.04	22.85	15.20	0.09	0.05	0.72
4	14.92	37.95	22.85	15.10	0.09	0.05	0.55
5	14.58	38.05	22.85	15.20	0.09	0.05	0.53
6	14.95	38.03	22.84	15.19	0.09	0.05	0.55
7	14.80	38.00	22.85	15.15	0.09	0.05	0.54
8	14.87	38.01	22.84	15.17	0.09	0.05	0.54
9	5.00	38.06	22.85	15.21	0.09	0.05	0.18
10	14.84	38.00	22.84	15.16	0.09	0.05	0.54
11	14.96	37.98	22.84	15.14	0.09	0.05	0.55
12	9.73	38.05	22.85	15.20	0.09	0.05	0.36
13	10.21	38.05	22.84	15.21	0.09	0.05	0.37
14	19.64	38.01	22.84	15.16	0.09	0.05	0.72
15	9.98	38.03	22.85	15.18	0.09	0.05	0.37

16	19.48	38.06	22.84	15.21	0.09	0.05	0.71
17	14.81	38.01	22.85	15.17	0.09	0.05	0.54
18	19.64	38.05	22.85	15.20	0.09	0.05	0.72
19	14.70	38.11	22.84	15.27	0.09	0.05	0.53
20	14.78	38.11	22.84	15.27	0.09	0.05	0.54
AVG		38.03	22.84				0.52

Table A5: Thermal Conductivity for OPSLWC-BPS-0.3% Panel at 7-days

Hours	Heat Flow, Q (W)	Avg Hot Plate Temp	Avg Cold Plate Temp	Avg Temp Different, ΔT (K)	Area, A (m ²)	Thickness, L (m)	Thermal Conductivity, K (W·K ⁻¹ ·m ⁻¹)
1	10.04	38.36	21.89	16.47	0.09	0.05	0.34
2	15.20	38.38	21.90	16.47	0.09	0.05	0.51
3	14.99	38.44	21.92	16.52	0.09	0.05	0.50
4	9.98	38.47	21.93	16.54	0.09	0.05	0.33
5	19.81	38.42	21.91	16.51	0.09	0.05	0.67
6	9.92	38.44	21.91	16.53	0.09	0.05	0.33

7	15.01	38.51	21.90	16.61	0.09	0.05	0.50
8	19.86	38.48	21.90	16.57	0.09	0.05	0.67
9	14.99	38.53	21.89	16.64	0.09	0.05	0.50
10	19.97	38.50	21.90	16.60	0.09	0.05	0.67
11	19.78	38.46	21.89	16.57	0.09	0.05	0.66
12	14.95	38.48	21.89	16.59	0.09	0.05	0.50
13	19.95	38.53	21.89	16.64	0.09	0.05	0.67
14	5.06	38.50	21.88	16.62	0.09	0.05	0.17
15	15.17	38.47	21.89	16.58	0.09	0.05	0.51
16	14.87	38.56	21.89	16.67	0.09	0.05	0.50
17	9.99	38.54	21.89	16.66	0.09	0.05	0.33
18	9.98	38.55	21.89	16.65	0.09	0.05	0.33
19	20.12	38.55	21.89	16.66	0.09	0.05	0.67
20	15.03	38.58	21.89	16.69	0.09	0.05	0.50
AVG		38.49	21.90				0.49

Table A6: Thermal Conductivity for OPSLWC-HYB-0.4% Panel at 7-days

Hours	Heat Flow, Q (W)	Avg Hot Plate Temp	Avg Cold Plate Temp	Avg Temp Different, ΔT (K)	Area, A (m ²)	Thickness, L (m)	Thermal Conductivity, K (W·K ⁻¹ ·m ⁻¹)
1	14.95	37.63	22.72	14.91	0.09	0.05	0.56
2	10.01	37.78	22.74	15.03	0.09	0.05	0.37
3	19.95	37.74	22.75	15.00	0.09	0.05	0.74
4	9.89	37.65	22.75	14.90	0.09	0.05	0.37
5	10.03	37.75	22.75	15.00	0.09	0.05	0.37
6	9.90	37.73	22.74	14.99	0.09	0.05	0.37
7	14.84	37.70	22.75	14.95	0.09	0.05	0.55
8	9.74	37.71	22.74	14.97	0.09	0.05	0.36
9	9.95	37.76	22.75	15.01	0.09	0.05	0.37
10	19.89	37.70	22.74	14.96	0.09	0.05	0.74
11	10.16	37.68	22.74	14.94	0.09	0.05	0.38
12	10.14	37.75	22.75	15.00	0.09	0.05	0.38
13	14.91	37.75	22.74	15.01	0.09	0.05	0.55
14	19.95	37.71	22.74	14.96	0.09	0.05	0.74
15	9.89	37.73	22.75	14.98	0.09	0.05	0.37

16	20.10	37.76	22.74	15.01	0.09	0.05	0.74
17	14.89	37.71	22.75	14.97	0.09	0.05	0.55
18	19.74	37.75	22.75	15.00	0.09	0.05	0.73
19	15.09	37.81	22.74	15.07	0.09	0.05	0.56
20	14.87	37.81	22.74	15.07	0.09	0.05	0.55
AVG		37.73	22.74				0.52

Table A7: Thermal Conductivity for OPSLWC-CTR-0% Panel at 28-days

Hours	Heat Flow, Q (W)	Avg Hot Plate Temp	AvgCold Plate Temp	Avg Temp Different, ΔT (K)	Area, A (m ²)	Thickness, L (m)	Thermal Conductivity, K (W·K ⁻¹ ·m ⁻¹)
1	19.51	37.86	22.42	15.44	0.09	0.05	0.70
2	24.87	37.92	22.46	15.46	0.09	0.05	0.89
3	10.10	37.94	22.52	15.42	0.09	0.05	0.36
4	19.96	37.91	22.58	15.33	0.09	0.05	0.72
5	24.82	37.93	22.65	15.28	0.09	0.05	0.90
6	15.06	37.90	22.87	15.04	0.09	0.05	0.56
7	14.84	37.94	23.03	14.91	0.09	0.05	0.55

8	20.15	37.92	23.05	14.87	0.09	0.05	0.75
9	15.05	37.94	23.06	14.88	0.09	0.05	0.56
10	10.06	37.97	23.06	14.91	0.09	0.05	0.37
11	5.03	37.93	23.06	14.87	0.09	0.05	0.19
12	10.08	37.94	23.06	14.88	0.09	0.05	0.38
13	20.06	37.97	23.07	14.91	0.09	0.05	0.75
14	14.95	37.92	23.07	14.85	0.09	0.05	0.56
15	20.06	37.96	23.07	14.89	0.09	0.05	0.75
16	9.97	37.96	23.08	14.89	0.09	0.05	0.37
17	19.67	37.91	23.07	14.84	0.09	0.05	0.74
18	25.00	37.96	23.09	14.87	0.09	0.05	0.93
19	5.06	37.98	23.09	14.89	0.09	0.05	0.19
20	15.00	37.97	23.07	14.90	0.09	0.05	0.56
AVG		37.94	22.92				0.59

Table A8: Thermal Conductivity for OPSLWC-MPS-0.1% Panel at 28-days

Hours	Heat Flow, Q (W)	Avg Hot Plate Temp	AvgCold Plate Temp	Avg Temp Different, ΔT (K)	Area, A (m ²)	Thickness, L (m)	Thermal Conductivity, K (W·K ⁻¹ ·m ⁻¹)
1	14.92	37.47	22.10	15.37	0.09	0.05	0.54
2	24.94	37.52	22.15	15.38	0.09	0.05	0.90
3	19.88	37.52	22.20	15.32	0.09	0.05	0.72
4	24.74	37.53	22.19	15.33	0.09	0.05	0.90
5	19.91	37.55	22.19	15.36	0.09	0.05	0.72
6	15.11	37.56	22.20	15.36	0.09	0.05	0.55
7	20.16	37.54	22.20	15.34	0.09	0.05	0.73
8	25.02	37.53	22.21	15.32	0.09	0.05	0.91
9	19.98	37.57	22.21	15.36	0.09	0.05	0.72
10	19.94	37.56	22.21	15.35	0.09	0.05	0.72
11	29.96	37.55	22.22	15.33	0.09	0.05	1.09
12	30.11	37.56	22.23	15.33	0.09	0.05	1.09
13	15.16	37.55	22.23	15.32	0.09	0.05	0.55
14	30.11	37.55	22.23	15.32	0.09	0.05	1.09
15	20.03	37.57	22.24	15.33	0.09	0.05	0.73

16	29.90	37.53	22.24	15.29	0.09	0.05	1.09
17	19.68	37.57	22.22	15.35	0.09	0.05	0.71
18	29.75	37.58	22.22	15.36	0.09	0.05	1.08
19	14.69	37.59	22.19	15.40	0.09	0.05	0.53
20	24.65	37.58	22.19	15.39	0.09	0.05	0.89
AVG		37.55	22.20				0.81

Table A9: Thermal Conductivity for OPSLWC-BPS-0.1% Panel at 28-days

Hours	Heat Flow, Q (W)	Avg Hot Plate Temp	AvgCold Plate Temp	Avg Temp Different, ΔT (K)	Area, A (m ²)	Thickness, L (m)	Thermal Conductivity, K (W·K ⁻¹ ·m ⁻¹)
1	19.88	38.17	21.92	16.24	0.09	0.05	0.68
2	14.94	37.55	21.77	15.77	0.09	0.05	0.53
3	19.95	38.22	21.97	16.25	0.09	0.05	0.68
4	20.05	38.20	22.06	16.14	0.09	0.05	0.69
5	9.90	38.20	22.12	16.08	0.09	0.05	0.34
6	19.90	38.21	21.96	16.24	0.09	0.05	0.68

7	20.16	38.21	22.17	16.03	0.09	0.05	0.70
8	15.24	38.21	22.02	16.20	0.09	0.05	0.52
9	19.97	38.19	22.15	16.04	0.09	0.05	0.69
10	15.02	38.20	22.27	15.93	0.09	0.05	0.52
11	19.87	38.21	22.07	16.15	0.09	0.05	0.68
12	14.74	38.25	22.23	16.02	0.09	0.05	0.51
13	19.80	38.26	22.18	16.08	0.09	0.05	0.68
14	10.01	38.28	22.15	16.14	0.09	0.05	0.34
15	14.90	38.25	22.23	16.02	0.09	0.05	0.52
16	15.18	38.22	22.16	16.06	0.09	0.05	0.53
17	14.89	38.25	22.25	16.00	0.09	0.05	0.52
18	10.18	38.25	22.23	16.02	0.09	0.05	0.35
19	15.36	38.24	22.18	16.06	0.09	0.05	0.53
20	19.88	38.22	22.30	15.92	0.09	0.05	0.69
AVG		38.19	22.12				0.57

Table A10: Thermal Conductivity for OPSLWC-MPS-0.3% Panel at 28-days

Hours	Heat Flow, Q (W)	Avg Hot Plate Temp	AvgCold Plate Temp	Avg Temp Different, ΔT (K)	Area, A (m ²)	Thickness, L (m)	Thermal Conductivity, K (W·K ⁻¹ ·m ⁻¹)
1	14.94	37.36	21.97	15.39	0.09	0.05	0.54
2	24.80	37.43	22.01	15.41	0.09	0.05	0.89
3	20.03	37.43	22.06	15.37	0.09	0.05	0.72
4	20.05	37.45	22.06	15.39	0.09	0.05	0.72
5	19.92	37.47	22.06	15.41	0.09	0.05	0.72
6	15.11	37.48	22.07	15.41	0.09	0.05	0.54
7	19.95	37.47	22.07	15.40	0.09	0.05	0.72
8	25.01	37.46	22.07	15.39	0.09	0.05	0.90
9	14.84	37.49	22.08	15.41	0.09	0.05	0.54
10	20.29	37.49	22.08	15.42	0.09	0.05	0.73
11	20.00	38.35	21.98	16.37	0.09	0.05	0.68
12	19.84	37.70	22.06	15.63	0.09	0.05	0.71
13	15.21	37.69	22.06	15.63	0.09	0.05	0.54
14	24.55	37.69	22.06	15.63	0.09	0.05	0.87

15	19.87	37.70	22.07	15.63	0.09	0.05	0.71
16	24.81	37.67	22.07	15.60	0.09	0.05	0.88
17	19.77	37.71	22.06	15.66	0.09	0.05	0.70
18	24.72	37.72	22.05	15.67	0.09	0.05	0.88
19	14.82	37.73	22.03	15.70	0.09	0.05	0.52
20	24.64	37.71	22.02	15.69	0.09	0.05	0.87
AVG		37.61	22.05				0.72

Table A11: Thermal Conductivity for OPSLWC-BPS-0.3% Panel at 28-days

Hours	Heat Flow, Q (W)	Avg Hot Plate Temp	AvgCold Plate Temp	Avg Temp Different, ΔT (K)	Area, A (m ²)	Thickness, L (m)	Thermal Conductivity, K (W·K ⁻¹ ·m ⁻¹)
1	9.90	38.63	22.38	16.25	0.09	0.05	0.34
2	9.86	38.68	22.42	16.26	0.09	0.05	0.34
3	24.90	38.73	22.44	16.29	0.09	0.05	0.85
4	24.96	38.71	22.45	16.26	0.09	0.05	0.85
5	19.99	38.73	22.45	16.27	0.09	0.05	0.68

6	0.00	38.80	22.46	16.34	0.09	0.05	0.00
7	24.98	38.76	22.46	16.31	0.09	0.05	0.85
8	15.19	38.79	22.46	16.33	0.09	0.05	0.52
9	20.32	38.79	22.45	16.34	0.09	0.05	0.69
10	14.91	38.83	22.46	16.37	0.09	0.05	0.51
11	9.95	38.83	22.45	16.37	0.09	0.05	0.34
12	9.97	38.82	22.46	16.36	0.09	0.05	0.34
13	14.70	38.81	22.46	16.35	0.09	0.05	0.50
14	24.64	38.82	22.45	16.37	0.09	0.05	0.84
15	20.12	38.88	22.40	16.48	0.09	0.05	0.68
16	19.97	38.81	22.38	16.42	0.09	0.05	0.68
17	0.00	38.80	22.37	16.43	0.09	0.05	0.00
18	20.01	38.84	22.36	16.48	0.09	0.05	0.67
19	20.33	38.80	22.35	16.44	0.09	0.05	0.69
20	20.02	38.77	22.35	16.42	0.09	0.05	0.68
AVG		38.78	22.42				0.55

Table A12: Thermal Conductivity for OPSLWC-HYB-0.4% Panel at 28-days

Hours	Heat Flow, Q (W)	Avg Hot Plate Temp	Avg Cold Plate Temp	Avg Temp Different, ΔT (K)	Area, A (m ²)	Thickness, L (m)	Thermal Conductivity, K (W·K ⁻¹ ·m ⁻¹)
1	20.02	38.31	22.39	15.92	0.09	0.05	0.70
2	19.79	38.33	22.40	15.92	0.09	0.05	0.69
3	24.86	38.31	22.41	15.90	0.09	0.05	0.87
4	19.75	38.31	22.41	15.90	0.09	0.05	0.69
5	9.82	38.30	22.43	15.87	0.09	0.05	0.34
6	19.94	38.33	22.44	15.89	0.09	0.05	0.70
7	19.91	38.35	22.47	15.88	0.09	0.05	0.70
8	19.81	38.36	22.48	15.87	0.09	0.05	0.69
9	19.74	38.34	22.49	15.85	0.09	0.05	0.69
10	20.14	38.36	22.51	15.85	0.09	0.05	0.71
11	25.19	38.35	22.50	15.85	0.09	0.05	0.88
12	20.24	38.38	22.50	15.87	0.09	0.05	0.71
13	29.98	38.37	22.51	15.86	0.09	0.05	1.05
14	19.09	38.38	22.52	15.87	0.09	0.05	0.67
15	15.20	38.37	22.51	15.86	0.09	0.05	0.53

16	15.25	38.39	22.51	15.88	0.09	0.05	0.53
17	20.07	38.39	22.51	15.88	0.09	0.05	0.70
18	20.29	38.39	22.51	15.88	0.09	0.05	0.71
19	19.97	38.41	22.51	15.90	0.09	0.05	0.70
20	10.03	38.41	22.51	15.90	0.09	0.05	0.35
AVG		38.36	22.48				0.68

LIST OF PUBLICATIONS

1. Loh, L. T., Yew, M. K. & Yew, M. C., 2018. A New Mixing Method for Lightweight Concrete with Oil Palm Shell as Coarse Aggregate. E3S Web of Conferences, 65, p.02012. Available at: <https://doi.org/10.1051/e3sconf/20186502012>.
2. Loh, L. T., Yew, M. K., Yew, M. C., Beh, J.H., Lee, F.W., Lim, S.K. & Kwong, K.Z., 2021. Mechanical and Thermal Properties of Polypropylene Fibre-Reinforced Renewable Oil Palm Shell Lightweight Concrete. Materials, 14, 2337. Available at: <https://doi.org/10.3390/ma14092337>